ULTRA FAST SPEED MEASUREMENT BY ROTATING MAGNETIC FIELD

ABSTRACT
OF THE
THESIS

SUBMITTED FOR THE AWARD OF THE DEGREE OF

Doctor of Philosophy

in

Electronics Engineering

SUBMITTED BY

SYED JAVED ARIF

DEPARTMENT OF ELECTRONICS ENGINEERING
ZAKIR HUSAIN COLLEGE OF ENGINEERING & TECHNOLOGY
ALIGARH MUSLIM UNIVERSITY
ALIGARH, UP (INDIA)

2013

Abstract

Accurate and fast speed measurement is one of the important requirements of the industrial drives, trains, cars, ships, space vehicles, aeroplanes, and fast propulsion or transportation systems. In this thesis, novel rotating magnetic field (RMF) based measurement techniques are proposed to measure speed, variation in speed, very low speed, seismic vibrations, foreshocks and to calibrate tachometers. The rotating member whose speed is to be measured is coupled with the rotor of a synchro. The stator of the synchro is energized by a balance three phase ac voltage which produces RMF rotating at a very high speed in the air gap of synchro. The RMF generates electromotive force (EMF) in the rotor circuit of synchro whose frequency depends upon slip speed i.e. the speed difference of RMF with the rotor of synchro. The RMF rotates in the air gap at a very fast speed and completes several rotations even before completion of one rotation of the rotor, hence, speed measurement becomes very fast. The frequency/time period of the induced EMF in the rotor circuit is measured using a digital storage oscilloscope (DSO) and a microcontroller, which is converted to give the speed of the rotating member. A 16-bit digital output of the microcontroller is also made available corresponding to speed which can be used as a feedback signal for speed control applications. Now if the speed of the rotating member gets changed abruptly, the proposed method is able to sense the new speed in a very short time (within 2.5 ms) due to the high speed of RMF. The time response of the proposed scheme is compared with the time response of a dc tachogenerator.

The fast measurement at low speed becomes very difficult due to slow response of transducers. At low speed (below 10 r/min), normally, transducers take several seconds to give the required output signal. In the proposed method, since the RMF revolves at a high speed, hence the measurement becomes very fast even at 1 r/min for a low speed machine. For the measurement of low speed, a

one-shot monostable multivibrator (OS) and logic gate circuits are used to give a pulse whose width corresponds to the speed. The proposed method is compared with a conventional tachogenerator method which confirms the fast measurement of speed by the proposed method. The output is also obtained in terms of dc voltage and dc current, which can be used for feed-back and control applications. Moreover, due to high accuracy of the proposed method, different types of tachometers, analog and digital, are calibrated using this technique.

The concept of fast RMF based measurement is also extended to measure the velocity and acceleration of seismic vibrations and foreshocks at high resolution and accuracy in millisecond range. To simulate the seismic vibrations and foreshocks mechanically, a microprocessor based rocking vibration arrangement is used. These vibrations are mechanically transmitted to the rotor of a synchro. According to the movement of the rotor of synchro, the RMF generates voltage signals at the rotor output and thereby a pulse train of variable pulse width is produced. The widths of these pulses are used to measure the instantaneous velocity of vibrations. The averaging circuits give the average velocity of vibrations in terms of dc voltage and dc current, corresponding to the widths of these pulses. The instantaneous values of acceleration of these vibrations are found from the related instantaneous values of velocity. The peak positive and negative velocity and acceleration of vibrations are also obtained with a resolution in millisecond range.

Work Done in this Thesis

The goal set for this thesis is in three important areas of instrumentation and measurement, namely; *fast measurement of angular speed of rotating machines, calibration of tachometers, and high resolution seismic vibration measurement.* The work done and the main contributions described in this thesis are explained below.

- A novel technique of measurement using RMF is proposed for the fast and accurate measurement of speed.
- A novel technique of measurement using RMF is proposed for the measurement of variation in speed.
- Experimental setups with circuits are developed for the generation of RMF based measurement of speed in acceleration and deceleration mode.
- A single-phase to three-phase convertor circuit is developed for the generation of RMF. To avoid the loading effect of the three-phase convertor circuit, a buffer amplifier circuit is designed to provide amplified signal to the stator winding of synchro.
- A program is developed using microcontroller (PIC 16F877A), to measure the time period of the output pulse which corresponds to speed. Hence the digital output becomes available for high resolution speed measurement and can also be used as a digital feedback signal for speed control applications.
- The proposed scheme is compared with the speed measurement by a dc tachogenerator in acceleration and deceleration mode.
- The RMF based measurement scheme is used for the calibration of various tachometers. Three different types of tachometers, (an analog/mechanical type, a digital non-contact type, and a digital contact type) are calibrated with the proposed scheme.
- The measurement technique is also extended for the fast and accurate measurement of low speed.
- Experimental setup is developed to realize very low speed from 0 to 10 r/min, using a three-phase induction motor (as a prime mover) and a vector controller adjustable frequency ac drive system.
- A digital logic circuit is designed to measure the pulse width corresponding to very low speed of the rotating member.
- An amplifier with averaging circuit is developed to obtain dc output voltage as well as dc current as feed-back signals for control applications.

- The RMF and synchro based measurement scheme is also proposed for the fast and accurate measurement of seismic vibrations and foreshocks.
- The velocity waveforms of various earthquakes are investigated. The waveforms of 2003 Lefkada (Greece), 1994 Northridge (USA), 1992 Landers (USA), and 1987 Whittier Narrows (USA) earthquakes are taken as reference for the simulation purpose.
- In order to mechanically simulate seismic vibrations in the laboratory, a microprocessor based vibration generation and measurement setup is developed to practically realize vibrations which resemble seismic vibrations of the reference earthquakes.
- Averaging circuits with amplifiers are used to obtain average velocity of vibrations in terms of dc voltage and dc current, corresponding to the widths of pulses generated due to these vibrations.
- A micro ammeter is calibrated in terms of velocity of vibrations.

Publications from the Thesis

Papers in International Journals

1. S. J. Arif, M. S. J. Asghar and Adil Sarwar, "Measurement of speed and calibration of tachometers using rotating magnetic field," *IEEE Tnans. on Inst. & Measr.*, Issue: 99, pp. 1-11, Published to IEEE Xplore (DOI: 10.1109/TIM.2013.2283136), 17 October 2013.
2. S. J. Arif, M. S. J. Asghar and K. F. Khan, "A high resolution measurement of foreshocks for the prediction of earthquakes", *International Journal on Earth Science and Climate Change* (USA), vol., 3, no., 2, pp. 1-6, Oct. 2012.
3. S. J. Arif, M. S. J. Asghar and Imdadullah, "Accurate measurement of velocity and acceleration of seismic vibrations near nuclear power plants," *Elsevier's Journal of Physics Procedia,* vol., 37, pp. 43-50, Oct. 2012.
4. S. J. Arif, M. S. J. Asghar and Imdadullah, "Very fast measurement of low speed of rotating machines using rotating magnetic field," *IEEE Tnans. on Inst. & Measr.*, vol., 61, no., 3, pp. 759-766, March 2012.

Filed and Published Patents

1. S. J. Arif and M. S. J. Asghar, "A rotating magnetic field based calibration of tachometers," Patent Application 2517/DEL/2013, *Indian Official Journal of the Patent Office, Issue No. 40/2013,* p-24845, Oct 04, 2013.
2. S. J. Arif and Shahedul Haque Laskar, "A rotating magnetic field based ultra fast measurement of speed," Patent Application 777/DEL/2011A, *Indian Official Journal of the Patent Office, Issue No. 18/2011,* p-8219, May 06, 2011.
3. S. J. Arif and Shahedul Haque Laskar, "A rotating magnetic field based high resolution measurement of velocity and acceleration of seismic vibration,"

Patent Application 778/DEL/2011A, *Indian Official Journal of the Patent Office, Issue No. 17/2011,* p-7116, Apr. 29, 2011.

4. S. J. Arif and M. S. J. Asghar, "A rotating magnetic field based ultra fast transducer for the measurement of very low speed," Patent Application 2183/DEL/2010A, *Indian Official Journal of the Patent Office, Issue No. 14/2011,* p-6126, Apr. 8, 2011.

Paper to be Communicated

1. S. J. Arif and M. S. J. Asghar, "Rotating magnetic field based measurement of seismic vibrations and foreshocks," *to be communicated in IEEE Transaction on Instrumentation & Measurement.*

ULTRA FAST SPEED MEASUREMENT BY ROTATING MAGNETIC FIELD

THESIS

SUBMITTED FOR THE AWARD OF THE DEGREE OF

Doctor of Philosophy

in

Electronics Engineering

SUBMITTED BY

SYED JAVED ARIF

DEPARTMENT OF ELECTRONICS ENGINEERING
ZAKIR HUSAIN COLLEGE OF ENGINEERING & TECHNOLOGY
ALIGARH MUSLIM UNIVERSITY
ALIGARH, UP (INDIA)

2013

CERTIFICATE

This is to certify that the thesis entitled "**Ultra Fast Speed Measurement by Rotating Magnetic Field**", submitted by **me** in the Department of Electronics Engineering, Zakir Husain College of Engineering and Technology, Aligarh Muslim University, Aligarh, India, for the award of the degree of ***Doctor of Philosophy in Electronics Engineering,*** is a record of my own work. The matter embodied in this thesis has not been submitted to any other University or Institute for the award of any other degree.

Syed Javed Arif
Assistant Professor
Department of Electronics Engineering,
Zakir Husain College of Engineering and Technology
Aligarh Muslim University
Aligarh
India

Acknowledgement

I take this opportunity to thank Prof. Mohammad Syed Jamil Asghar for his enthusiastic support, continuous encouragement and keen interest throughout this research. It is through his concern and continuous help that I have been able to write and submit this thesis.

I express my thanks to Prof. Z. A. Abbasi, Prof. M. A. Siddiqi, and Prof. Salim Beg, current and past Chairmen, Department of Electronics Engineering, AMU Aligarh, for extending all types of administrative help and providing facilities in the department.

I am thankful to Prof. Ekram Khan, Dr. Athar Ali Moinuddin, Dr. Syed Atiqur Rahman, M. Sarosh Umar, Imdadullah, and Dr. Samar Ansari for their time, encouragement and helpful suggestions. I am also grateful to all my teachers, colleagues and friends and in particular Prof. M. Hasan, Dr. Shah Alam, M. R. Abidi, Dr. Omar Farooq, Ale Imran, Anwar Sadat, Adil Sarwar, Ayyub and Sadaf Zaidi for their continuous support and valuable suggestions. Thanks are also due to Haji Shamsuddin, University Polytechnic, AMU Aligarh, for his technical support in realization of the hardware for experimentation, throughout my research work.

My deepest gratitude goes to my parents to whom I owe all my achievements and they did not stay to see me earn my Ph.D. I really don't have words to express my gratitude to my wife for her immense patience, support and continuous encouragement during the hard times of my research work. Also, I want to express love to my sons Hamza, Hammad and especially to Hisham who have always released my tension whenever I was over stressed.

I would like to acknowledge the financial support of TEQIP Program and DRS Program of University Grants Commission, Government of India, without which doing research at AMU Aligarh, would not have been possible.

I would also like to extend my thanks to all the non-teaching staff of my department, in particular Shakeel Ahmad, S. A. Farooqi, Khan M. Akmal, Wasim Ahmad, M. Sulaiman, Sabil Ahmad, Nadeem Nami, Mushir Khan and Ameeruzzaman for their time and help whenever required.

Abstract

Accurate and fast speed measurement is one of the important requirements of the industrial drives, trains, cars, ships, space vehicles, aeroplanes, and fast propulsion or transportation systems. In this thesis, novel rotating magnetic field (RMF) based measurement techniques are proposed to measure speed, variation in speed, very low speed, seismic vibrations, foreshocks and to calibrate tachometers. The rotating member whose speed is to be measured is coupled with the rotor of a synchro. The stator of the synchro is energized by a balance three phase ac voltage which produces RMF rotating at a very high speed in the air gap of synchro. The RMF generates electromotive force (EMF) in the rotor circuit of synchro whose frequency depends upon slip speed i.e. the speed difference of RMF with the rotor of synchro. The RMF rotates in the air gap at a very fast speed and completes several rotations even before completion of one rotation of the rotor, hence, speed measurement becomes very fast. The frequency/time period of the induced EMF in the rotor circuit is measured using a digital storage oscilloscope (DSO) and a microcontroller, which is converted to give the speed of the rotating member. A 16-bit digital output of the microcontroller is also made available corresponding to speed which can be used as a feedback signal for speed control applications. Now if the speed of the rotating member gets changed abruptly, the proposed method is able to sense the new speed in a very short time (within 2.5 ms) due to the high speed of RMF. The time response of the proposed scheme is compared with the time response of a dc tachogenerator.

The fast measurement at low speed becomes very difficult due to slow response of transducers. At low speed (below 10 r/min), normally, transducers take several seconds to give the required output signal. In the proposed method, since the RMF revolves at a high speed, hence the measurement becomes very fast even at 1 r/min for a low speed machine. For the measurement of low speed, a

one-shot monostable multivibrator (OS) and logic gate circuits are used to give a pulse whose width corresponds to the speed. The proposed method is compared with a conventional tachogenerator method which confirms the fast measurement of speed by the proposed method. The output is also obtained in terms of dc voltage and dc current, which can be used for feed-back and control applications. Moreover, due to high accuracy of the proposed method, different types of tachometers, analog and digital, are calibrated using this technique.

The concept of fast RMF based measurement is also extended to measure the velocity and acceleration of seismic vibrations and foreshocks at high resolution and accuracy in millisecond range. To simulate the seismic vibrations and foreshocks mechanically, a microprocessor based rocking vibration arrangement is used. These vibrations are mechanically transmitted to the rotor of a synchro. According to the movement of the rotor of synchro, the RMF generates voltage signals at the rotor output and thereby a pulse train of variable pulse width is produced. The widths of these pulses are used to measure the instantaneous velocity of vibrations. The averaging circuits give the average velocity of vibrations in terms of dc voltage and dc current, corresponding to the widths of these pulses. The instantaneous values of acceleration of these vibrations are found from the related instantaneous values of velocity. The peak positive and negative velocity and acceleration of vibrations are also obtained with a resolution in millisecond range.

Publications from the Thesis

Papers in International Journals

1. S. J. Arif, M. S. J. Asghar and Adil Sarwar, "Measurement of speed and calibration of tachometers using rotating magnetic field," *IEEE Tnans. on Inst. & Measr.*, Issue: 99, pp. 1-11, Published to IEEE Xplore (DOI: 10.1109/TIM.2013.2283136), 17 October 2013.
2. S. J. Arif, M. S. J. Asghar and K. F. Khan, "A high resolution measurement of foreshocks for the prediction of earthquakes", *International Journal on Earth Science and Climate Change* (USA), vol., 3, no., 2, pp. 1-6, Oct. 2012.
3. S. J. Arif, M. S. J. Asghar and Imdadullah, "Accurate measurement of velocity and acceleration of seismic vibrations near nuclear power plants," *Elsevier's Journal of Physics Procedia,* vol., 37, pp. 43-50, Oct. 2012.
4. S. J. Arif, M. S. J. Asghar and Imdadullah, "Very fast measurement of low speed of rotating machines using rotating magnetic field," *IEEE Tnans. on Inst. & Measr.*, vol., 61, no., 3, pp. 759-766, March 2012.

Filed and Published Patents

1. S. J. Arif and M. S. J. Asghar, "A rotating magnetic field based calibration of tachometers," Patent Application 2517/DEL/2013, *Indian Official Journal of the Patent Office, Issue No. 40/2013,* p-24845, Oct 04, 2013.
2. S. J. Arif and Shahedul Haque Laskar, "A rotating magnetic field based ultra fast measurement of speed," Patent Application 777/DEL/2011A, *Indian Official Journal of the Patent Office, Issue No. 18/2011,* p-8219, May 06, 2011.
3. S. J. Arif and Shahedul Haque Laskar, "A rotating magnetic field based high resolution measurement of velocity and acceleration of seismic vibration,"

Patent Application 778/DEL/2011A, *Indian Official Journal of the Patent Office, Issue No. 17/2011,* p-7116, Apr. 29, 2011.

4. S. J. Arif and M. S. J. Asghar, "A rotating magnetic field based ultra fast transducer for the measurement of very low speed," Patent Application 2183/DEL/2010A, *Indian Official Journal of the Patent Office, Issue No. 14/2011,* p-6126, Apr. 8, 2011.

Paper to be Communicated

1. S. J. Arif and M. S. J. Asghar, "Rotating magnetic field based measurement of seismic vibrations and foreshocks," *to be communicated in IEEE Transaction on Instrumentation & Measurement.*

Table of Contents

List of Figures

List of Tables

List of Acronyms and Abbreviations

ADC	: analog to digital convertor
A_I	: instantaneous acceleration of vibrations
ASIC	: Application Specific Integrated Circuit
A_{p+}	: peak positive acceleration
A_{p-}	: peak negative acceleration
C	: capacitance
^oC	: degree centigrade
CH	: channel
cm/s	: centimeter per second
CSDT	: constant sample-time digital tachometer
dc	: direct current
DSO	: digital storage oscilloscope
EMF	: electromotive force
EMI	: electromagnetic interference
EX-OR	: Exclusive OR
f_r	: frequency of induced EMF in the rotor circuit of synchro
f_R	: frequency of signal V_R at the output of zero crossing detector
f_s	: frequency of voltage or current in the stator winding of synchro
f_z	: frequency of signal V_Z at the output of zero crossing detector
F.G	: function generator
FPGA	: field programming gate arrays
FSR	: full scale reading
G-1	: Exclusive OR gate
H	: Hexadecimal
Hz	: Hertz
I_{dc}	: dc current
kΩ	: kilo ohms

LED	: light emitting diode
LSB	: least significant bit
ms	: milliseconds
MSB	: most significant bit
mV	: milivolts
NGT	: negative going transition
n_r	: speed of the rotating member or rotor of synchro
n_s	: synchronous speed of rotating magnetic field
OS	: one shot mono-stable multi-vibrator
OP-AMP	: operational amplifier
P	: number of poles
PC	: personal computer
PGT	: positive going transition
ppm	: parts per million
Q	: output of one shot mono-stable multi-vibrator
Q′	: inverted output of one shot mono-stable multi-vibrator
r	: radius of rotor of synchro
R	: resistance
R_{ex}	: external resistance of the armature circuit of dc motor
RMF	: rotating magnetic field
r/min	: revolution per minute
s	: seconds
SEI	: serial encoder interface
SW	: switch
T	: time period of pulse at the output of gate G-1
t_{on}	: on time of pulse at the output of gate G-1
T_R	: time period of the signal V_R at the input of One Shot
T_{WG-}	: negative width of the pulse at the output of Exclusive OR gate
T_{WQ+}	: positive width of signal Q
T_{WQ-}	: negative width of signal Q′
T_{WR-}	: negative width of the signal V_R

T_{WR+} : positive width of the signal V_R

T_z : time period of rectangular waveform of zero crossing detector

V : volts

V_1, V_2, V_3 : three-phase voltages at the output of phase-split circuit

V_4, V_5, V_6 : three-phase voltages at the input of power amplifiers

V_7, V_8, V_9 : three-phase voltages at the output of power amplifiers

V_{dc} : dc voltage

V_I : instantaneous velocity of vibrations

V_{P+} : peak positive velocity of vibrations

V_{P-} : peak negative velocity of vibrations

V_{max} : maximum amplitude of pulse at the output of gate G-1

V_r : single-phase voltage of rotor winding of the synchro

V_R : square waveform at the output of zero crossing detector

V_s : three-phase voltages of stator winding of the synchro

V_z : rectangular waveform at the output of zero crossing detector

ZCD : zero crossing detector

μA : micro ampere

μF : micro Farad

μHz : micro Hertz

μs : micro seconds

Ω-m : ohm meter

ω : angular speed of rotor of synchro in radian per second

Chapter 1

Introduction

1.1 Background and Motivation from Literature

Feed back control systems require fast measurement of speed and generation of control signals. Accurate and fast speed measurement is one of the important requirements of space vehicles, aeroplanes, warships, rocket propellers, high speed trains, high speed cars, fast synchronous motors, induction motors, dc motors and fast propulsion or transportation systems. Very fast and accurate speed measurement is also one of the important requirements of low speed machines like rotors of cement kilns, rolling machines in paper mills, mining industries, textile mills and heavy stone crushing machines, where the speed varies from 0 to 10 revolutions per minute (r/min) [1]-[4]. Even the drives with speed less than 2 r/min are very common in industries [1]. Different contact type and non-contact type tachometers are used for speed measurement as well as for generation of feedback signals for control applications. Usually these tachometers suffer from calibration drift and they have also got drawbacks of low resolution and noise contaminations [5]-[11]. Moreover, several revolutions are required to detect the deviation in speed and therefore only after a significant delay, the outputs of these tachometers become stable. In case of many non-contact type transducers, several seconds are required due to delay in time response [8]-[11]. Both ac and dc tachogenerators are commonly used for speed measurement. But the commutator and brushes in dc tachogenerators need periodic maintenance [12]. Also, if the armature current is large, it distorts the field of the permanent magnet and hence causes non-linearity [13]. Similarly, in case of ac tachogenerators, the ripples of

the output voltage are susceptible to speed variations and therefore smoothening filters become necessary [7]. These filter circuits increase the delay in time response of ac tachogenerators. On the other hand, the digital tachometers are preferred over their analog counterparts as they have better accuracy and give immunity to noise. Thus the delay in time response due to analog filters is avoided. The digital tachometers are generally of two types. One is based on counting the pulses of a pulse-train over a fixed duration of measurement time, which exhibits very accurate result at high speed but the errors are dramatically increased at lower speed [14]-[16]. At low speed, this duration is kept large, therefore, a significant delay appears in the response time of the measurement. Moreover, the method results in a loss of one pulse during the count of pulses. At high speed, as the number of pulses are large, the loss of one pulse is insignificant; therefore, the accuracy of the measurement is not affected. At low speed, the loss of one pulse causes significant error. An appreciable improvement is made in the above method by the constant elapsed time method [14]-[15]. However, this method has a serious limitation of minimum measurable speed, within a given maximum response time. Therefore, it does not work effectively for a speed below 30 r/min [15]. The Application Specific Integrated Circuit (ASIC) method of digital tachometers combines the advantages of both the above mentioned methods and gives high accuracy of measurement over a wide range of speed. However, the response time of ASIC method is slow which is of the order of seconds [16]. The ADC based methods are also commonly used in angular speed measurement [17]-[19]. They require longer period of measurement as these methods are based on averaging processes [18]-[19]. In optical encoder based methods, the increase in sampling time improves the read-out accuracy but these methods are costly and intricate [20]-[23]. In fact, they require additional accessories like serial encoder interface (SEI) bus adapter, power supply and a PC with supporting software to monitor the displacement and position of the rotating member [24]-[25]. Moreover, the encoder coupling to the machine shaft has rubber inserts which gives heavy damping and backlash [23]. For accurate measurement of speed, Hall sensors and optical sensors have also been reported in

the literature. However, they have large response time, which is of the order of seconds [26]-[27]. The speed measurement by sensor less methods has got momentum in last decade [28]-[40]. The drives with sensor less control have advantages of increased reliability (no tachometer failure), elimination of sensor cables and reduced size of drive systems. However, these measurement methods experience problems due to variation in machine parameters (stator and rotor resistances etc), resulting in deterioration of accuracy [36]. Moreover, the delay in time response becomes high due to output filters [36], [38]. Also, the output filters, may alter the information output at low speed [39]-[40]. The Constant Sample-time Digital Tachometer (CSDT) method is used to measure both low and high speeds. However, the non idealities in optical incremental encoders and sensors produce very large errors. Also, the phasing between encoding channel generates significant errors at the output of tachometer [41]-[44]. With the help of FPGA, CSDT method is improved, however, it gives faster response at low speed only [45]. The contact type measurement methods are simple and cost effective. They are being used in remote locations, for example, off shore wind turbines, and cost effective condition monitoring [46]. With the advancement in technology, the measurement using contact type methods is not a problem anymore. The true zero backlash flexible shaft couplings are available for the shaft coupling up to 30,000 r/min for continuous use in a temperature range of -40 °C to +120 °C [47].

The delay in time response of the existing methods varies from one tenth of a second to several seconds as detailed earlier. Therefore, these techniques are not suitable for fast speed measurement or where fast feedback signals are required for control applications. To overcome these drawbacks, a novel technique of measurement using rotating magnetic field (RMF) is proposed in this thesis for fast and accurate measurement of speed and variation in speed [48]-[49]. A balanced three-phase ac voltage with a frequency of 400 Hz is applied to the stator winding of a synchro which produces an RMF rotating at a very fast speed in the air gap of synchro. Consequently, an electromotive force (EMF) is generated in the rotor circuit of synchro which is coupled with a rotating member

whose speed is being measured. The frequency of the induced EMF in the rotor circuit of synchro depends upon slip speed i.e. the speed difference of RMF with the rotor of synchro. With a frequency of 400 Hz, the RMF revolves at a speed of 24000 r/min which is purposely kept very high in comparison to the speed of the rotor or rotating member. Thus the measurement becomes very fast and the change in speed is sensed within 2.5 ms. The synchro and a dc shunt motor with a zero crossing detector (ZCD) are used for the measurement. Separate circuits are designed for the measurement of speed in acceleration and deceleration mode. The time response of the proposed scheme is compared with the time response of a dc tachogenerator. A program is developed using microcontroller (PIC 16F877A), to measures the time period which corresponds to speed and deviation in speed of the rotating member. The 16-bit digital output of the microcontroller is made available as a feedback signal for control applications.

The effect of fast rotation of magnetic field is much more pronounced at low speed. Hence, the method of RMF based fast measurement is highly suitable for low speed machines [50]-[51]. Since the time of measurement depends on the slip speed of RMF with the rotor/rotating member, very fast measurement is achieved even at very low speed (1-10 r/min). Here, the frequency of the balanced three-phase ac voltage applied to the stator winding of synchro is taken as 40 Hz. At this frequency, the RMF rotates at a speed of 2400 r/min. Hence, even at 1 r/min the speed is measured at the speed of RMF (2400 r/min), which is 2400 times faster than the speed of rotating member. An experimental setup is developed to realize low speed from 0 to 10 r/min, using a three-phase induction motor (as a prime mover) and an adjustable frequency ac drive system. A digital logic circuit is designed to measure the pulse width corresponding to very low speed of the rotating member. An amplifier with averaging circuit is also developed to obtain dc output voltage or dc current as feed-back signals for control applications. The proposed scheme is compared with the speed measurement by a dc tachogenerator.

Fast and accurate method is also required for the calibration of tachometers. Different tachometers which include contact type, non-contact type, and both analog and digital tachometers are being used for speed measurement in the industries and laboratories etc. The calibration of a tachometer refers to comparing its readings (speed) with a more accurate (standard) speed measuring instrument than the tachometer being calibrated [52]-[53]. The tachometers are manufactured by physical materials and they are used in the real world of humidity, heat, physical stress, noise and vibrations etc., and as a consequence their performance gets affected and deteriorates. Hence, regular calibration of tachometers is required to maintain their accuracy within the manufacturer's specifications.

Several state-of-the-art methods are being used in industries for calibration of both contact type and non-contact type tachometers [54]-[58]. The contact type tachometers are calibrated using pulse generator, electronic counter along with discrete variable components (like resistors). The performance of these components deteriorates with aging and causes inaccuracies in calibration [54]. A simple method has also been reported to calibrate the contact type tachometers, using a computer with tone generating program [55]. The method calibrates the tachometers up to 8500 r/min. In the lower range of speed the calibration is limited to 200 r/min. The non-contact optical tachometers are calibrated up to a range 12000 r/min to 60000 r/min using universal frequency counter and pulse signals of laser diode, and LEDs, driven by very accurate and calibrated function generator [56]-[58]. These methods are complex and the instruments and software involved with attachments like calibration adapter are costly. The non-contact optical tachometers are also calibrated using a stroboscope. However, the high light of stroboscope sometimes makes the results of calibration unacceptable [59].

An improved method is developed using the RMF based measurement technique using a synchro, coupled with a dc motor (rotating member) for the calibration of tachometers. The calibration is based on the fundamental principle where the frequency of the induced EMF in the rotor circuit of synchro is directly

proportional to the speed of rotating member. For a particular speed the exact frequency is found and thereby, the actual time period is calculated for this speed. The rotating member (dc motor) is allowed to run and the speed is controlled by varying the voltage across its armature winding. The exact time period is adjusted and set accurately, by varying the speed of dc motor. Consequently, the speed of dc motor becomes exactly equal to the theoretical value. Three different types of tachometers (an analog/mechanical type, a digital non-contact type, and a digital contact type) are calibrated with the proposed method [60]-[62].

High resolution, fast and accurate measurement is equally important for measuring the speed/velocity of seismic vibrations. The earthquake is one of the prime causes of natural disasters, human loss, technological disasters, and damage to heavy building structures, electric power and water delivery system. Enormous destruction and economic losses are common due to earthquakes and landslides provoked by geological instabilities and rock impacts [63]. The earthquake of Japan on March 11, 2011 has raised alarm worldwide regarding nuclear power generation. The earth quake in Haiti on January 12, 2010 has killed more than 230,000 people. The earth quake of Sumatra (Tsunami) on December 26, 2004 killed more than 300,000 people in 11 countries. The heavy destruction from big earthquakes [Friuli, Mexico City 1985, Aegion 1995, Umbria 1997, Turkey 1999, Sumatra (Tsunami) 2004, Sichuan 2008, Samoa 2009, Chile 2010 and Japan 2011] is beyond contemplation. The instruments like seismometers and accelerometers, used for monitoring seismic vibrations have been mainly developed in view of measuring acceleration, which is only one of the parameters [64]. Furthermore, the present seismometers fail to record the peak values of acceleration, displacement, speed, rise time caused by strong motions in the critical area near field of strong earthquakes, with high resolution [65]. Hence, due to poor resolution, the peak values of seismic wave's parameters are missed, which causes problems in the reliable design of nuclear power plants, industrial plants and buildings, resistant to strong earthquakes. This fact has been demonstrated by the destruction of heavy constructions in the recent strong earthquakes. Therefore, for a more consistent design of buildings, it would be an

advantage to measure directly the seismic waves acting on the buildings.

A reduction in disasters due to earthquakes requires a rigorous effort over a wide range of solutions-oriented multi-disciplinary, multi-institutional research. An accurate prediction of earthquake will minimize the loss of life, severe injuries, and disruption of important services. Therefore, the prediction of location and time, of large earthquakes, has regained a great importance. A high resolution measurement of velocity and acceleration of foreshocks helps more accurate prediction of earthquakes [66]-[67].

Generally, before any earthquake, there are foreshocks with hidden signatures of velocity and acceleration. The fact has been established recently that the foreshocks are the best accredited forecaster of earthquakes [68]. This thinking has been supported by the seismic response time histories and comparison of measured and identified data records of seismic vibrations [69]. The researchers have found that there is a strong correlation and resemblance in the pattern of velocity and acceleration of foreshocks and main shock. This is helpful in the prediction of earthquakes [70]-[74]. The foreshocks consist of very low frequency waves with superimposed high frequency spikes, which have extremely high instantaneous velocity and acceleration. Due to this adverse combination, the existing low resolution accelerometers and seismometers are unable to get an insight of signatures of these foreshocks [68]-[69], [75].

For the prediction of earthquakes, several experiments have been carried out in Greece, based on the change of electric current in dielectric media and soil [76]-[80]. However, the prediction is too vague and no feasible decision such as to evacuate the population of a certain area for a given period of time, can be made [64], [81]-[82]. The VAN method gives a good prediction of earth quake to vacate a certain area. However, the large numbers of dipoles (buried at the depth of 2 meters) are required at a distance of 100 meters to 10 km. Therefore, large connecting wires required to supply the signal to a difference amplifier, make the system costly and intricate [83]. Attempts were also made in Japan for the

prediction of earthquakes, based on chemical changes in mineral water [84]-[85]. However, the implementation of the technique is very expensive and complex [86]. Various techniques, for measuring the velocity and acceleration of foreshocks and main shock, have been proposed in the literature. The resolution of measurement of existing methods is in the range of few seconds to tens of seconds. Moreover these methods are slow, less accurate, and unreliable for the prediction of earthquakes [75], [87]-[90]. Hence a high resolution measurement technique for the measurement of seismic vibrations and foreshocks is required.

In this thesis, the RMF based measurement scheme is proposed for fast and accurate measurement of velocity of seismic vibrations and foreshocks [91]-[93]. In order to mechanically simulate seismic vibrations in the laboratory, the velocity waveforms of various earthquakes are investigated [87]-[90]. Some of these earthquake waveforms [2003 Lefkada (Greece), 1994 Northridge (USA), 1992 Landers (USA), 1987 Whittier Narrows (USA)] are taken as reference for the simulation of seismic vibrations [90]. A microprocessor based system with stepper motor and a synchro is developed to practically realize vibrations which resemble seismic vibrations of these earthquakes. The fast back and forth movement of different angular length, which resembles the seismic vibrations, is generated by stepper motor and transmitted to the rotor of the synchro. Consequently, the movement varies the frequency of rotor voltage of synchro. Thereby, a pulse train of variable pulse width is obtained and recorded in millisecond range. A digital logic circuit measures the width of these pulses which corresponds to the instantaneous velocity of vibrations. The averaging circuits are also developed and the average velocity of vibrations is obtained in terms of dc voltage and current. The instantaneous values of acceleration of these vibrations are found using the corresponding instantaneous velocity. The values of peak positive and negative velocity and acceleration of vibrations are also obtained with a resolution in millisecond range.

1.2 Work Done in this Thesis

The goal set for this thesis is in three important areas of instrumentation and measurement, namely; *fast measurement of angular speed of rotating machines, calibration of tachometers, and high resolution seismic vibration measurement.* The work done and the main contributions described in this thesis are explained below.

- A novel technique of measurement using RMF is proposed for the fast and accurate measurement of speed.
- A novel technique of measurement using RMF is proposed for the measurement of variation in speed.
- Experimental setups with circuits are developed for the generation of RMF based measurement of speed in acceleration and deceleration mode.
- A single-phase to three-phase convertor circuit is developed for the generation of RMF. To avoid the loading effect of the three-phase convertor circuit, a buffer amplifier circuit is designed to provide amplified signal to the stator winding of synchro.
- A program is developed using microcontroller (PIC 16F877A), to measure the time period of the output pulse which corresponds to speed. Hence the digital output becomes available for high resolution speed measurement and can also be used as a digital feedback signal for speed control applications.
- The proposed scheme is compared with the speed measurement by a dc tachogenerator in acceleration and deceleration mode.
- The RMF based measurement scheme is used for the calibration of various tachometers. Three different types of tachometers, (an analog/mechanical type, a digital non-contact type, and a digital contact type) are calibrated with the proposed scheme.
- The measurement technique is also extended for the fast and accurate measurement of low speed.

- Experimental setup is developed to realize very low speed from 0 to 10 r/min, using a three-phase induction motor (as a prime mover) and a vector controller adjustable frequency ac drive system.
- A digital logic circuit is designed to measure the pulse width corresponding to very low speed of the rotating member.
- An amplifier with averaging circuit is developed to obtain dc output voltage as well as dc current as feed-back signals for control applications.
- The RMF and synchro based measurement scheme is also proposed for the fast and accurate measurement of seismic vibrations and foreshocks.
- The velocity waveforms of various earthquakes are investigated. The waveforms of 2003 Lefkada (Greece), 1994 Northridge (USA), 1992 Landers (USA), and 1987 Whittier Narrows (USA) earthquakes are taken as reference for the simulation purpose.
- In order to mechanically simulate seismic vibrations in the laboratory, a microprocessor based vibration generation and measurement setup is developed to practically realize vibrations which resemble seismic vibrations of the reference earthquakes.
- Averaging circuits with amplifiers are used to obtain average velocity of vibrations in terms of dc voltage and dc current, corresponding to the widths of pulses generated due to these vibrations.
- A micro ammeter is calibrated in terms of velocity of vibrations.

1.3 Organization of Thesis

The thesis is organized such that the background of the work done in this thesis is discussed in chapter 1. Also the contribution and organization of the thesis is given in this chapter.

In chapter 2, an RMF based measurement technique is proposed which provides fast measurement of speed and deviation in speed. The time response of the proposed scheme is compared with the time response of a conventional dc

tachogenerator. The use of a microcontroller is also discussed which generates a 16-bit digital output, corresponding to speed.

The chapter 3 describes the proposed technique which was discussed in chapter 2, is successfully applied for the calibration of different contact type and non-contact type tachometers. The calibration of three different types of tachometers (an analog/mechanical type, a digital non-contact type, and a digital contact type) is discussed.

The chapter 4 describes the application of the RMF based speed measurement technique for the fast measurement of very low speed. The proposed method is compared with a conventional tachogenerator method which confirms the fast response of the proposed method. The output measurand is also made available in terms of dc voltage and current for feedback control applications.

In chapter 5, a seismic vibration measurement technique is proposed using RMF which provides fast measurement of seismic vibrations including foreshocks with high accuracy and high resolution. The use of a microprocessor based system is discussed to simulate or generate the vibrations in the range of -20 cm/s to +20 cm/s, with a frequency of about 1 Hz. Here, the use of an amplifier circuit for the measurement of vibrations is also discussed. The output is obtained in terms of dc voltage and current for the direct measurement of the vibrations.

Chapter 6 of the thesis contains the conclusion of work as well as possible future investigations.

Chapter 2

Ultra Fast Measurement of Speed and Deviation in Speed Using Rotating Magnetic Field

2.1 Introduction

In this chapter, the concept of using RMF for fast measurement of speed is being proposed. RMF based measurement technique for fast and accurate measurement of speed and the variation in speed is described. A contact type synchro is used as a primary transducer. A balanced three-phase ac voltage is applied to the stator winding of synchro which produces an RMF in the air gap. An EMF is generated by RMF in rotor circuit of the synchro which is coupled with the rotating member whose speed is being measured. The frequency of induced EMF in the rotor circuit of synchro depends upon the slip speed of RMF with the rotor/rotating member. An operational amplifier in open-loop mode is used as a ZCD to eliminate the effect of noise, distortion in waveform and varying magnitude of EMF. Moreover, as the rotation of magnetic field is kept as fast as possible (24000 r/min, 400 Hz), the speed and the change in speed are quickly monitored by the deviation in frequency of rotor circuit. Since the RMF rotates at very high speed and it completes one revolution within 1/400 s, therefore, the deviation in speed is immediately detected in the very next cycle i.e., within 2.5 ms. A digital storage oscilloscope (DSO) and a microcontroller are used for the measurement of time period and frequency, corresponding to the speed and the change in speed of

the rotating member. The digital output of microcontroller is made available as a digital feedback signal for controlling the speed and the deviation in speed. The time response of the proposed scheme is also compared with the time response of a dc tachogenerator.

2.2 Theory

A synchro is an electromechanical device which has a three-phase stator winding and a single-phase rotor winding. Its physical construction is similar to a three-phase alternator. A synchro is suitable for the operation in heavy noise industrial environment as it can tolerate high temperature, high shock, vibration and humidity [94]. When the three-phase stator winding of a synchro is energized by a three-phase balanced current, the RMF is produced in the air gap [48], [51], [94]. The RMF in the air gap rotates at synchronous speed (in r/min) is given by

$$n_s = \frac{120\, f_s}{P} \qquad (2.1)$$

where f_s is the frequency of voltage or current in the stator winding, in Hz and P is the number of poles of the stator winding.

The RMF generates EMF in the rotor circuit of synchro whose frequency depends upon slip speed i.e. the speed difference of RMF with the rotor of synchro. Here, for the speed measurement, this principle is employed and a synchro is used as a part of the speed transducer.

If the rotor of a synchro is mechanically connected or linked with a rotating member, the frequency of induced EMF, in the rotor circuit of synchro is given by

$$f_r = \frac{(n_s \mp n_r)P}{120} \qquad (2.2)$$

where n_r is the speed of the rotating member or rotor of synchro in r/min

From (2.1) and (2.2),

$$f_r = \frac{n_s P}{120} \mp \frac{n_r P}{120} = f_s \mp \frac{n_r P}{120} \qquad (2.3)$$

Since P, n_s and f_s are constant, f_r linearly varies with the rotor speed n_r. When the rotating member or the rotor of synchro is stationary, f_r becomes equal to f_s. However, when the rotating member rotates along with (direction of) RMF, f_r is proportional to the slip ($n_s - n_r$). Whereas, if the direction of rotation is opposite, f_r is proportional to the slip ($n_s + n_r$). Here, the speed of the rotor of synchro or rotating member (dc motor) is few hundred r/min only, whereas, the speed of RMF is 24000 r/min for a supply frequency of 400 Hz. At this frequency, for each revolution of the rotating member, the RMF rotates 24000 times. Therefore, any change in speed is sensed immediately, within the completion of one revolution of the RMF i.e. within 1/400 seconds. Consequently, the measurement becomes very fast. In the proposed method, the high resolution of speed measurement depends upon the high resolution of the pulse-width (time period) measurement. Here, both microcontroller and DSO based measurement offer high resolution. For example, for 1500 r/min, the resolution of a 16-bit microcontroller is very high, i.e. $1500/2^{16}$ or 0.0225 r/min.

2.3 Realization of the Scheme for Fast Measurement of Speed

The shaft of the rotating member (dc shunt motor) is mechanically coupled to the rotor of synchro. The detailed specifications of dc shunt motor and synchro are given in appendix A.1. An adjustable dc voltage is realized by using an adjustable ac voltage source and a bridge rectifier. The field winding of the dc motor is energized by a constant dc voltage. The dc voltage of the armature winding of the motor is adjustable which is controlled by an auto transformer. Figure 2.1 shows the circuit diagram of setup for the measurement of speed. A switch (SW) is connected across the external resistance R_{ex} to change the dc voltage of the armature circuit which changes the speed of motor promptly.

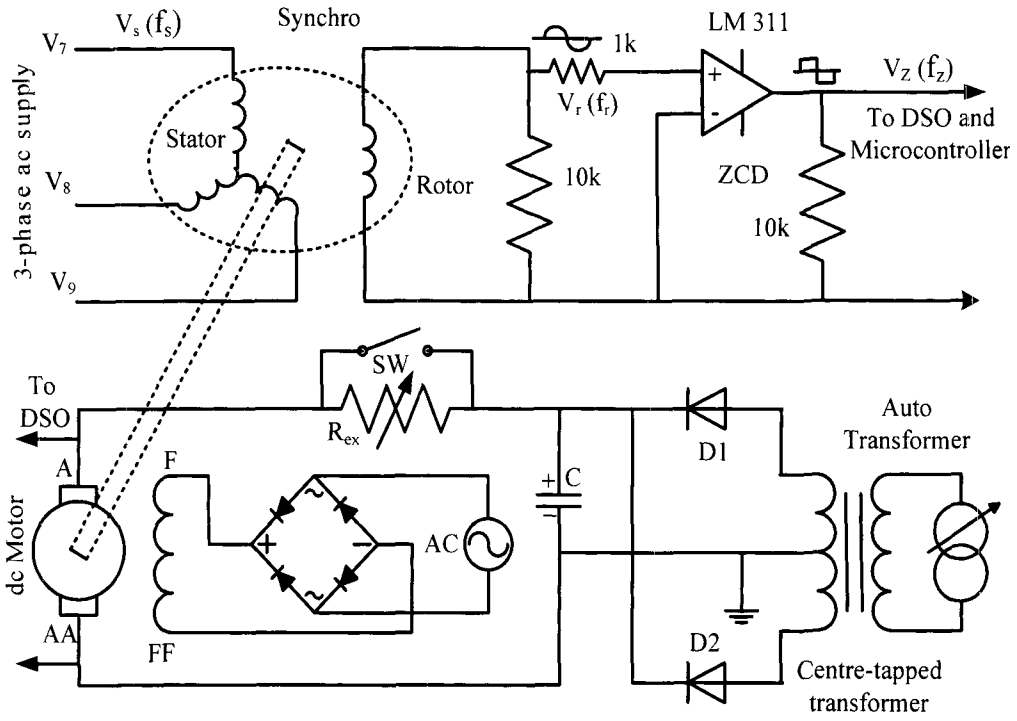

Figure 2.1 Setup for RMF based speed measurement (acceleration mode).

A sine wave signal of 400 Hz (20V peak-to-peak) from a stable arbitrary function generator (F.G) is supplied to a center-tapped transformer with two phase-split circuits (Figure 2.2). It generates two voltage waveforms as shown in Figure 2.3. The phase-split circuits are adjusted to get two signals V_2 and V_3 which lag and lead by 120° with respect to V_1. These output signals V_1, V_2 and V_3 are balanced three-phase 400 Hz voltages (Figure 2.4). These voltage signals are reduced to a value of about 100 mV (V_4, V_5 and V_6), before feeding into three buffer amplifiers (Figure 2.5). Since, the synchro requires sufficient current to generate the desired RMF. Therefore, to avoid the loading effect of the single-phase to three-phase conversion circuit, a buffer amplifier (LM 384 N) is used to amplify each voltage signal (Figure 2.2). These amplified signals (V_7, V_8 and V_9), with frequency f_s are applied to the stator winding of the synchro and marked as V_s (Figure 2.1).

As long as the synchro is standstill, it acts as a transformer and generates a sine wave with the same frequency in its rotor circuit ($f_r = f_s$) as shown in Figure

2.6. A ZCD using LM 311 of very high slew rate [95] gives a rectangular waveform V_z with the same frequency ($f_z = f_r = f_s$), as shown in Figure 2.7. A microcontroller (PIC 16F877A [96]) is used to measures the time period T_z of signal V_z which corresponds to speed and deviation in speed of the rotating member. The 16-bit digital output of microcontroller is recorded on 16-digital channels of DSO.

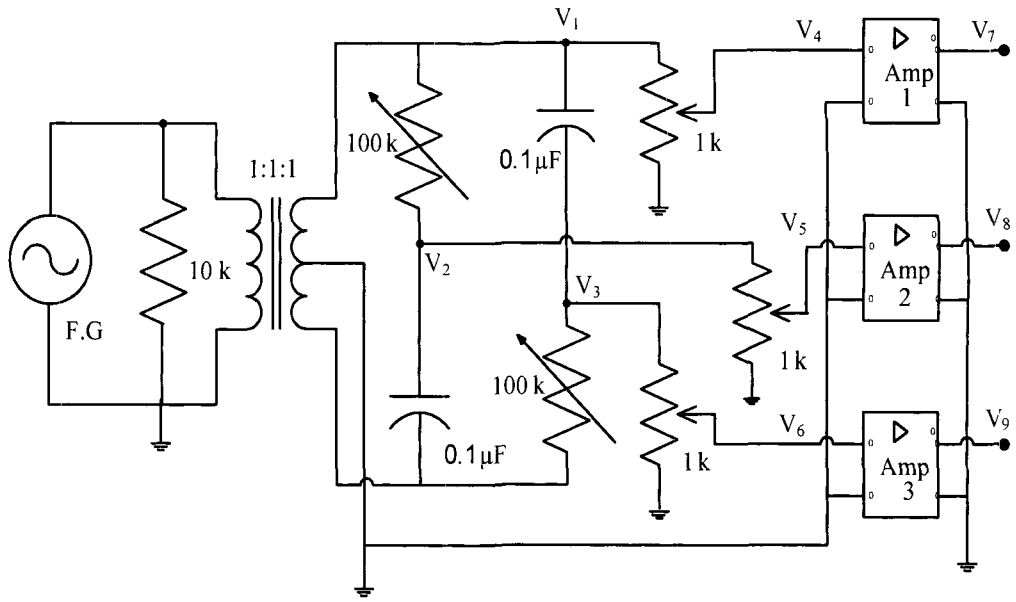

Figure 2.2 Single-phase to three-phase conversion circuit with a centre-tapped transformer and power amplifiers.

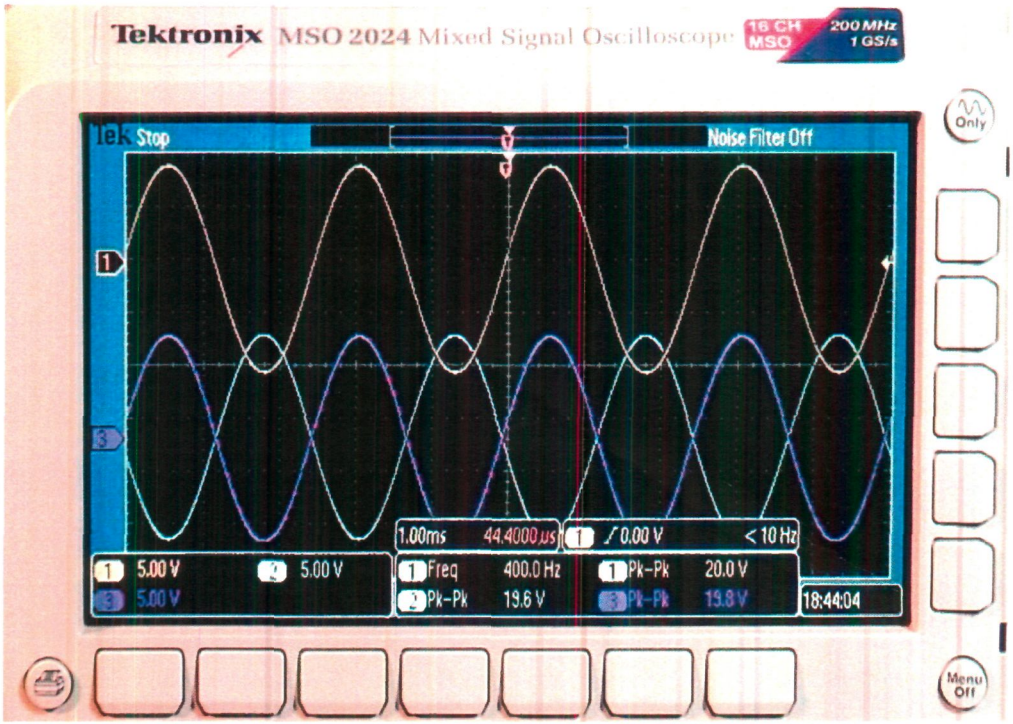

Figure 2.3 Waveforms of the input and output voltages of center-tapped transformer.

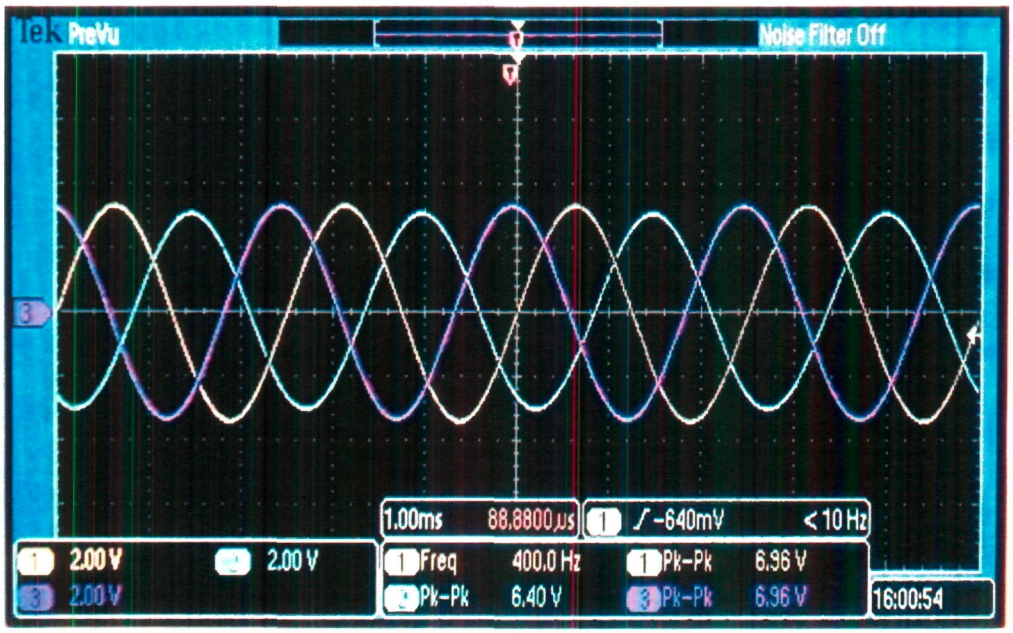

Figure 2.4 Waveforms V_1 (CH#1), V_2 (CH#2) and V_3 (Ch#3) at the output of phase-splitting circuits, respectively.

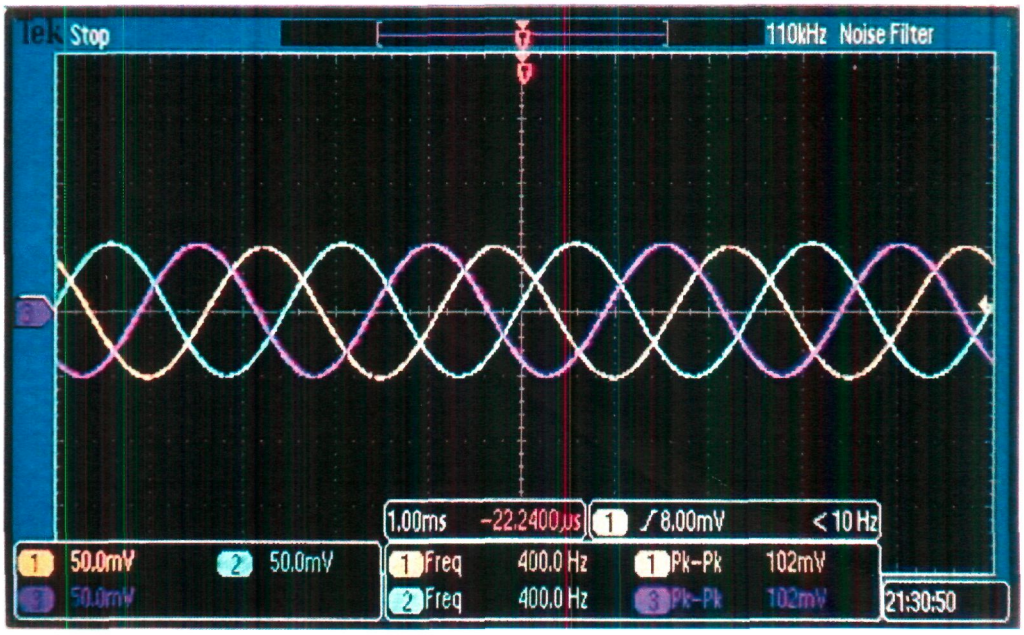

Figure 2.5 Waveforms V_4 (CH#1), V_5 (CH#2), and V_6 (Ch#3) applied at the input of power amplifiers, respectively.

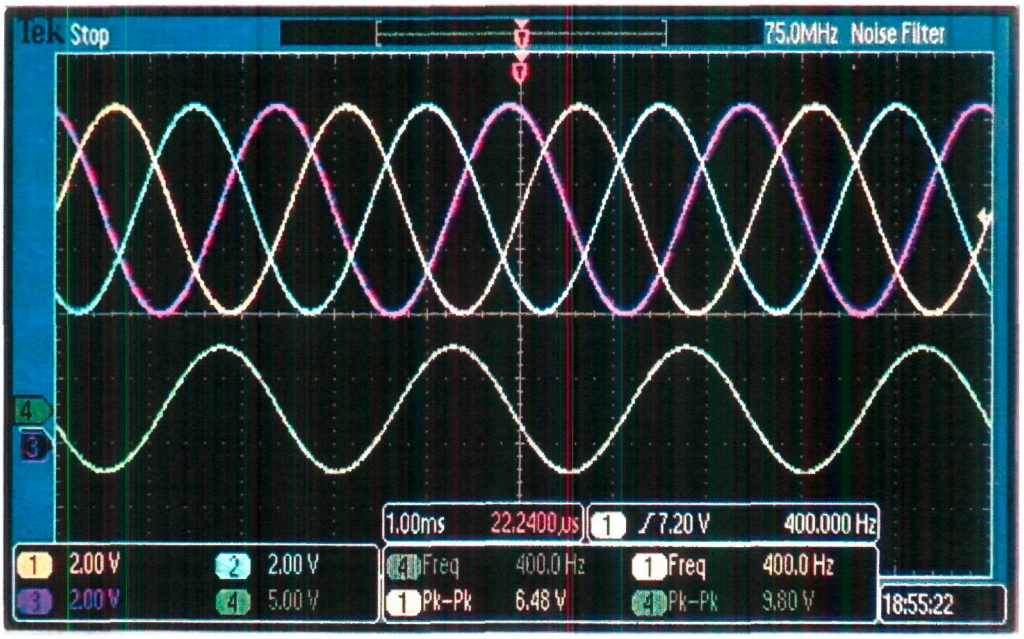

Figure 2.6 V_7 (CH#1), V_8 (CH#2), and V_9 (Ch#3) of stator winding of synchro with frequency f_s, and rotor output V_r (CH#4) with frequency f_r.

2.4 Speed Measurement

The experiments are carried out for measurement of speed and the variation of speed in acceleration as well as deceleration mode. The speed of rotating member is measured at different values within a range of 0 to 1500 r/min. For each speed of the rotating member, time period of the rotor EMF of synchro is measured using a high resolution DSO. The same time period is also measured by a microcontroller.

The accuracy of measurement is related with the stability in output frequency of function generator. Thus a high resolution arbitrary function generator (Tektronix, AFG-2022 B), is used [± 1 parts per million (ppm) ± 1μHz, 0 ^{o}C to 50 ^{o}C]. However, the output level of signal, at zero crossing point may change due to the ambient noise caused by electromagnetic interference (EMI). This problem may be solved by properly shielding the setup with low carbon steel casing having a saturation permeability of 276.81, a linear permeability of 1161.36, resistivity of 10^{-8} Ω-m and a shielding efficiency of 67.89 %. The ambient temperature variation and the electrical noise in the common wire may also cause a voltage offset in the output of ZCD and consequently, its pulse width may vary. Therefore, an instrument grade operational amplifier (LM 311) is used which is immune to noise over large extent. Hence, the circuit operates satisfactorily for the proposed instrumentation.

2.4.1 Stationary Mode

In standstill condition, the frequency f_r of signal V_r of the rotor circuit is equal to f_s (400 Hz). The ZCD produces a rectangular waveform V_z with the same frequency ($f_z = f_r$) of 400 Hz (with a time period T_z of 2.5 ms), as shown in Figure 2.7. T_z is also measured by the microcontroller to produce a 16-bit binary weighted digital output 0618H (in Hexadecimal code), as shown in the oscillographic record (Figure 2.8). The label D0 indicates the least significant bit

(LSB) and D15 shows the most significant bit (MSB) of digital output of microcontroller (Figure 2.8).

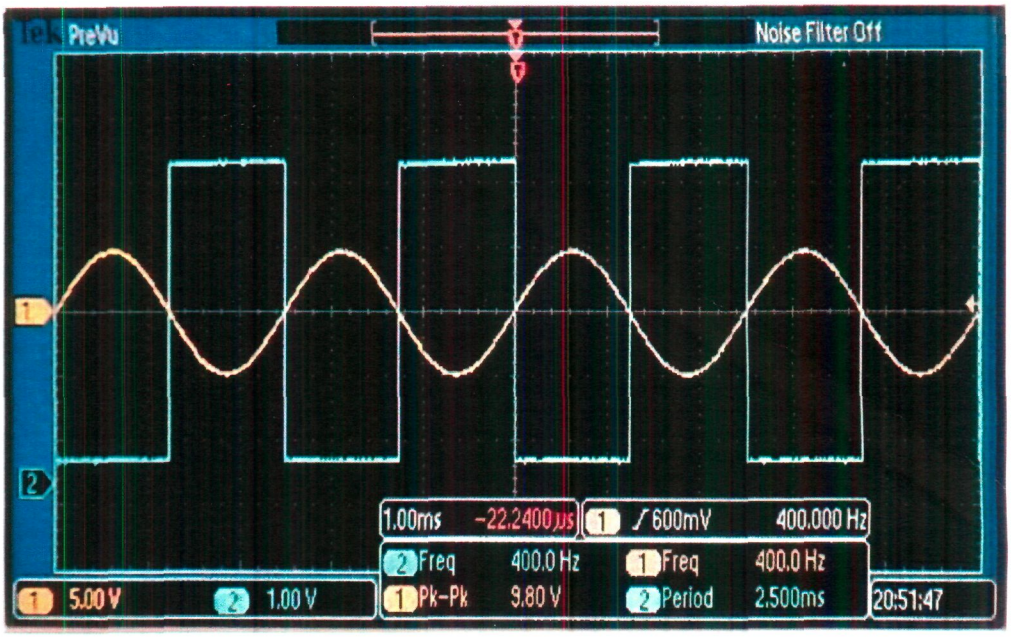

Figure 2.7 V_r (Ch#1) and V_z (Ch#2) at standstill (f_z = 400 Hz).

Figure 2.8 Output of microcontroller (0618H) on16 digital channels (D15-D0) of DSO at standstill.

2.4.2 Acceleration Mode

In acceleration mode, the dc motor (rotating member) is initially allowed to run at a particular speed. As long as the SW is open, the armature current of dc motor is limited by R_{ex} and the dc voltage across armature winding is kept at a low level of about 20 V. The time period T_z at this condition is 2.49 ms and therefore f_z = 401.61 Hz, as measured by DSO (Figure 2.9). T_z is also measured by the microcontroller, which gives a digital output 0610H corresponding to 2.49 ms (Figure 2.10). The actual speed corresponding to this time period is 96.39 r/min which is found from (2.3) as shown in Table 2.1.

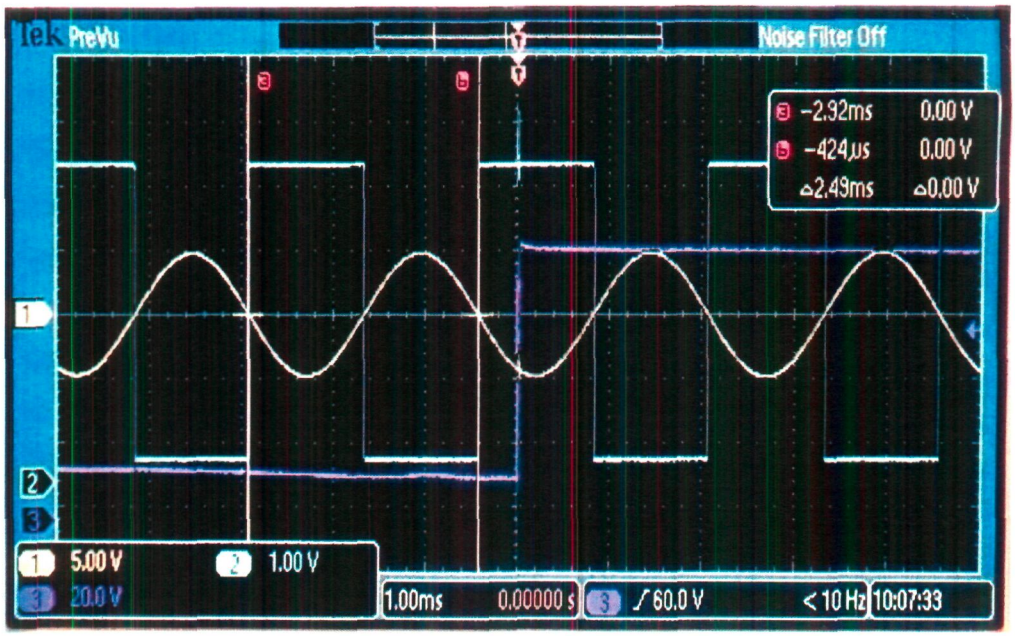

Figure 2.9 V_r (Ch#1), V_z (T_z = 2.49 ms and f_z = 401.61 Hz) at 96.39 r/min (Ch#2), when the armature voltage (Ch#3) is 20 V (acceleration mode before switching).

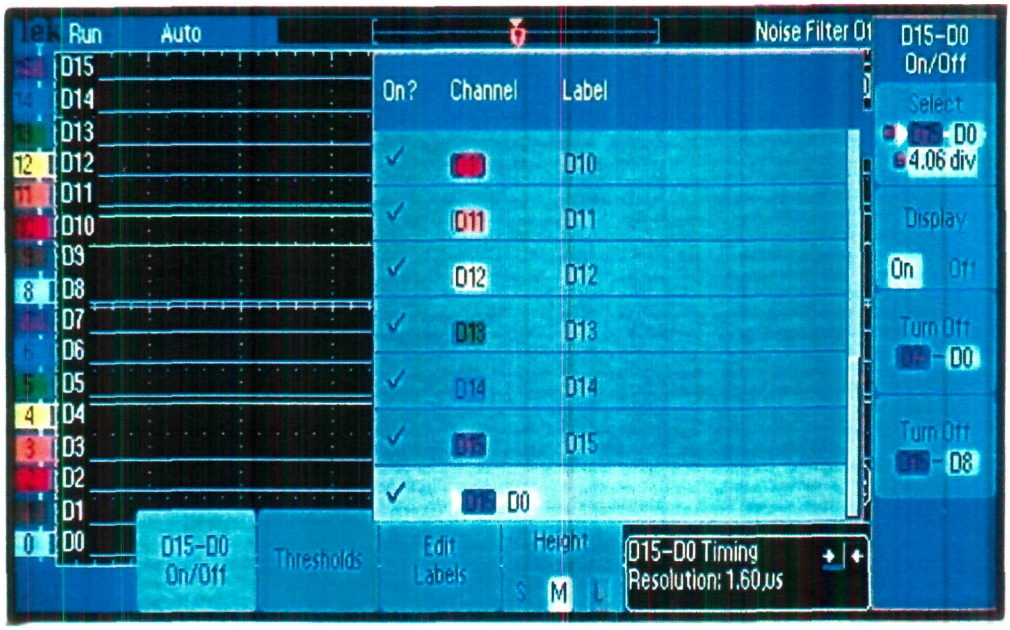

Figure 2.10 Output of microcontroller (0610H) on 16 digital channels (D15-D0) of DSO at (T_z = 2.49 ms, f_z = 401.61 Hz) 96.39 r/min, when the armature voltage is 20 V (acceleration mode before switching).

Now, the SW is closed, the voltage across armature winding shoots up to a new level of about 85 volts (Figure 2.11). This sudden increase in the speed increases f_z immediately. Hence, T_z decreases to a value of 2.47 ms (f_z = 404.86 Hz), as shown in Figure 2.11. T_z is also measured by the microcontroller (Figure 2.12) that gives a digital output 0604H corresponding to 2.47 ms. The speed corresponding to this time period is 291.6 r/min as shown in Table 2.1. It is evident from DSO records that the time period changes in the very next cycle which is measured here within a time frame of 2.5 ms (Figures 2.9 and 2.11). This is possible due to the fast movement of the RMF in the air gap around the rotor (24000 r/min) which register any change in the rotor speed quickly. For example, for a rotor speed of 100 r/min, the RMF revolves at a speed, 240 times faster than the speed of rotor. Thus, even before the completion of one revolution of the rotating member, the change in speed is exposed by the change in frequency. The DSO and the microcontroller senses the change in frequency immediately and gives the output accordingly, within 2.5 ms. Therefore, the speed measurement becomes extremely fast.

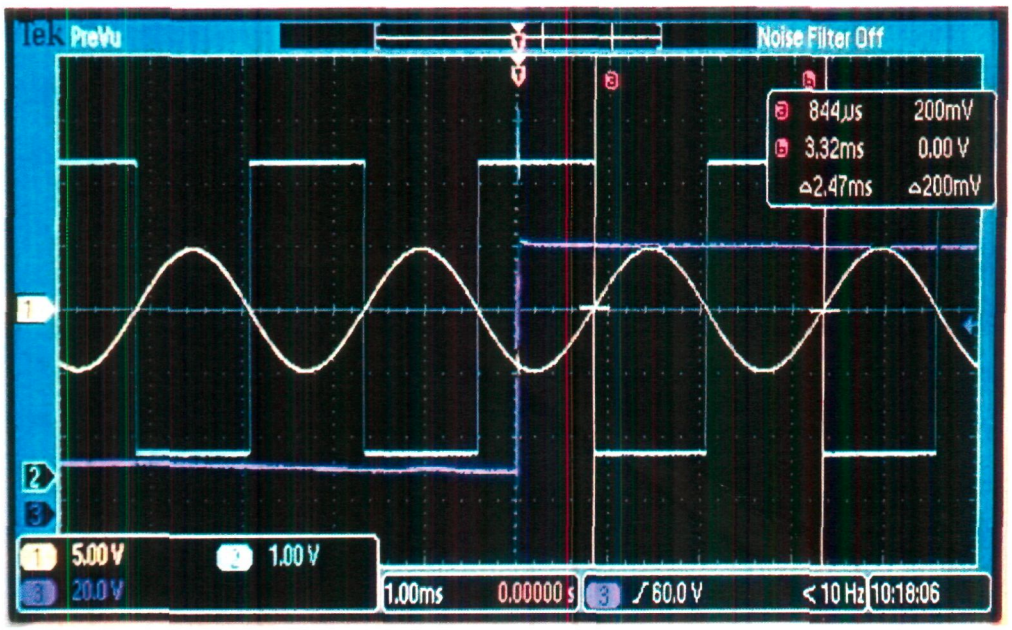

Figure 2.11 V_r (Ch#1), V_z (T_z = 2.47 ms and f_z = 404.86) at 291.6 r/min (Ch#2), when the armature voltage (Ch#3) is 85 V (acceleration mode after switching).

Figure 2.12 Output of microcontroller (0604H) on 16 digital channels (D15-D0) of DSO (T_z = 2.47 ms and f_z = 404.86 Hz) at 291.6 r/min when the armature voltage is 85 V (acceleration mode after switching).

Experiments are also carried out for different level of change in speed (in acceleration mode). The change in speed is measured in terms of time period or frequency using DSO. The microcontroller also measures the time periods which is represented in Hexadecimal code in Table 2.1. It is evident from the oscillographic records (Figures 2.13-2.24), that the change in speed is sensed in the very next cycle of signal V_z. The microcontroller generates a unique 16-bit digital output that can be used as a digital feed-back signal for controlling the speed of motor. It also gives a high resolution of the speed measurement. The chance of error is there in the measurement with DSO due to gross error (human error). However this effect is eliminated using the microcontroller which measures the pulse width accurately. For the 16-bit digital output of microcontroller and 1500 r/min dc motor, the resolution becomes $1500/2^{16}$ i.e. 0.0225 r/min.

Table 2.1: Measurement of speed in acceleration mode

S. No.	Armature voltage for different values of R_{ex} (V)		T_z measured by DSO (ms)		Related frequency $f_z = 1/T_z$ (Hz)		Actual speed from (3) (r/min)		T_z measured by microcontroller (in HEX code)		Decimal equivalent of binary weighted output	
	Before switc-hing	After switc-hing	Before switc-hing	After switc-hing	Before switc-hing	After switc-hing	Before switc-hing	After switc-hing	Before switc-hing	After switc-hing	Before switc-hing	After switc-hing
1	0	0	2.50	-	400.00	-	0	0	0618H	-	1560	-
2	20	85	2.49	2.47	401.61	404.86	96.39	291.6	0610H	0604H	1552	1540
3	70	170	2.46	2.44	406.50	409.84	390.24	590.4	05FCH	05F0H	1532	1520
4	60	140	2.45	2.41	408.16	414.94	489.60	896.4	05F8H	05E0H	1528	1504
5	100	190	2.41	2.37	414.94	421.94	896.40	1316.4	05E0H	05C4H	1504	1476

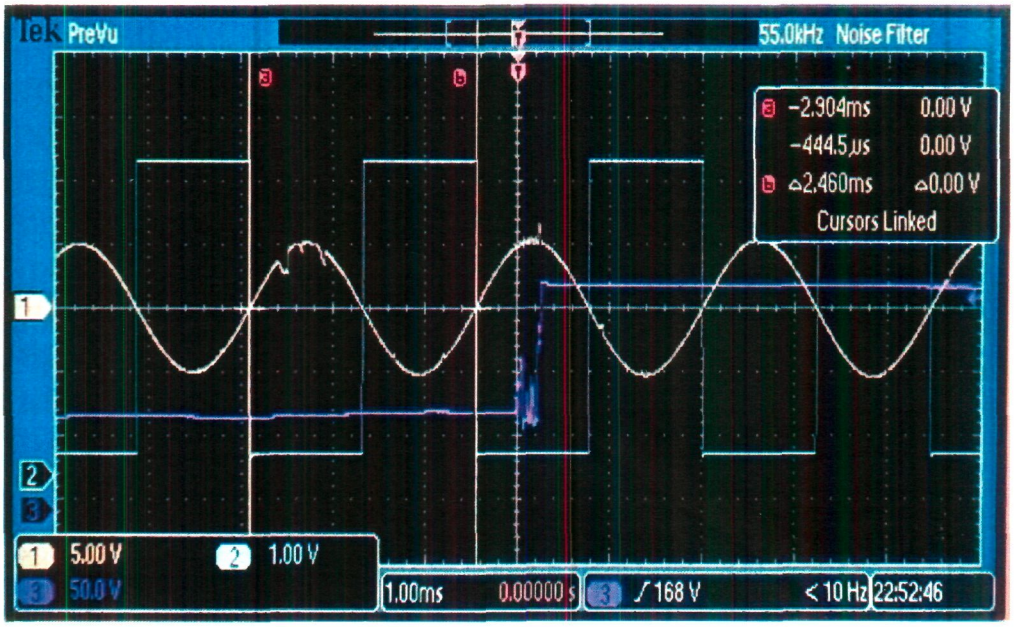

Figure 2.13 V_r (Ch#1), V_z (T_z = 2.46 ms and f_z = 406.5 Hz) at 390.24 r/min (Ch#2), when the armature voltage (Ch#3) is 70 V (acceleration mode before switching).

Figure 2.14 Output of microcontroller (05FCH) on16 digital channels (D15-D0) of DSO (T_z = 2.46 ms and f_z = 406.5 Hz) at 390.24 r/min (acceleration mode before switching).

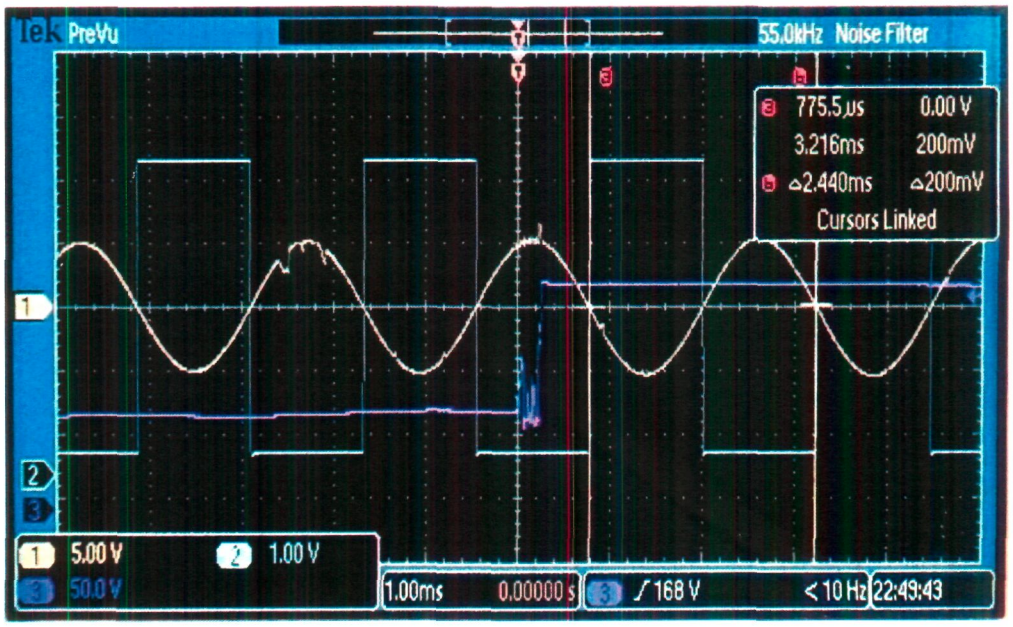

Figure 2.15 V_r (Ch#1), V_z (T_z = 2.44 ms and f_z = 409.84 Hz) at 590.4 r/min (Ch#2), when the armature voltage (Ch#3) is 170 V (acceleration mode after switching).

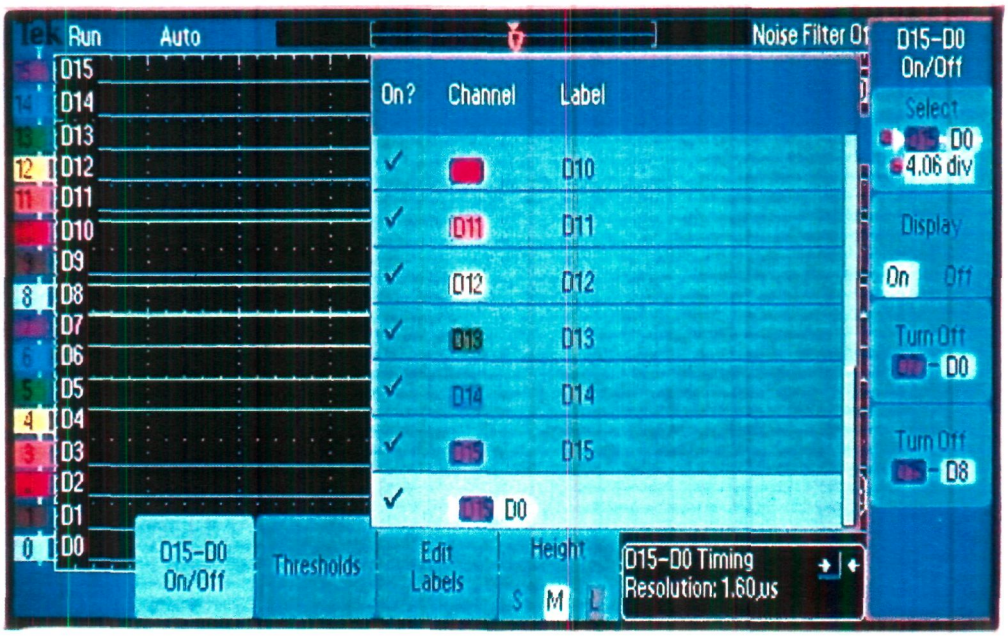

Figure 2.16 Output of microcontroller (05F0H) on 16 digital channels (D15-D0) of DSO (T_z =2.44 ms and f_z = 409.84 Hz) at 590.4 r/min (acceleration mode after switching).

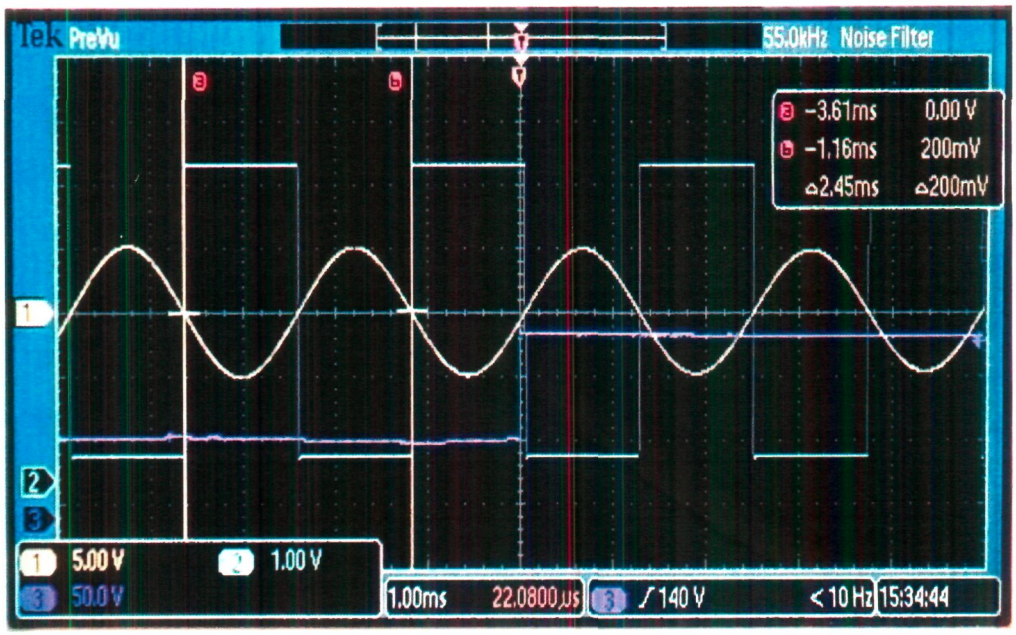

Figure 2.17 V_r (Ch#1), V_z (T_z = 2.45 ms and f_z = 408.16 Hz) at 489.6 r/min (Ch#2), when the armature voltage (Ch#3) is 60 V (acceleration mode before switching).

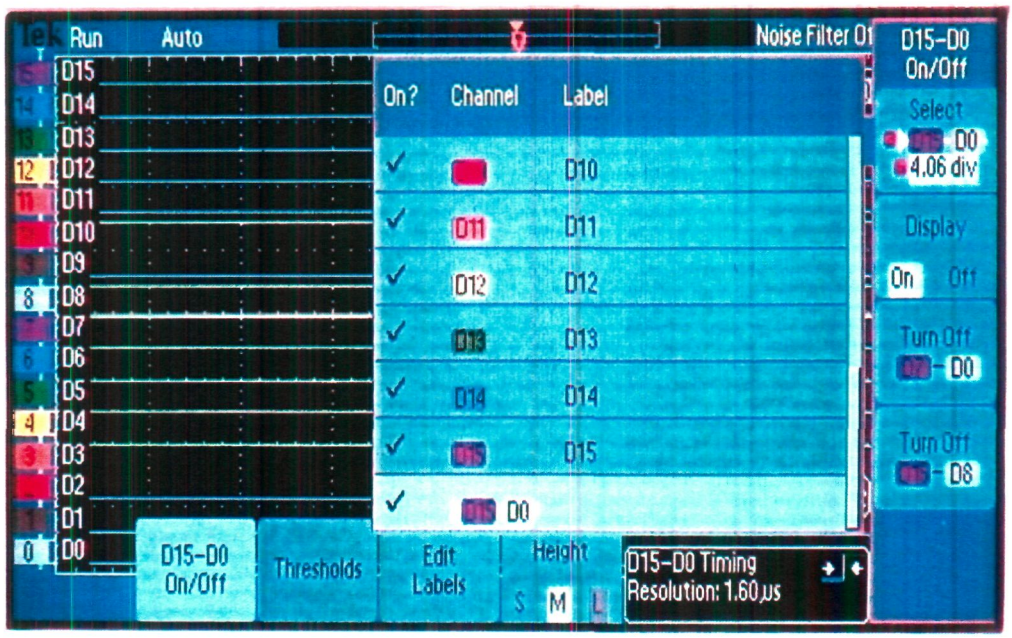

Figure 2.18 Output of microcontroller (05F8H) on 16 digital channels (D15-D0) of DSO (T_z = 2.45 ms and f_z = 408.16 Hz) at 489.6 r/min (acceleration mode before switching).

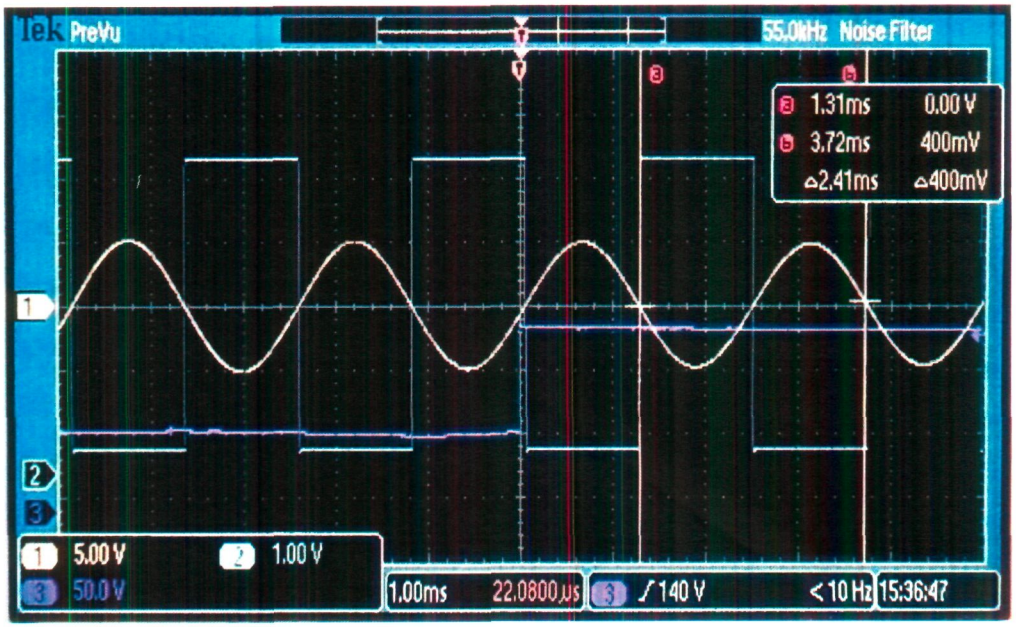

Figure 2.19 V_r (Ch#1), V_z (T_z = 2.41 ms and f_z = 414.94 Hz) at 896.4 r/min (Ch#2), when the armature voltage (Ch#3) is 140 V (acceleration mode after switching).

Figure 2.20 Output of microcontroller (05E0H) on 16 digital channels (D15-D0) of DSO (T_z = 2.41 ms and f_z = 414.94 Hz) at 896.4 r/min (acceleration mode after switching).

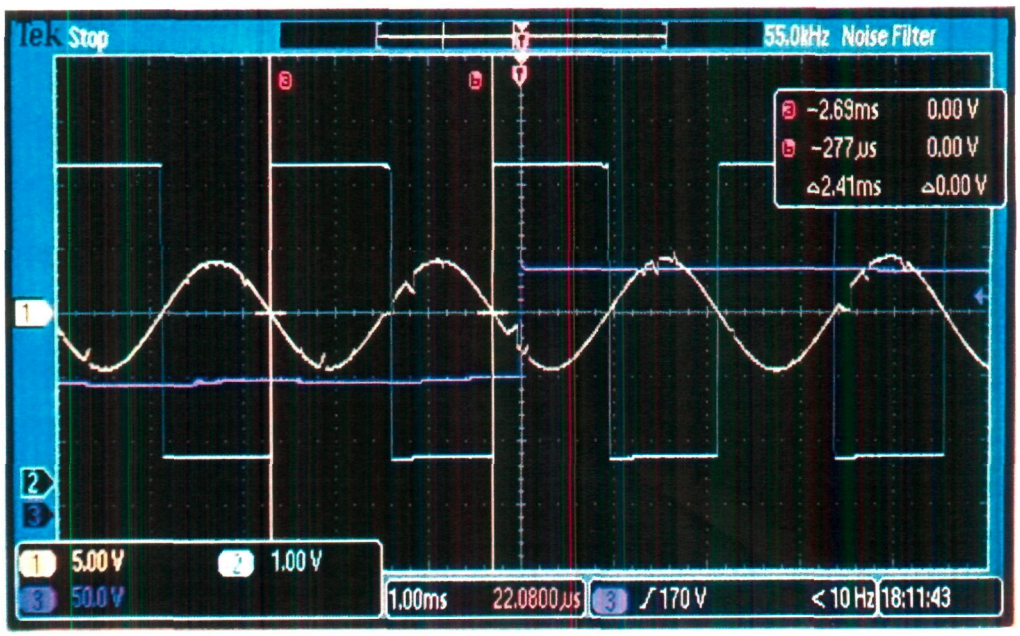

Figure 2.21 V_r (Ch#1), V_z (T_z = 2.41 ms and f_z = 414.94 Hz) at 896.4 r/min (Ch#2), when the armature voltage (Ch#3) is 100 V (acceleration mode before switching).

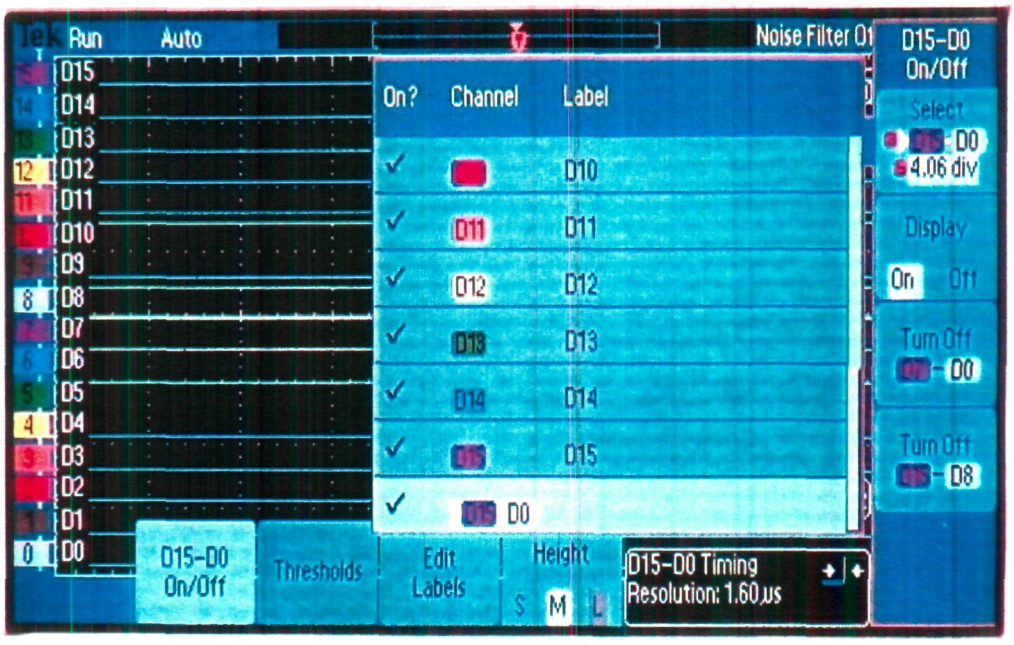

Figure 2.22 Output of microcontroller (05E0H) on 16 digital channels (D15-D0) of DSO (T_z = 2.41 ms and f_z = 414.94 Hz) at 896.4 r/min (acceleration mode before switching).

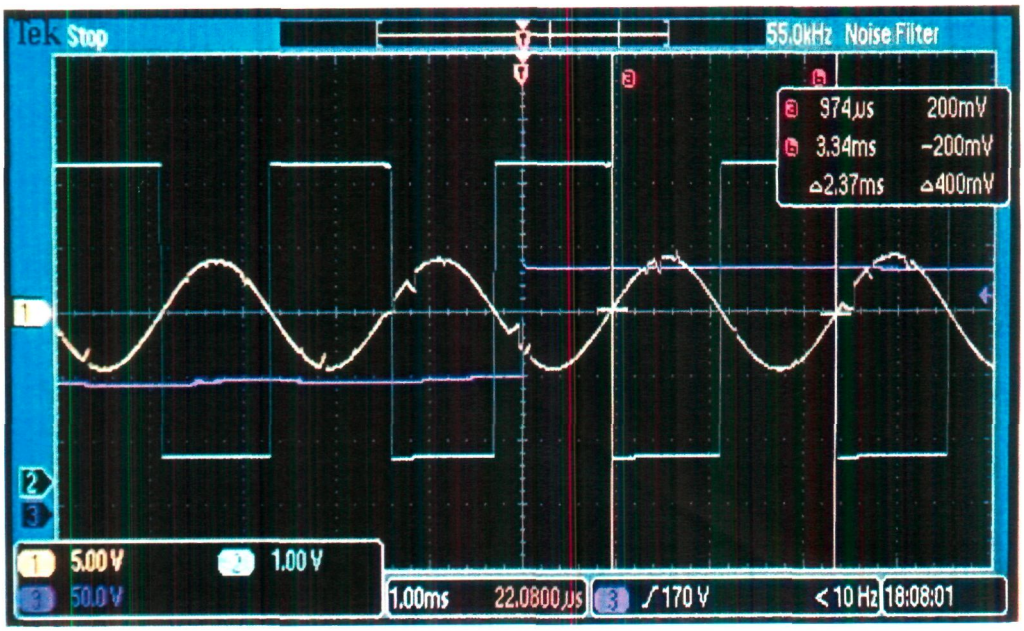

Figure 2.23 V_r (Ch#1), V_z (T_z = 2.37 ms and f_z = 421.94 Hz) at 1316.4 r/min (Ch#2), when the armature voltage (Ch#3) is 190 V (acceleration mode after switching).

Figure 2.24 Output of microcontroller (05C4H) on 16 digital channels (D15-D0) of DSO (T_z = 2.37 ms and f_z = 421.94 Hz) at 1316.4 r/min (acceleration mode after switching).

2.4.3 Deceleration Mode

For the deceleration mode, the circuit shown in Figure 2.1 is slightly modified (highlighted by **bold** lines) as shown in Figure 2.25. Initially, the SW is kept closed and the armature winding of dc motor is directly energized by a dc voltage source. The dc motor is allowed to run at an arbitrary armature voltage (40 V) and an arbitrary speed. At this speed, T_z is recorded which is 2.47 ms (f_z = 404.86 Hz) as shown in Figure 2.26. T_z is also measured by the microcontroller, which gives a digital value 0604H corresponding to 2.47 ms (Figure 2.27). According to (2.3), the speed corresponding to this time period is 291.6 r/min. To decelerate the motor, the SW is opened. The speed and f_z decrease instantly. Finally, the motor becomes standstill and T_z becomes equal to 2.50 ms (f_z = 400 Hz) as shown in Figure 2.28. T_z is also measured by the microcontroller which gives a digital output 0618H corresponding to 2.50 ms (Figure 2.29).

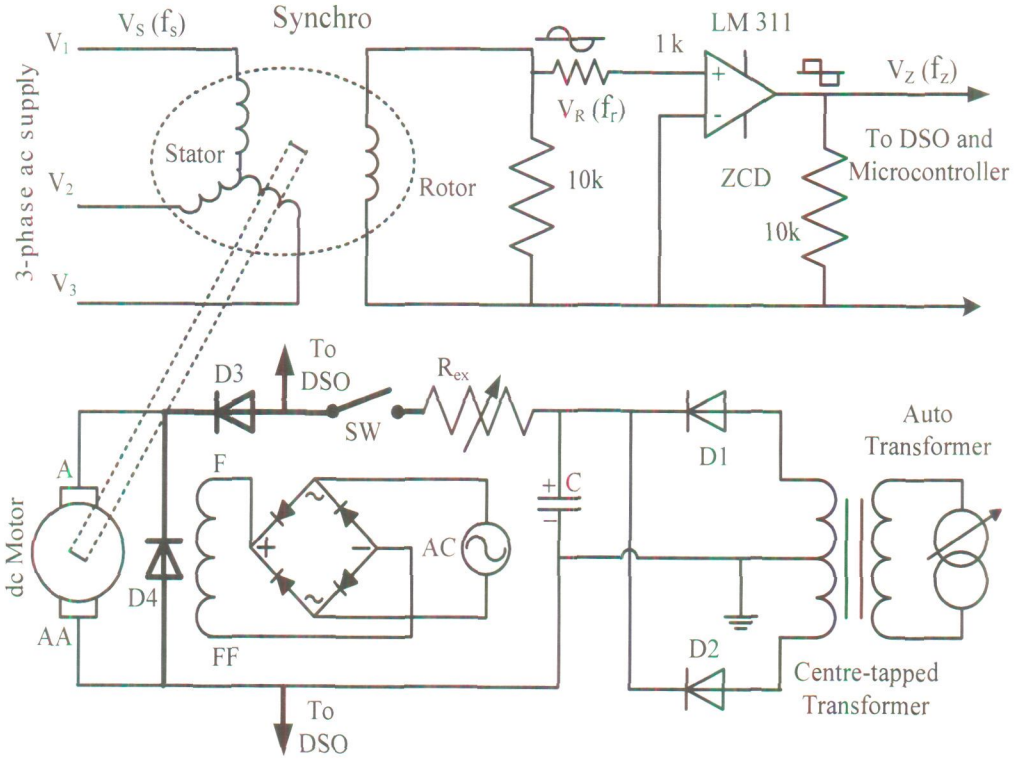

Figure 2.25 RMF based speed measurement setup in deceleration mode.

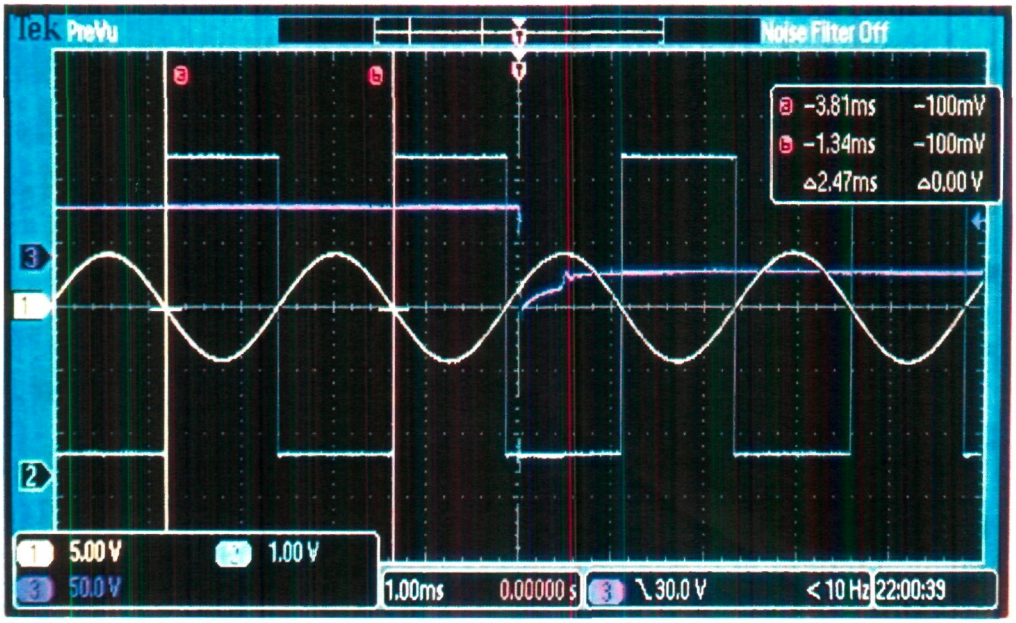

Figure 2.26 V_r (Ch#1), V_z (T_z = 2.47 ms and f_z = 404.86 Hz) at 291.6 r/min (Ch#2), and the armature voltage (Ch#3) is 40 V before switching and 0 V after switching (deceleration mode).

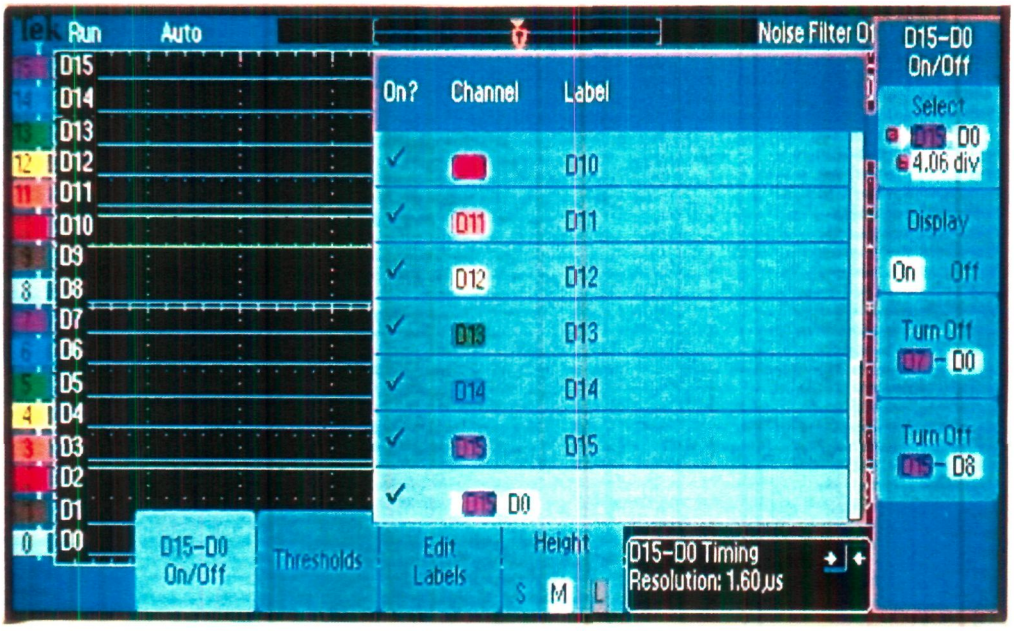

Figure 2.27 Output of microcontroller (0604H) on 16 digital channels (D15-D0) of DSO (T_z = 2.47 ms and f_z = 404.86 Hz) at 291.6 r/min before switching (deceleration mode).

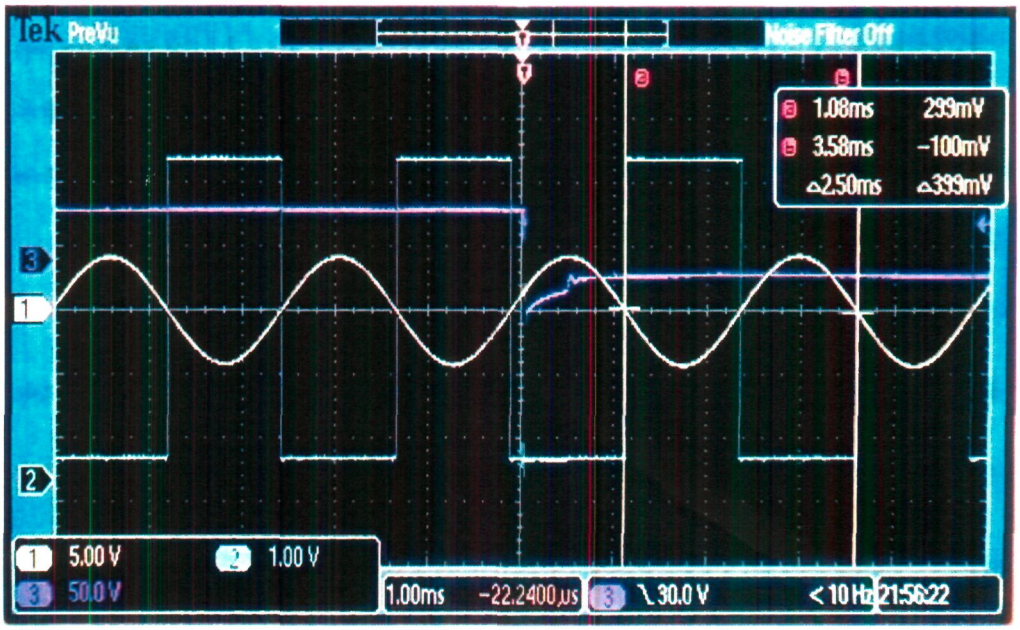

Figure 2.28 V_r (Ch#1), V_z (T_z = 2.5 ms and f_z = 400 Hz) at 0 r/min (Ch#2), when armature voltage (Ch#3) becomes zero after switching (deceleration mode).

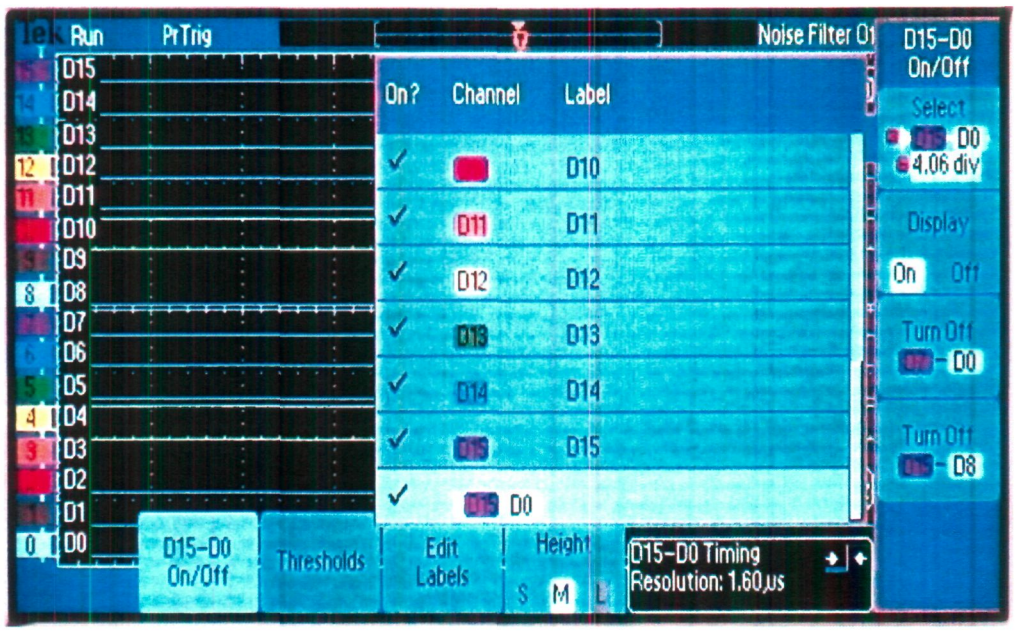

Figure 2.29 Output of microcontroller (0618H) on 16 digital channels (D15-D0) of DSO (T_z = 2.5 ms and f_z = 400 Hz) at 0 r/min after switching (deceleration mode).

The program of microcontroller for the fast measurement of T_z is given in Appendix A.2 and the flow chart of program is described as follows.

1. PIC 16F877A, an 8 bit microcontroller from Microchip is used for the measurement of time period of the square wave signal from ZCD.
2. OPTION_REG register is initialized for RB0 interrupt for every rising edge on the RB0 pin of port B.
3. Output is a 16 bit digital signal. Since all I/O ports are 8 bits, Port C and Port D are made output ports.
4. Enable the Global Interrupt Enable bit (**GIE**) and RB0/INT External Interrupt Enable bit (**INTE**). RB0/INT External Interrupt Flag bit (**INTF**) is cleared for RB0 interrupt to occur. All these bits are in INTCON register.
5. Pause till interrupt occurs.
6. When an interrupt occurs, check whether the interrupt is due to RB0, by checking the status of INTF bit of INTCON register.
7. For RB0 interrupt, move the value of TMR1L to PORTC and move the value of TMR1H to PORTD.
8. Initialize the TIMER1 in T1CON register.
9. Start the TIMER1.
10. Return from the interrupt routine.

2.4.5 Comparison with Time Response of Tachogenerator

The results of the proposed method are also compared with the response of a dc tachogenerator which generates 24.3 mV per r/min (Appendix A.2). Figures [2.31(a)-(d)] show the variation in time response of tachogenerator in acceleration mode for different speed. It is evident that the response of dc tachogenerator is slow and it takes sufficiently large time to show the change in speed. It is due to spikes at commutator segments which are low at lower speed [Figures 2.31 (a)-(b)] and becomes high at higher speed [Figures 2.31 (c)-(d)]. A significant variation in the output voltage of dc tachogenerator [Figure 2.31 (a)] is not

available unless armature moves to the next position of commutator segment. For example, in this case, the initial speed before switching is 96.39 r/min. Thus,

the time for one revolution = 60/96.39 = 0.62247 s

the time to pass (past) one commutator segment = 0.62247/12 = 51.8726 ms

Therefore at this speed, the maximum resolution of the measurement (time period) is 51.8726 ms for this dc tachogenerator. However, the proposed measurement system senses the change in speed immediately and gives the response accordingly within 2.5 ms. The response time of measurement is found by DSO records (Figures 2.9 and 2.11) for the proposed method and for the dc tachogenerator (Figures 2.31 and 2.32) which are tabulated in Table 2.2. Moreover, a significant amount of noise is present in the output dc voltage of tachogenerator which is evident from Figures 2.31 and 2.32. A smoothening filter is therefore required at the output which would further increase the delay in its response time. The rubber coupling between tachogenerator and motor may also cause the delay in response time. The complete setup of the measurement system is shown in Figure 2.33.

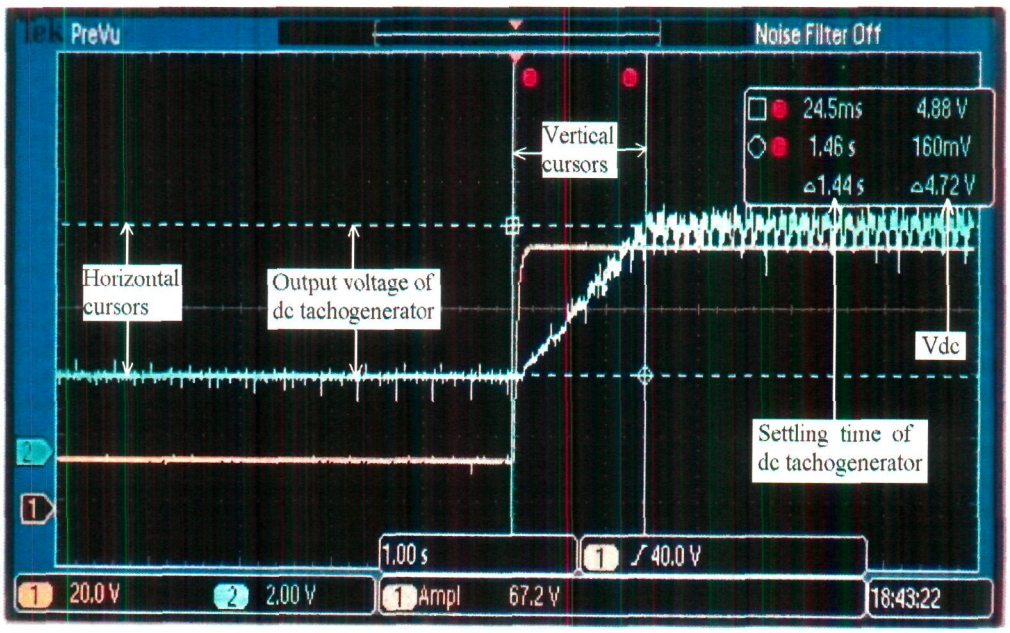

(a)

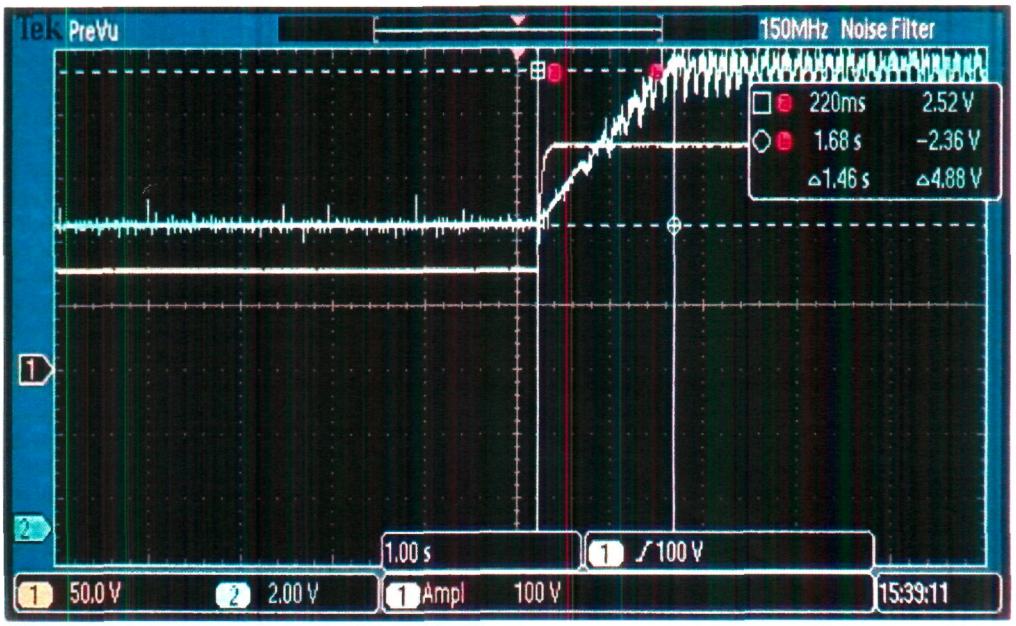
Tek PreVu
150MHz Noise Filter
220ms 2.52 V
1.68 s -2.36 V
Δ1.46 s Δ4.88 V
1.00 s
1 ⨍ 100 V
1 50.0 V
2 2.00 V
1 Ampl 100 V
15:33:11

(b)


Tek PreVu
150MHz Noise Filter
-84.5ms 9.86 V
2.76 s 60.0mV
Δ2.84 s Δ9.80 V
2.00 s
1 ⨍ 100 V
1 50.0 V
2 5.00 V
1 Ampl 80.0 V
14:38:18

(c)

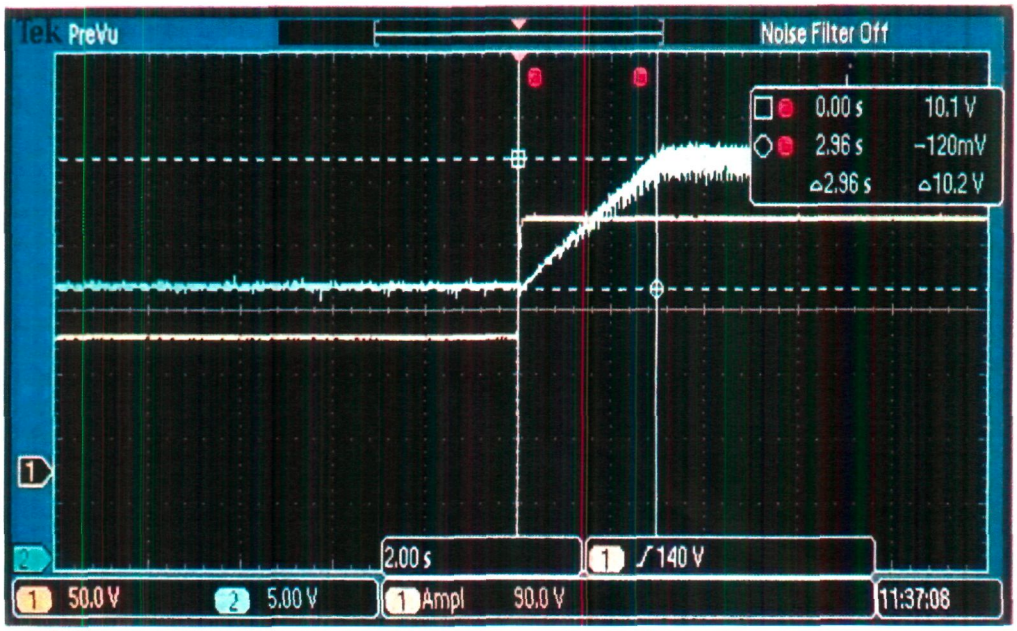

(d)

Figures 2.31 (a)-(d) Step change in input dc voltage (Ch#1), and time response of tachogenerator (Ch#2) for different variation in speed (acceleration mode).

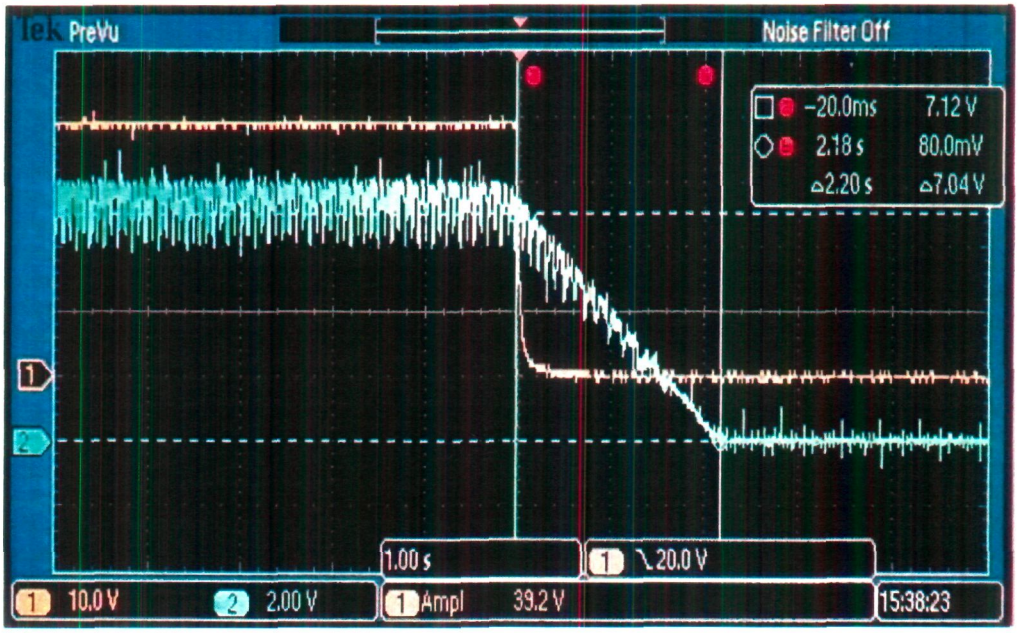

Figure 2.32 Step change in input dc voltage (Ch#1) and time response of tachogenerator (Ch#2) for variation in speed (deceleration mode).

Table 2.2 Time response of proposed method and dc tachogenerator in acceleration mode and deceleration mode

S. No.	T_z measured by DSO (ms)		Related frequency $f_z = 1/T_z$ (Hz)		Actual speed [from (3)] (r/min)		Speed variation (r/min)	Output of dc tachogenerator			Response time	
	Before switching	After switching	Before switching	After switching	Before switching (S1)	After switching (S2)	(S2 – S1)	Output dc voltage (V_{dc})	Speed variation V_{dc} /0.0243 (r/min)	Settling time (s)	Proposed Scheme (ms)	Dc Tachogenerator (ms)
1	2.49	2.47	401.61	404.86	96.39	291.60	195.21	4.72	194.24	1.44	2.5	100
2	2.46	2.44	406.50	409.84	390.00	590.40	200.40	4.88	200.82	1.46	2.5	120
3	2.45	2.41	408.16	414.94	489.60	896.40	406.80	9.80	403.29	2.84	2.5	150
4	2.41	2.37	414.94	421.94	896.40	1316.40	420.00	10.20	419.75	2.96	2.5	200
5	2.47	2.50	404.86	400.00	291.60	0	291.60	7.04	289.71	2.20	2.5	80

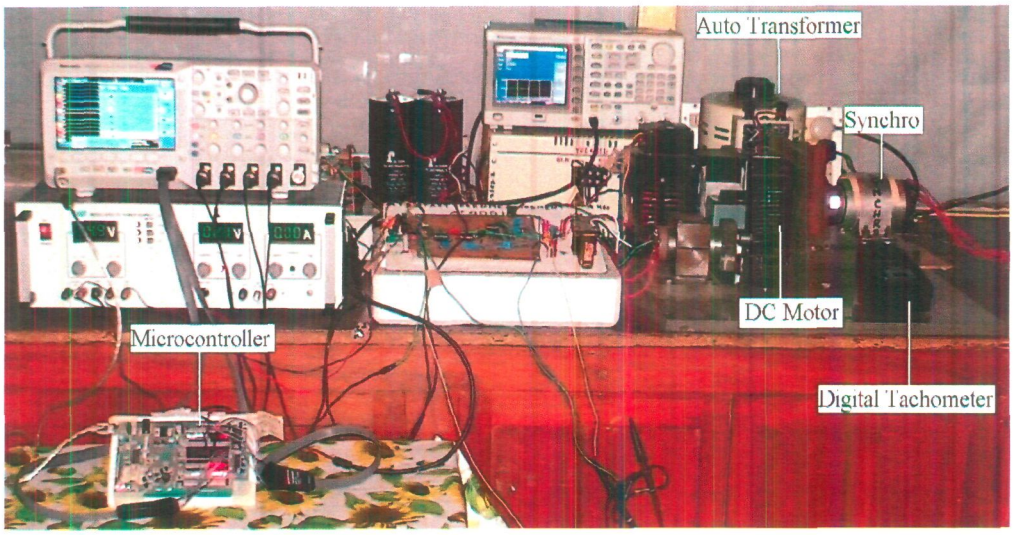

Figure 2.33 The complete setup of the measurement system.

2.5 Conclusion

In this chapter, a novel contact type RMF based measurement technique is proposed which provides fast measurement of speed and deviation in speed while retaining high accuracy. The change in speed, changes the frequency of induced EMF in the rotor circuit of synchro instantly which is monitored by the change in pulse width corresponding to the time period. As the RMF rotates at a high speed (24000 r/min) for an input voltage frequency of 400 Hz, the measurement of speed and the deviation in speed are sensed in the very next cycle of the induced EMF (within 2.5 ms). In comparison to a dc tachogenerator, the time response of proposed method is very fast and the measurement is more accurate which is directly related to the frequency of rotor EMF of synchro. A microcontroller is also used for the measurement of speed and the variation in speed to give a 16-bit digital output, which also confirms the accuracy and the fast response of proposed method. The digital output of the microcontroller can be used as a feedback signal for controlling the speed and deviation in speed accurately. For fast speed motors, the resolution may be increased to a very high value by utilizing 32-bit digital output signal of microcontroller or by increasing the frequency of the input voltage which generates the RMF. However, practically the frequency of the input

ac voltage and current which produces RMF is restricted by the magnetic material of the synchro. For example, a synchro made of silicon steel can be used up to 400 Hz effectively. The high accuracy of measurement of the proposed technique is also successfully applied for calibration of different contact type and non-contact type tachometers and described in the following chapter.

Chapter 3

Calibration of Tachometers

3.1 Introduction

Fast and accurate method is also required for the calibration of tachometers. Different types of tachometers which include contact type, non-contact type, and both analog and digital tachometers are being used for speed measurement in the industries as well as laboratories. The calibration of a tachometer refers to comparing its readings (speed) with a more accurate (standard) speed measuring instrument whose accuracy should be at least four times better than the tachometer being calibrated [52]-[53]. The tachometers are manufactured by physical materials and they are used in the real world of humidity, heat, physical stress, noise and vibrations etc., hence their performance gets affected and deteriorates. Moreover the magnetic field strength of a dc tachometer as well as tachogenerator decreases due to aging effect. Therefore for accurate speed measurement and feedback control applications, a regular calibration of these devices is necessary according to manufacturer's specifications. The main benefits of a calibrated tachometer include uniformity between measurements, assurance of measurement accuracy, and reduction in measurement errors.

Usually, instead of providing the error curve for the whole speed range, the manufacturers of tachometers supply the data of Absolute Error or Guarantee Error for a range of speed. For an analog tachometer which is calibrated by the

proposed method, the Maximum Point-Error provided by the manufacturer at different speed is given as [60]

Speed of Tachometer #1	**Point error**
300 r/min	± 3 r/min
600 r/min	± 6 r/min
900 r/min	± 9 r/min
1500 r/min	± 10 r/min
3000 r/min	± 15 r/min
4500 r/min	± 23 r/min

The data does not tell anything about the error in between two given speeds. Similarly, the error of a digital non-contact tachometer is specified by the manufacturer as [62]

Speed of Tachometer #2	**Point error**
5 – 500 r/min	± 1 r/min
1000 r/min	± 5 r/min
20002 r/min	± 10 r/min
40004 r/min	± 20 r/min
80008 r/min	± 40 r/min

This does not indicate the actual error of measurement for the speed between specified ranges. The accuracy of measurement is also specified by the manufacturer's Guarantee Error in terms of percentage of full scale reading (FSR) for the entire range of speed. Hence, the absolute error remains same for the whole range of measurement. Consequently, at lower range, the percentage of error becomes significantly high. For a digital contact type tachometer with 5 digit display, the error at the maximum speed of 10000 r/min is 6 r/min (± 0.05 % + 1digit) [61]. However, for a lower speed of 10 r/min, the error (± 6 r/min)

becomes 60 %. Hence, it becomes necessary to calibrate the tachometer for the whole range to obtain the accuracy of measurement at any desired speed.

In this chapter, the proposed scheme (Figure 2.25) is used for the calibration of tachometers. For calibration of tachometers, the measurement is based on the fundamental principle of electromagnetic theory where the frequency of the induced EMF in the rotor circuit of synchro is directly proportional to the speed of rotating member [94]. Therefore, the proposed method of measurement can be used for the calibration of tachometers. Three different types of tachometers (an analog/mechanical type, a digital non-contact type, and a digital contact type) are calibrated with the proposed scheme. The detailed specifications of these tachometers are given in Appendix A.3. The calibration curves are also drawn for lower and higher speed ranges. The results of calibration are compared with the data specification sheets of these tachometers.

3.2 Realization of Scheme for the Calibration of Tachometers

It is evident from the equation (2.3), as discussed in chapter 2, that there is a unique output frequency for a particular speed of rotor of synchro or the rotating member. Therefore, for the calibration of tachometers, for a particular speed n_r, the exact frequency f_r ($f_r = f_z$) of signal V_r is found using (2.3). Thereby, the actual time period ($T_z = 1/f_z$), is calculated for this speed (actual value). The rotating member (dc motor) is allowed to run and its speed is controlled by varying the voltage across the armature winding using the external resistance R_{ex} (Figure 2.25). For 100 r/min, the exact time period is 2.4896 ms according to (2.3). Now, by varying the speed of the dc motor, T_z is set accurately, equal to the exact time period i.e. 2.4896 ms. Thus, the speed of the dc motor becomes exactly equal to 100 r/min. The waveform at this condition is recorded by DSO and shown in Figure 3.1 (b).

Although the measurement technique is simple which is based on fundamental principle of frequency measurement. However, a negligible amount

of error may be introduced in the measurement due to a slight deviation in the frequency of signal generator and due to the measurement error of DSO. Here, a very high resolution, arbitrary function generator (Tektronix, AFG-2022 B) is used with an error of ± 1ppm, ± 1μHz at 0 to 50 °C [97]. Likewise, the DSO used (LeCroy, MSO-10MXs-B4), has the sampling rate of 10 GS/s with an update rate up to 22000 waveforms/s [98]. Moreover, the DSO has a very high resolution and measures T_z accurately up to nine decimal places [Figures 3.1 (a)-(e)]. At higher speed, the high frequency noise signals, superimposed over V_r, introduce error in the measurement of T_z. These noise signals are removed from V_r using a low pass filter (π filter) with a cut-off frequency of 478 Hz [$f_c = 1/(2\pi RC)$, R = 3.33 kΩ, C = 0.1 μF]. It is also evident from figure 2.15, 2.21, 2.23 and 3.1 (e) that the measurement of output voltage of synchro is unaffected even in the presence of noise and spikes over large extent due to square wave shape of the output voltage of ZCD. As all the measurements are done with the output signal of ZCD instead of the ac output of synchro, hence, V_z and the measurement of T_z remain unaffected.

Three different types of tachometers (an analog/mechanical type, a digital non-contact type, and a digital contact type) are calibrated with the proposed method. The experiment is carried out for different speed of dc motor [Figures 3.1 (a)-(e)]. The readings of these three tachometers deviate from the actual speed as shown in Table 3.1 and the errors are shown in Figure 3.2. The percentage errors shown in Fig. 3.2 are calculated using basic relationship [22], [53].

$$\text{Percentage Error} = [(\text{Observed speed} - \text{Actual speed})/\text{Actual speed}] \times 100$$

where, the actual speed is the measured speed by proposed method and the observed speed is the measured speed by tachometers #1, #2, and #3 respectively.

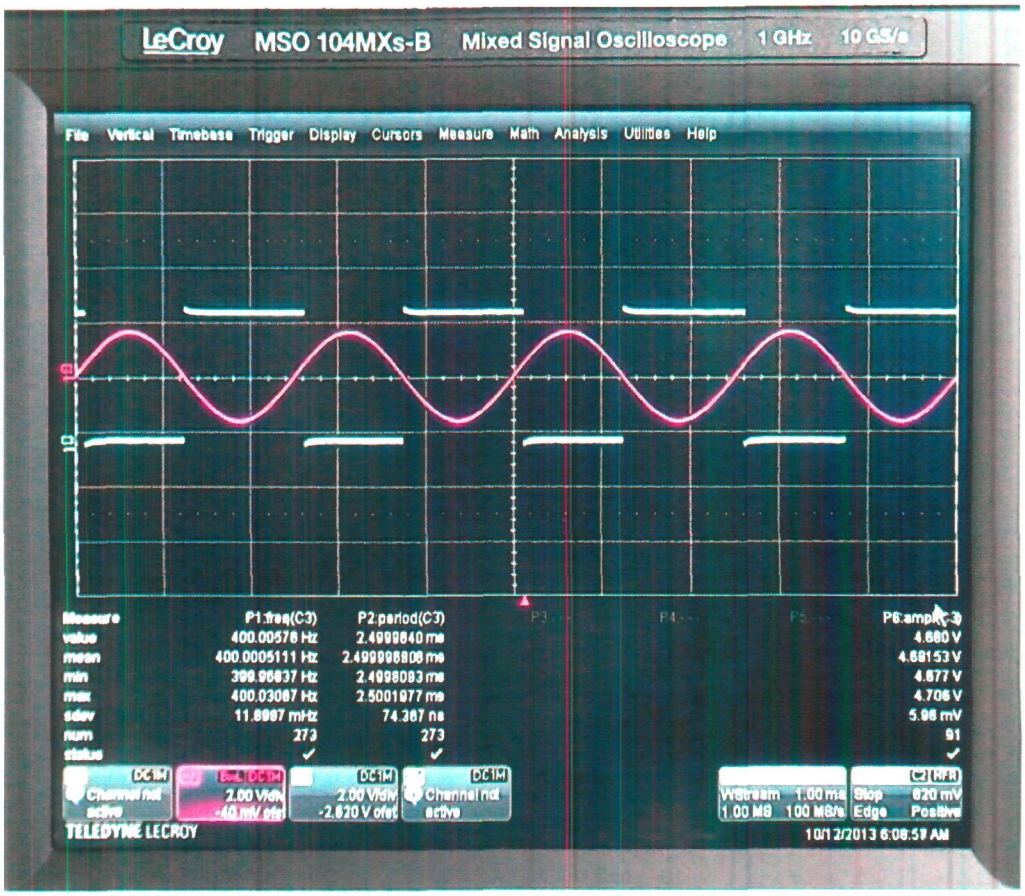
LeCroy MSO 104MXs-B Mixed Signal Oscilloscope 1 GHz 10 GS/s
File Vertical Timebase Trigger Display Cursors Measure Math Analysis Utilities Help
Measure P1:freq(C3) P2:period(C3) P6:ampl(C3)
value 400.00578 Hz 2.4999640 ms 4.680 V
mean 400.0005111 Hz 2.499998808 ms 4.68153 V
min 399.96837 Hz 2.4998083 ms 4.677 V
max 400.03087 Hz 2.5001977 ms 4.706 V
sdev 11.8987 mHz 74.367 ns 5.98 mV
num 273 273 91
status ✓ ✓ ✓
DC1M 2.00 V/div -40 mV ofst
DC1M 2.00 V/div -2.620 V ofst
DC1M Channel not active
Wavestream 1.00 ms/div 1.00 MS 100 MS/s
Stop 620 mV Edge Positive
TELEDYNE LECROY
10/12/2013 6:08:57 AM

(a)

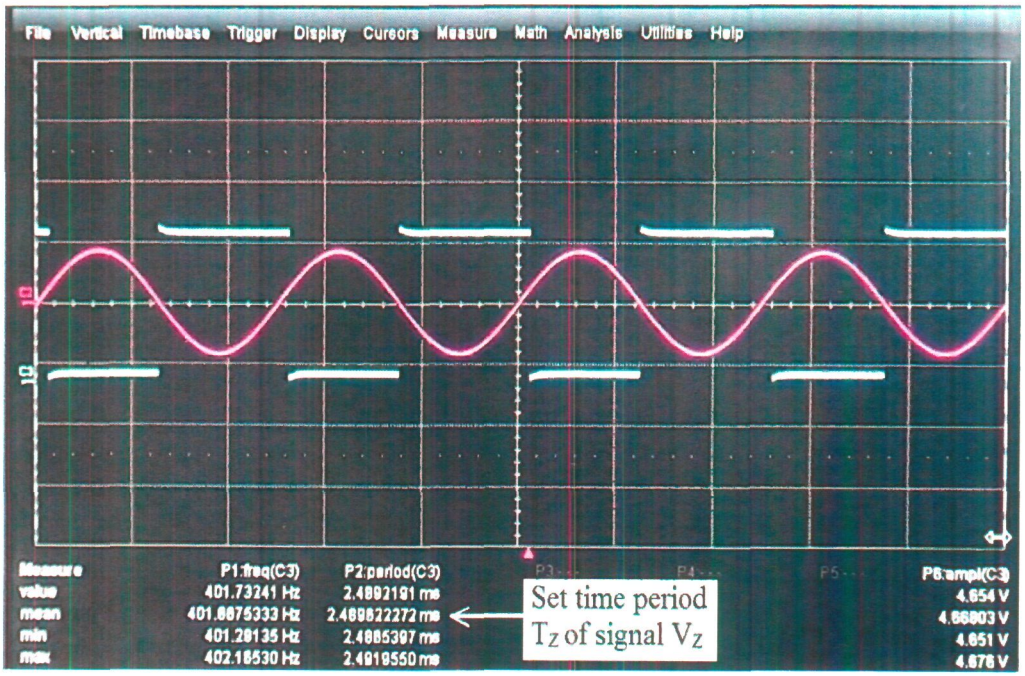
File Vertical Timebase Trigger Display Cursors Measure Math Analysis Utilities Help
Measure P1:freq(C3) P2:period(C3) P6:ampl(C3)
value 401.73241 Hz 2.4892191 ms 4.654 V
mean 401.8875333 Hz 2.489822272 ms 4.66903 V
min 401.28135 Hz 2.4865397 ms 4.651 V
max 402.18530 Hz 2.4919550 ms 4.676 V
Set time period
Tz of signal Vz

(b)

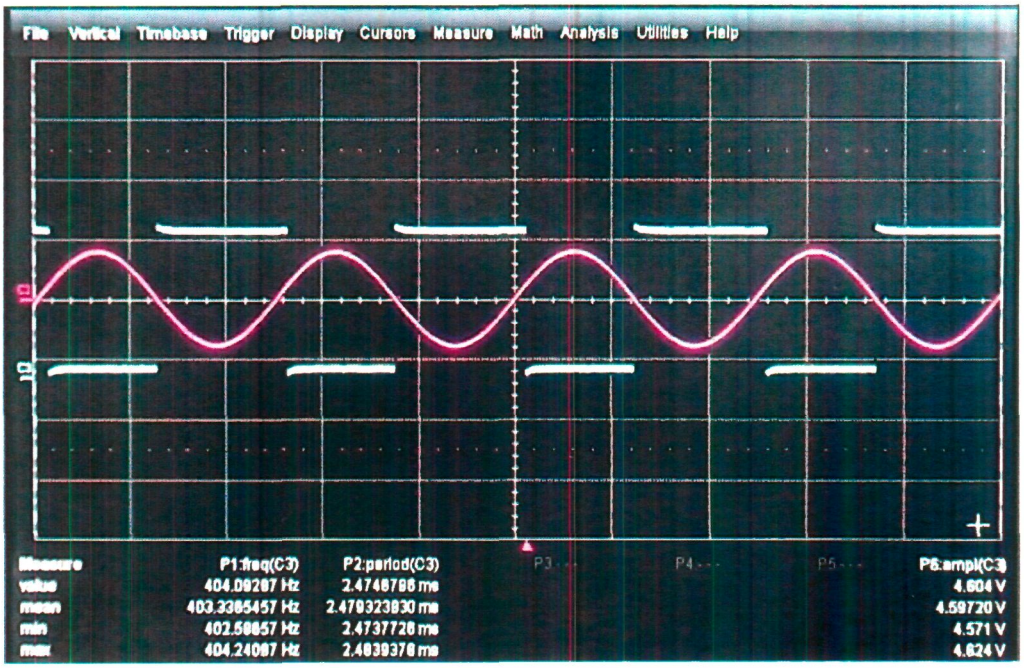
File Vertical Timebase Trigger Display Cursors Measure Math Analysis Utilities Help
C3
Measure P1:freq(C3) P2:period(C3) P3 P4 P5 P6:ampl(C3)
value 404.09287 Hz 2.4746766 ms 4.604 V
mean 403.3385457 Hz 2.479323830 ms 4.59720 V
min 402.58657 Hz 2.4737726 ms 4.571 V
max 404.24087 Hz 2.4839376 ms 4.624 V

(c)

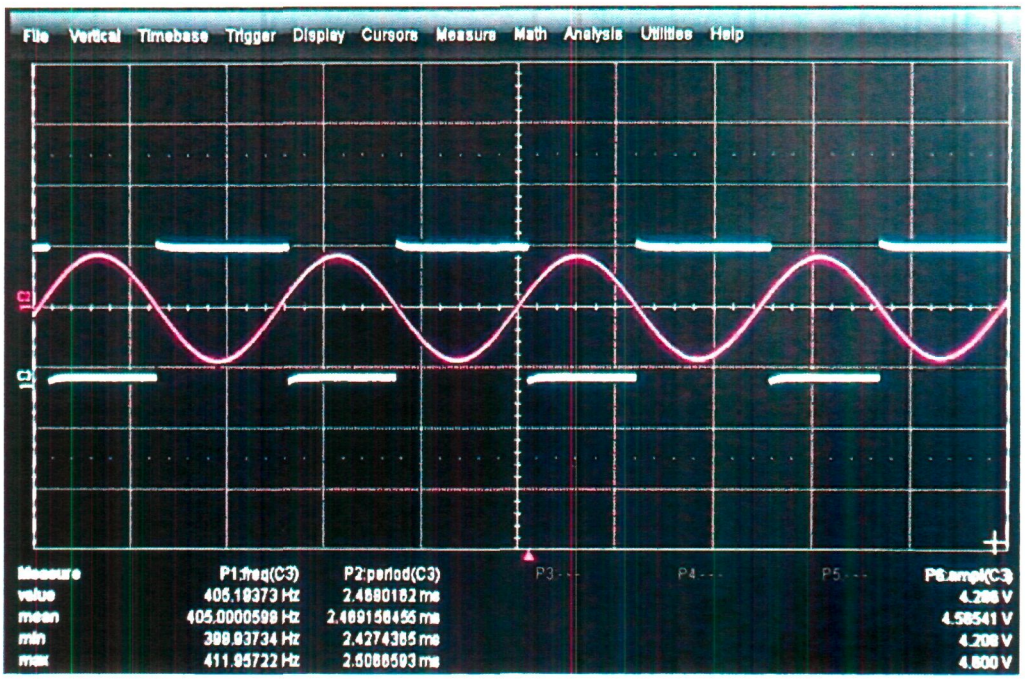
File Vertical Timebase Trigger Display Cursors Measure Math Analysis Utilities Help
C3
Measure P1:freq(C3) P2:period(C3) P3 P4 P5 P6:ampl(C3)
value 405.19373 Hz 2.4680182 ms 4.206 V
mean 405.0000599 Hz 2.469156455 ms 4.59541 V
min 399.93734 Hz 2.4274385 ms 4.208 V
max 411.95722 Hz 2.5006593 ms 4.800 V

(d)

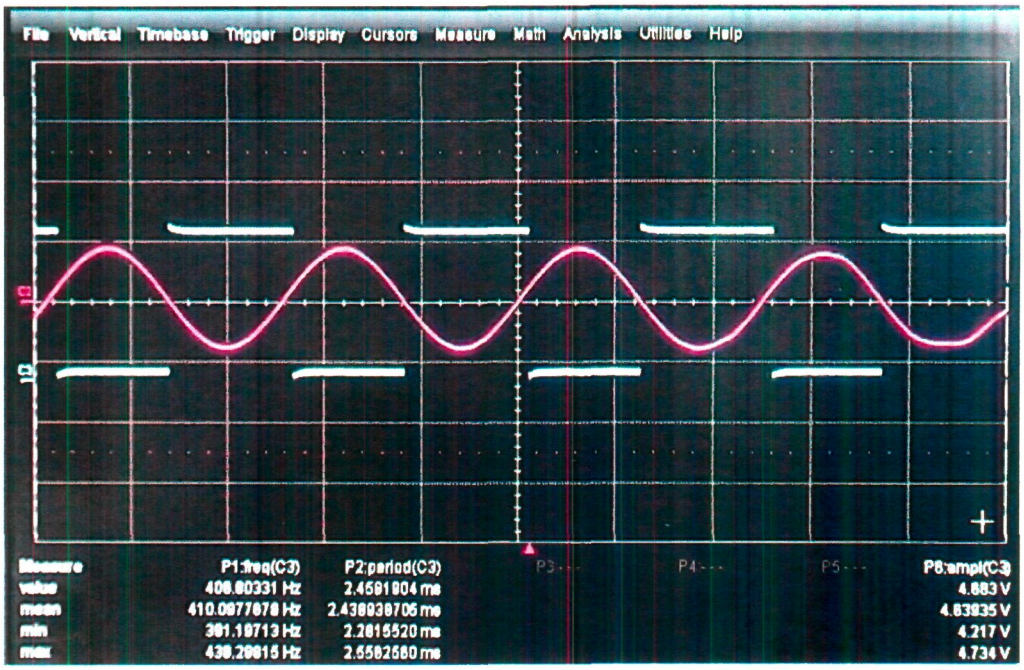

(e)

Figure 3.1 (a)-(e) V_r (Ch#2), and the exact set time period T_z (Ch#3) for **(a)** 0 r/min, **(b)** 100 r/min, **(c)** 200 r/min, **(d)** 300 r/min and **(e)** 600 r/min.

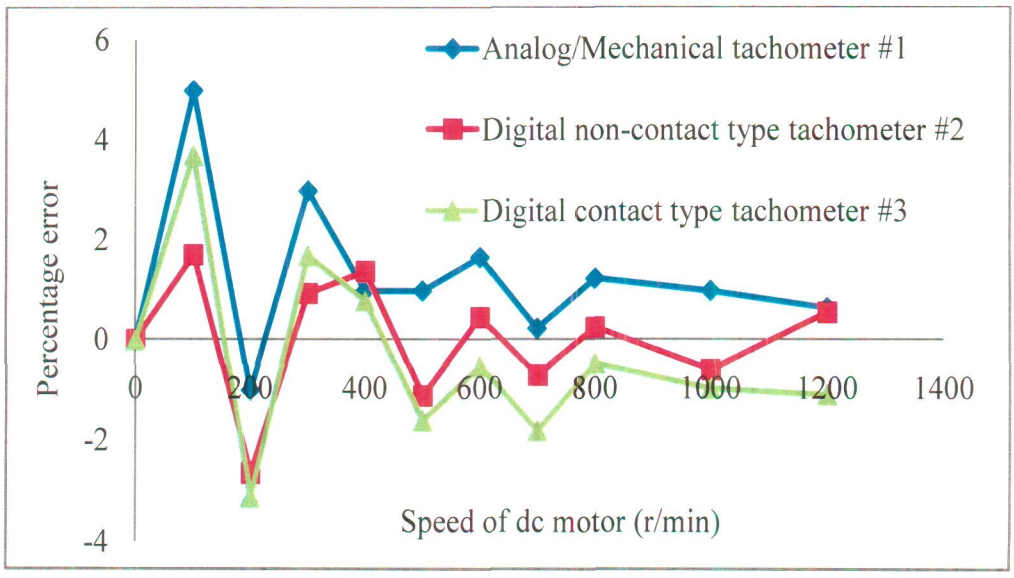

Figure 3.2 Errors of different tachometers under test.

Table 3.1: Performances of the Tachometers under Test

S. No.	Actual speed of dc motor (r/min)	Exact frequency f_z (Hz)	Set time period T_z (ms)	Speed measured by analog/ mechanical tachometer #1 (r/min)	Error of analog/ mechanical tachometer #1 (%)	Speed measured by digital non-contact type tachometer #2 (r/min)	Error of digital non-contact type tachometer #2 (%)	Speed measured by digital contact type tachometer #3 (r/min)	Error of digital contact type tachometer #3 (%)
1	0	400.0000	2.5000	0	0	0	0	0	0
2	100	401.6666	2.4896	105	5.00	101.8	1.80	103.7	3.70
3	200	403.3333	2.4793	198	-1.00	194.7	-2.65	193.8	-3.10
4	300	405.0000	2.4691	309	3.00	302.8	0.93	305.1	1.70
5	400	406.6666	2.4590	404	1.00	405.5	1.25	403.2	-0.80
6	500	408.3333	2.4489	505	1.00	495.6	-0.88	492.2	-1.60
7	600	410.0000	2.4390	610	1.67	602.7	0.45	596.9	-0.52
8	700	411.6666	2.4291	702	0.24	695.0	-0.71	687.4	-1.80
9	800	413.3333	2.4193	810	1.25	802.0	0.25	796.3	-0.46
10	1000	416.6666	2.4000	1010	1.00	994.0	-0.60	990.4	-0.96
11	1200	420.0000	2.3809	1208	0.66	1206.6	0.55	1187.0	-1.08

Experiments are carried out further at specified low speed range (0-200 r/min) and at high speed range (800-1000 r/min) with the steps of 50 r/min. These results are tabulated in Tables 3.2 and 3.3. Figures 3.3 and 3.4 show the deviation of the measured values (speed) in these ranges.

Table 3.2: Performance of tachometers under test (low speed range)

S. No.	Actual speed of motor (r/min)	Exact frequency f_z (Hz)	Set time period T_z (ms)	Speed measured by analog/ mechanical tachometer #1 (r/min)	Speed measured by digital non-contact type tachometer #2 (r/min)	Speed measured by digital contact type tachometer #3 (r/min)
1	0	400.0000	2.5000	0	0.0	0.0
2	50	400.8333	2.4948	54	56.2	57.9
3	100	401.6666	2.4896	105	101.8	103.7
4	150	402.5000	2.4844	160	158.0	158.7
5	200	403.3333	2.4793	198	194.7	193.8

Table 3.3: Performance of tachometers under test (high speed range)

S. No.	Actual speed of motor (r/min)	Exact Frequency f_z (Hz)	Set time period T_z (ms)	Speed measured by analog/ mechanical tachometer #1 (r/min)	Speed measured by digital non-contact type tachometer #2 (r/min)	Speed measured by digital contact type tachometer #3 (r/min)
1	800	413.333	2.419	810	802.0	796.3
2	850	414.166	2.414	856	842.1	844.8
3	900	415.000	2.409	918	907.4	903.5
4	950	415.833	2.404	961	953.4	947.2
5	1000	416.666	2.400	1010	994.0	990.4

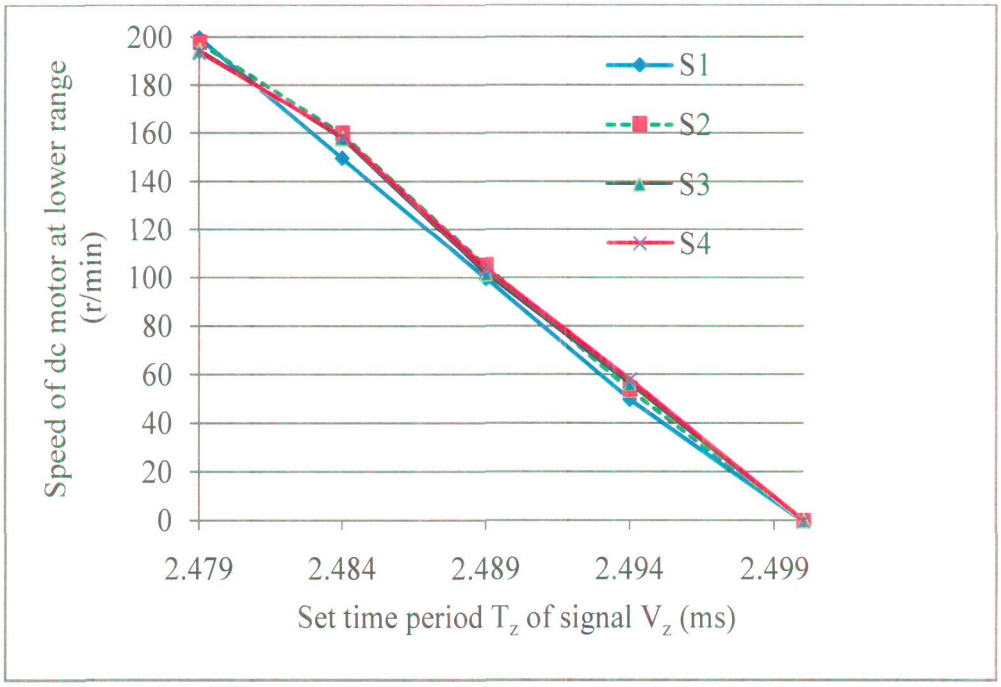

Figure 3.3 Comparison of tachometers at lower speed range.

S1- Actual (Exact)

S2- Analog/Mechanical tachometer #1

S3- Digital non-contact type tachometer #2

S4- Digital contact type tachometer #3

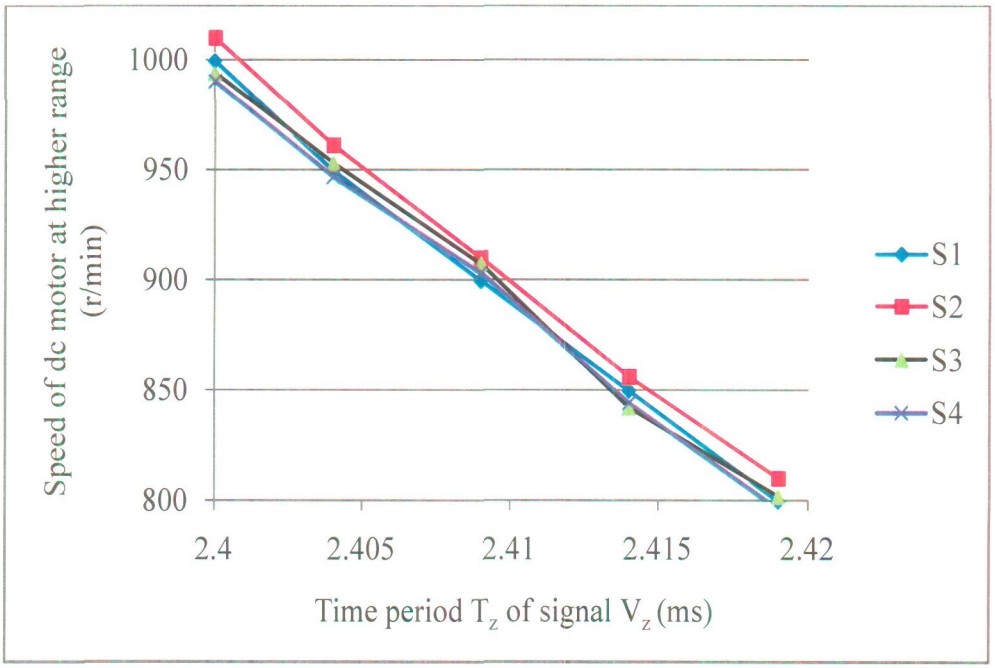

Figure 3.4 Comparison of tachometers at higher speed range.

S1- Actual (Exact)

S2- Analog/Mechanical tachometer #1

S3- Digital non-contact type tachometer #2

S4- Digital contact type tachometer #3

3.3 Conclusion

The experimental results of errors of the tachometer are summarized in Table 3.4. It clearly shows the variation in error from the manufacturer's specifications. Thus using the calibration curve, the proposed method can be used to obtain the accurate speed at any desired value, as in general, manufacturers do not provide errors curve for all speed range.

Table 3.4 Comparison of the errors of tachometers under test with proposed method.

	Errors of tachometers	
Tachometers	Manufacturers specification	Experimentally found by proposed method
Tachometer # 1	± 3 r/min for 300 r/min ± 10 r/min for 1200 r/min	± 2 r/min to ± 10 r/min for 0 to 1200 r/min
Tachometer # 2	± 1 r/min for 5 to 1200 r/min	± 2 r/min to ± 6 r/min for 0 to 1200 r/min
Tachometer # 3	± 7 r/min for 5 to 1200 r/min	± 3 r/min to ± 13 r/min for 0 to 1200 r/min

The proposed method is used for the calibration of different tachometers which includes contact type, non-contact type, and both analog and digital tachometers. Significant errors of the order of 5% are found in these tachometers using the proposed method. The error of analog contact type tachometer provided in the data specification sheet varies from ± 3 r/min to ± 10 r/min, in the range of

300 r/min to 1200 r/min [60]. The errors found by the proposed method are ± 2 r/min to ± 10 r/min, over this range. The accuracy of digital non-contact type tachometer is ± 1 r/min in the range of 5 r/min to 1200 r/min, according to calibration report provided with the tachometer [62]. Whereas, the error found by the proposed method is ± 2 r/min to ± 6 r/min in this range. Similarly, the error (Guarantee Error) of digital contact type tachometer is claimed as ± 7 r/min for the entire range of 5 r/min to 1200 r/min, according to manufacturer's data specification sheet [61]. However, the error found by the proposed method is ± 3 r/min to ± 13 r/min in this range.

Chapter 4

Very Fast Measurement of Low Speed of Rotating Machines Using Rotating Magnetic Field

4.1 Introduction

Sophisticated speed control applications require very fast and accurate speed measurement. It is one of the important requirements of low speed machines like rotors of cement kilns, rolling machines in paper mills, mining industries, textile mills and heavy stone crushing machines etc, where the speed varies from 0 to 10 r/min [1]-[4]. The measurement at low speed becomes very difficult due to the slow response of transducers. At low speed (below 10 r/min), normally transducers take several seconds to give the required output signal [14]-[16]. Therefore, the existing techniques are not suitable where fast feedback signals are required for control applications.

In the proposed technique, as explained in chapter 2, a fast RMF is used to measure the speed as well as deviation in speed for low-speed machines. A three-phase balanced voltage supply is realized with the help of a stable arbitrary function generator and a single-phase to three-phase convertor using three power amplifiers. The three windings placed on the stator of the synchro are energized by this three-phase balanced voltage/current. They create RMF in the air gap which links with the rotor circuit of the synchro and generates an EMF in it [99]-

[100]. The rotor of the synchro is mechanically coupled with a rotating member. Both the magnitude and frequency of the output voltage at the rotor circuit of synchro depend upon the speed and difference in speed. The effect of variation in the magnitude of the output voltage is eliminated by using a ZCD in open-loop mode at the output. Here, the speed of the rotor of synchro or rotating member (three-phase induction motor) is few r/min only, whereas, the speed of RMF is 2400 r/min for a supply frequency of 40 Hz. At this frequency, for each revolution of the rotating member, the RMF rotates 2400 times. Thus the deviation in the speed of rotor is quickly picked up by the RMF which causes a fast deviation in frequency of the rotor voltage. Hence the measurement, even at 1 r/min, becomes extremely fast. The proposed scheme is tested successfully from 1 r/min to 10 r/min and the results of measurements are compared with a conventional method (techogenerator) which shows the fast response of proposed method. The output is also obtained in terms of dc voltage and dc current, which can be used for feed-back and control applications.

4.2 Realization of the Scheme for Fast Measurement of Low Speed

Figure 4.1 shows the set up for the realization of low speed measurement. To realize low speed from 0 to 10 r/min, a three-phase induction motor (as a prime mover) is connected to an adjustable frequency ac drive system (Appendix A.4). On one side of the prime mover the synchro is connected whereas on the other side a dc tachogenerator is connected for comparison of measurement of speed simultaneously.

Figure 4.2 shows the circuit for the realization of balanced three-phase voltages for stator winding of synchro. This circuit has been given in chapter 2 as Figure 2.2, is redrawn here for ready reference. Here, a sine wave signal of 40 Hz (18.8 V peak-to-peak) from a stable arbitrary function generator (F.G) is supplied to a centre-tapped transformer (Figure 4.3). The output of transformer is applied to an RC network (R=100 kΩ and C = 0.1μF), to generate three phase, 40 Hz

voltages V_1, V_2, and V_3 (Figure 4.4). These voltages are attenuated to a value of about 150 mV [V_4, V_5, and V_6 (Figure 4.5)], before feeding into three audio power amplifiers (LM 384N). The outputs of these amplifiers, V_7, V_8 and V_9 with frequency f_s are in turn applied to the stator winding of synchro and marked as V_s (Figure 4.1). Therefore at stationary condition, a sinusoidal signal V_r with frequency f_r (40 Hz) is generated at the rotor winding of synchro (Figure 4.6).

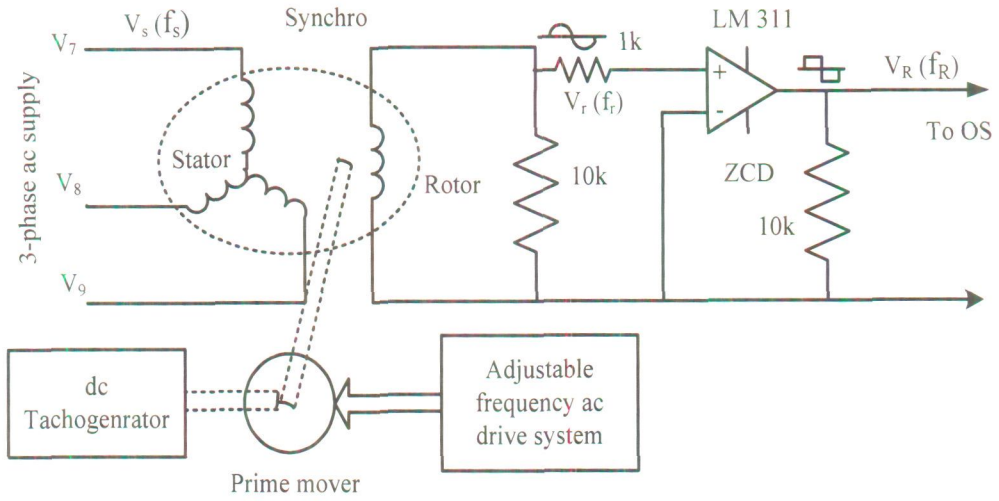

Figure 4.1 RMF based low speed measurement setup.

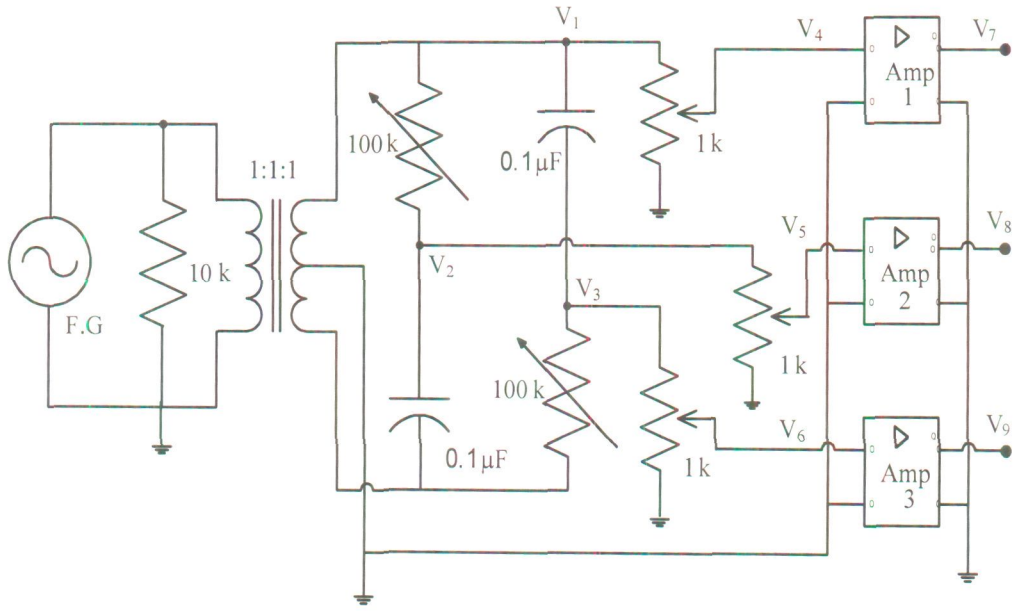

Figure 4.2 Single-phase to three-phase conversion system to generate balanced three-phase voltages V_7, V_8 and V_9 for stator winding of synchro.

Figure 4.3 Sine wave signals of 40 Hz from a stable arbitrary function generator (CH#1) and output of centre-tapped transformer (CH#2 and Ch#3).

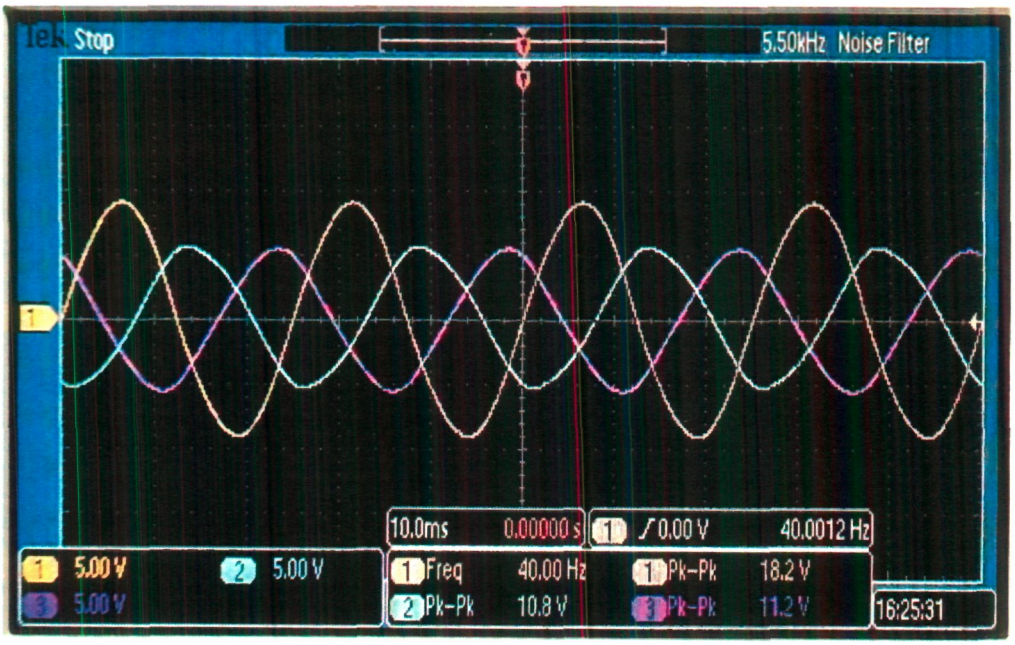

Figure 4.4 Three phase voltages, V_1, V_2, and V_3 at the output of RC network (CH#1, CH#2 and Ch#3)

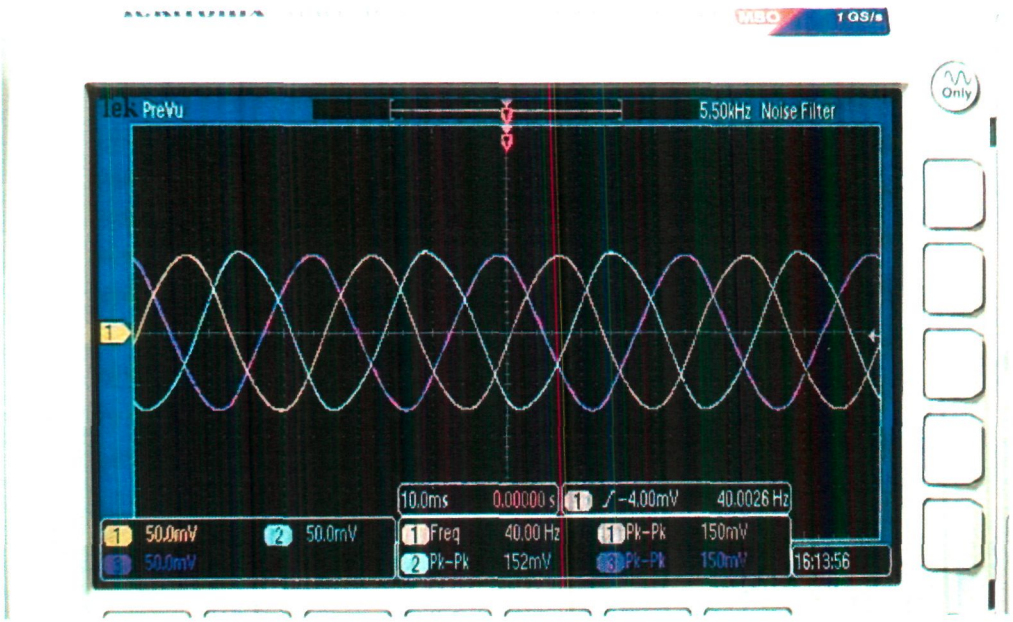

Figure 4.5 Waveforms V_4, V_5, and V_6 applied at the input of power amplifiers (CH#1, CH#2 and Ch#3 respectively).

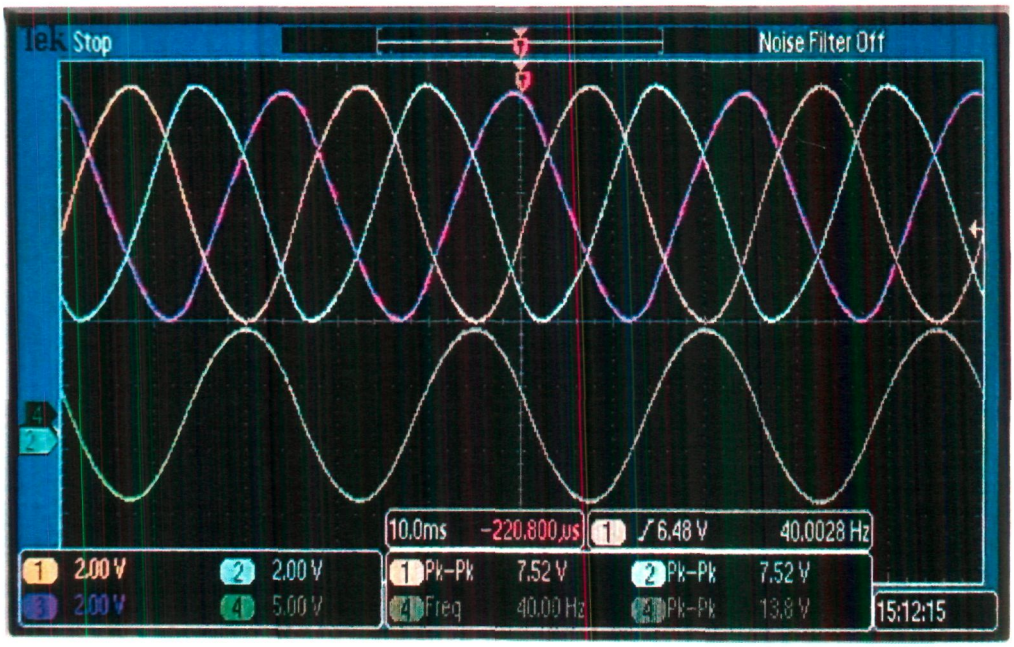

Figure 4.6 V_7 (CH#1), V_8 (CH#2) and V_9 (Ch#3) with frequency f_s, applied to stator winding of synchro as V_s, and rotor voltage V_r (CH#4) with frequency f_r.

Figure 4.7 Output voltage of rotor, V_r (Ch#1) and output of ZCD, V_R (Ch#2) at 40 Hz.

4.3 Experimental Results

4.3.1 When the Rotating Member Is Stationary

As long as the rotating member is stationary, the speed of rotor of synchro is zero. The frequency f_r of V_r of the rotor circuit is equal to f_s of V_s of the stator circuit (Figure 4.6). The signal V_r is now passed through a ZCD to produce a square waveform V_R with the same frequency ($f_R = f_r$), as shown in Figure 4.7. The negative going transition (NGT) of signal V_R is used to trigger a one shot mono-stable multi-vibrator (OS, 74LS121N) to produce a signal Q of a stable fixed positive width T_{WQ+} of 12.5 ms, as shown in Figure 4.8. These two signals (V_R and Q) are applied to an EX-OR gate (G-1). The output of G-1 becomes high as the negative width (T_{WR-}) of the signal V_R is equal to positive width (T_{WQ+}) of signal Q and vice versa. This is also explained using (2.3), which is re-written here for easy reference as (4.1).

$$f_r = f_s \mp \frac{n_r P}{120} \qquad (4.1)$$

f_r = Frequency of induced EMF (V_r) of rotor of synchro

f_s = Frequency of stator voltage (V_s) of synchro

f_R = Frequency of signal V_R at the output of ZCD ($f_R = f_r$)

T_R = Time period of the signal V_R at the input of OS

T_{WR-} = Negative width of the signal V_R

T_{WQ+} = Positive width of signal Q

T_{WG-} = Negative width of the pulse at the output of G-1

$T_{WG-} = T_{WR-} - T_{WQ+}$

Consider the case when the rotating member is stationary (i.e. n_r = 0 r/min)

From (4.1), it can be observed that $f_R = f_r = f_s = 40$ Hz

Therefore, $T_R = (1/f_R) = 25$ ms

$T_{WR-} = (T_R / 2) = 12.5$ ms

$T_{WQ+} = 12.5$ ms

$T_{WG-} = T_{WR-} - T_{WQ+}$

$T_{WG-} = 12.5 - 12.5$

$T_{WG-} = 0$

Thus, the output of EX-OR gate G-1 = 1 (HIGH).

The wave forms V_r, V_R, Q, and T_{WG-} are also shown in the DSO records (Figure 4.9).

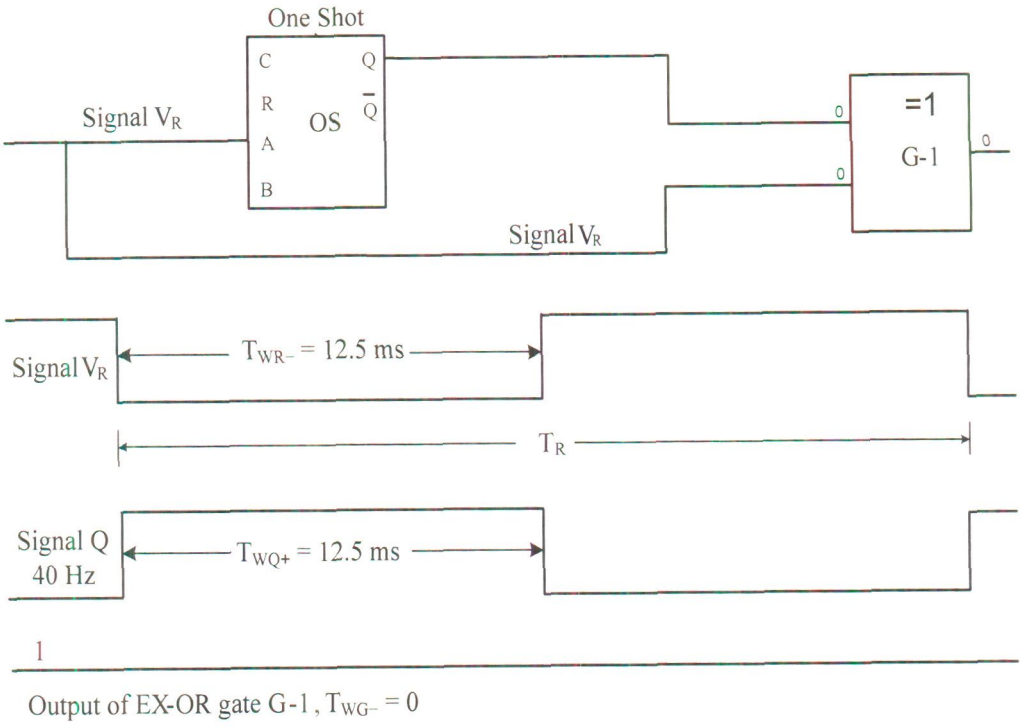

Figure 4.8 Waveforms of signals, V_R, Q and output T_{WG-}.

Figure 4.9 Output of the rotor V_r of synchro (Ch#1), V_R with T_{WR-} (Ch#2), signal Q with T_{WQ+} (Ch#3), and output T_{WG-} of G-1 (Ch#4), at stationary condition.

4.3.2 *When the Rotating Member Rotates in the Clockwise Direction (f_R Decreases)*

When the rotating member crawls to a low speed in clockwise direction, the frequency f_r of the induced EMF V_r in the rotor circuit of synchro decreases. The time period T_R or $(1/f_R)$ and, hence, the negative width T_{WR-} of signal V_R at the output of ZCD increases accordingly. The NGT of V_R triggers OS to produce a signal Q with stable positive width T_{WQ+} of 12.5 ms. When the signals V_R and Q are applied to G-1, a pulse with negative width is generated at its output, as shown in Figure 4.10. The duration of this pulse depends on the speed of rotation of rotor and is obtained using (4.1)

When n_r = 1 r/min (rotation is clockwise)

$f_s = 40$ Hz

Using (4.1), $f_R = f_r = 40 - \frac{1 \times 2}{120}$

$f_R = 39.983$

$T_R = (1/f_R) = 25.010$ ms

$T_{WR-} = T_R/2 = 12.505$ ms

$T_{WQ+} = 12.5$ ms

$T_{WG-} = T_{WR-} - T_{WQ+}$

$T_{WG-} = 12.505 - 12.5$

$T_{WG-} = 5.211$ µs

Figures 4.11(a)-(j) show the DSO records for a speed range, corresponding to 1-10 r/min in clockwise direction. These results are also tabulated in Table 4.1.

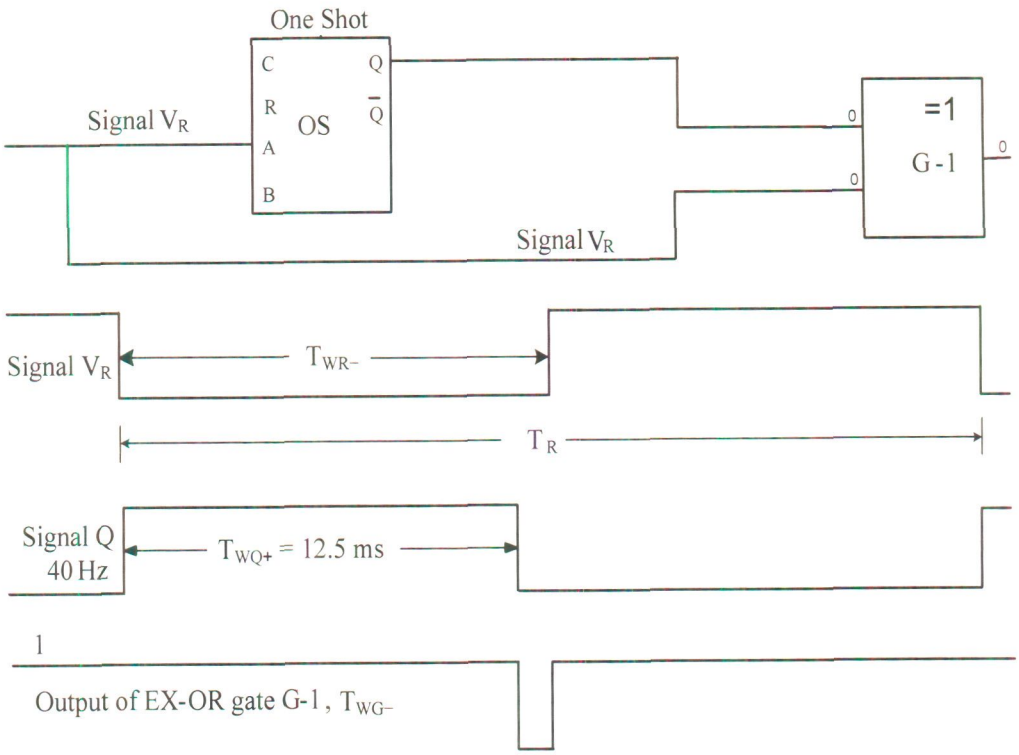

Figure 4.10 Waveforms of signals, V_R, Q and output T_{WG-}.

(a)

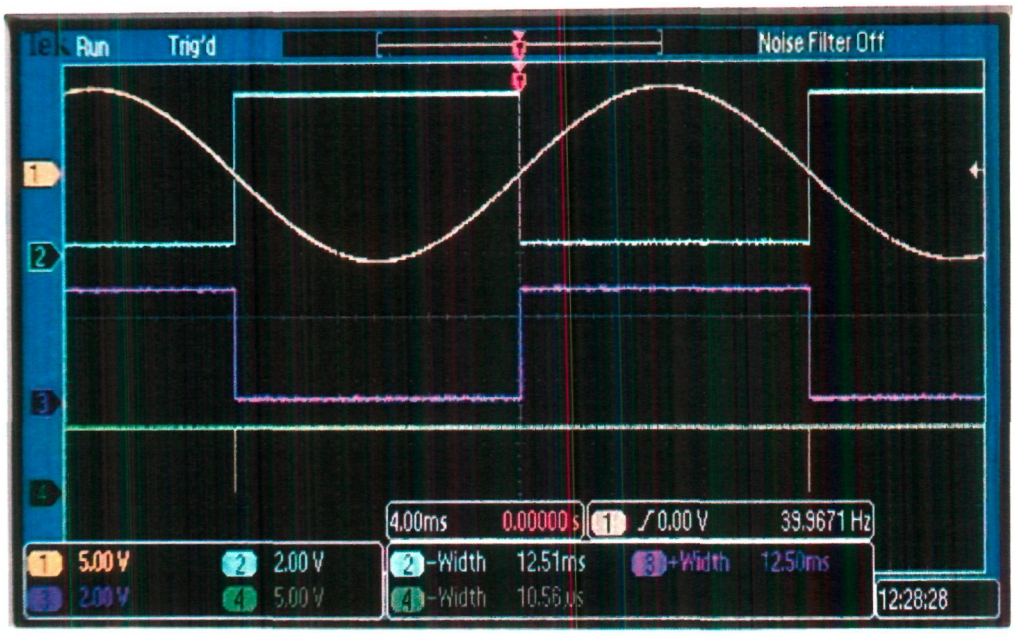
Run
Trig'd
Noise Filter Off
4.00ms
0.00000 s
0.00 V
39.9671 Hz
5.00 V
2.00 V
-Width
12.51ms
+Width
12.50ms
-Width
10.56 µs
12:28:28

(b)

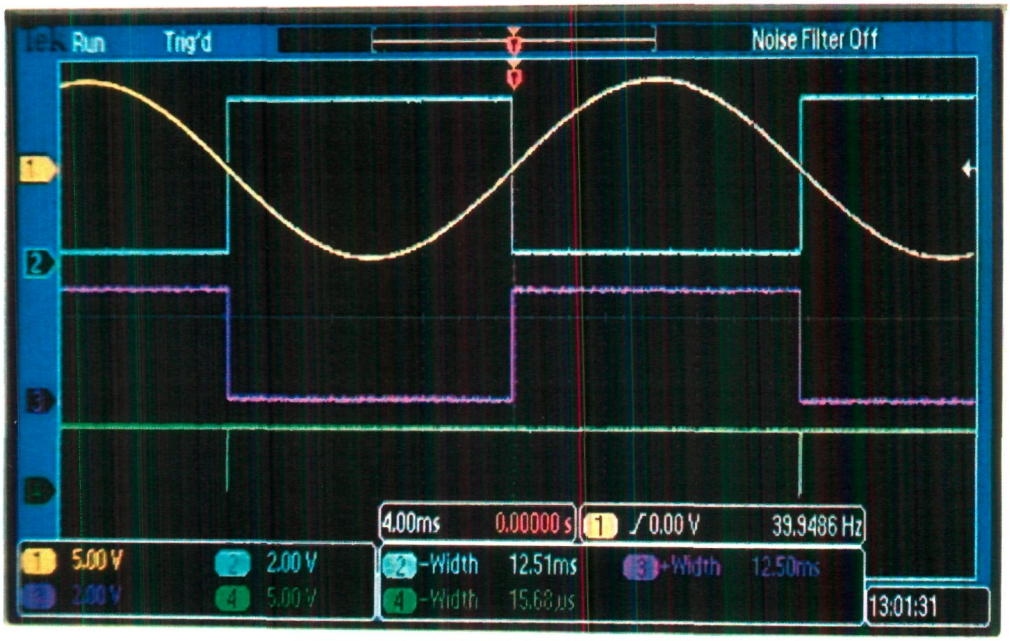
Run
Trig'd
Noise Filter Off
4.00ms
0.00000 s
0.00 V
39.9486 Hz
5.00 V
2.00 V
-Width
12.51ms
+Width
12.50ms
-Width
15.68 µs
13:01:31

(c)

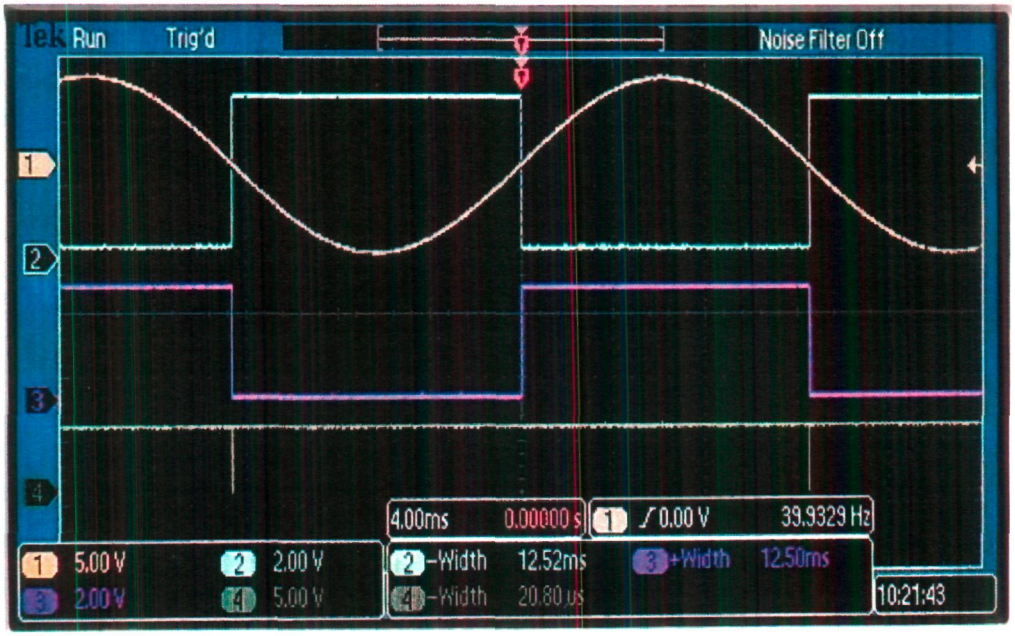
Tek Run Trig'd
Noise Filter Off
4.00ms 0.00000 s
1 ⨍ 0.00 V 39.9329 Hz
1 5.00 V
2 2.00 V
3 2.00 V
4 5.00 V
2 -Width 12.52ms
3 +Width 12.50ms
4 -Width 20.80 µs
10:21:43

(d)

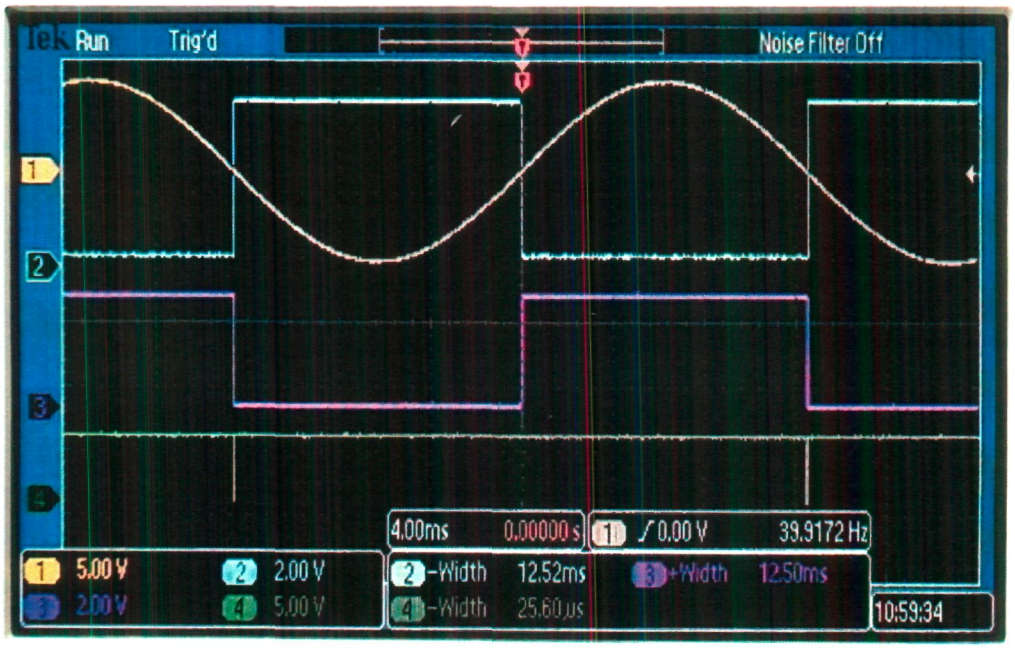
Tek Run Trig'd
Noise Filter Off
4.00ms 0.00000 s
1 ⨍ 0.00 V 39.9172 Hz
1 5.00 V
2 2.00 V
3 2.00 V
4 5.00 V
2 -Width 12.52ms
3 +Width 12.50ms
4 -Width 25.60 µs
10:59:34

(e)

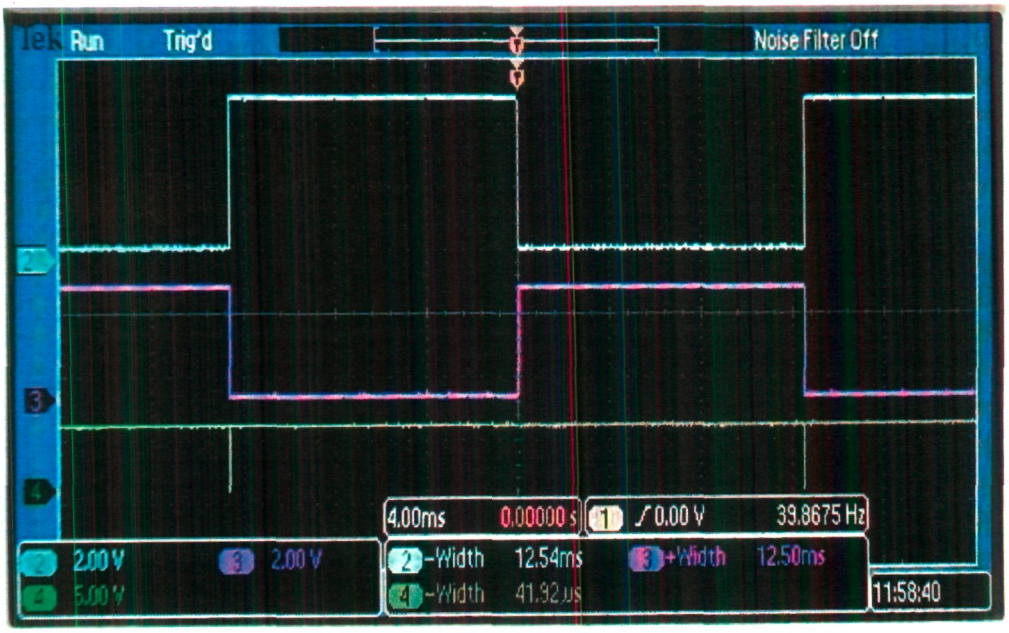
Tek Run Trig'd
Noise Filter Off
4.00ms 0.00000 s
/ 0.00 V
39.8675 Hz
2.00 V
2.00 V
-Width 12.54ms
+Width 12.50ms
5.00 V
-Width 41.92 µs
11:58:40

(h)


Tek Run Trig'd
Noise Filter Off
4.00ms 0.00000 s
/ 0.00 V
39.8495 Hz
5.00 V
2.00 V
-Width 12.54ms
+Width 12.50ms
2.00 V
5.00 V
-Width 47.07 µs
11:17:57

(i)

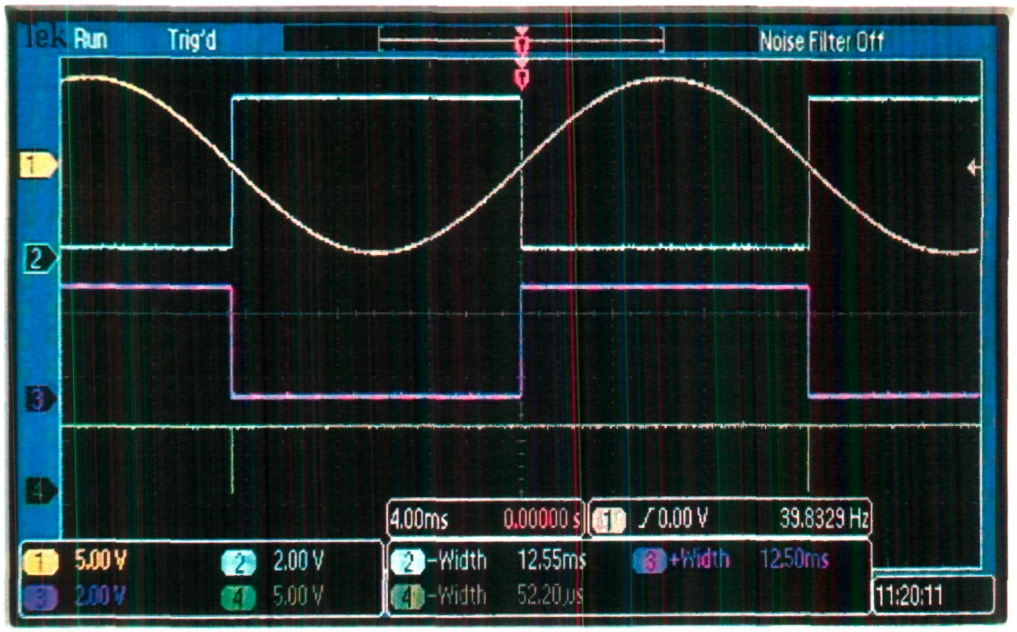

(j)

Figure 4.11 (a)-(j) Output voltage of rotor V_r of synchro (Ch#1), V_R with T_{WR-} (Ch#2), signal Q with T_{WQ+} (Ch#3), and negative width (T_{WG-}) at the output of G-1, corresponding to 1-10 r/min (Ch#4), respectively.

Table 4.1: Theoretical and observed results of the test

T_{WQ+} ms	n_r r/min	f_R (V_R) Hz Theoretical	f_R (V_R) Hz Observed	$T_R=1/f_R$ ms Theoretical	$T_{WR-}=T_R/2$ ms Theoretical	$T_{WR-}=T_R/2$ ms Observed	T_{WG-} (μs) = $T_{WR-}-T_{WQ+}$ Theoretical	T_{WG-} (μs) = $T_{WR-}-T_{WQ+}$ Observed
12.5	0	40	40.000	25.00	12.50	12.50	0	0
12.5	1	39.983	39.982	25.010	12.505	12.50	05.211	5.76
12.5	2	39.966	39.967	25.021	12.510	12.51	10.425	10.56
12.5	3	39.95	39.948	25.031	12.515	12.51	15.645	15.68
12.5	4	39.933	39.932	25.042	12.521	12.52	20.868	20.80
12.5	5	39.916	39.917	25.052	12.526	12.52	26.096	25.60
12.5	6	39.90	39.901	25.063	12.531	12.53	31.328	31.04
12.5	7	39.883	39.884	25.073	12.536	12.53	36.564	36.49
12.5	8	39.866	39.865	25.084	12.541	12.54	41.806	41.92
12.5	9	39.85	39.849	25.094	12.547	12.54	47.051	47.07
12.5	10	39.833	39.832	25.104	12.552	12.55	52.301	52.20

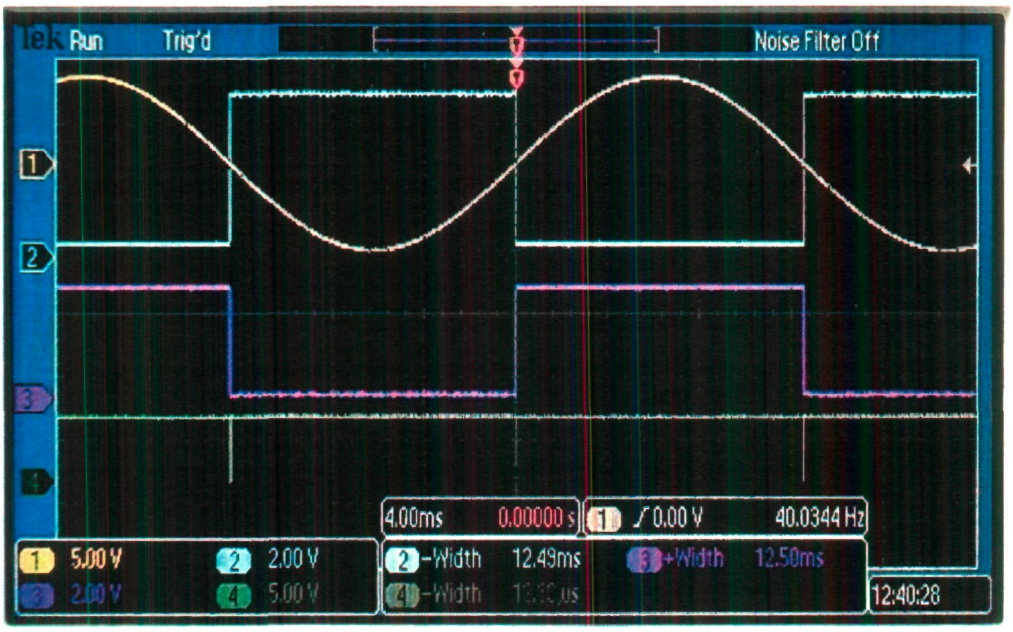
Tek Run Trig'd
Noise Filter Off
4.00ms 0.00000 s
0.00 V 40.0344 Hz
5.00 V
2.00 V
-Width 12.49ms
+Width 12.50ms
12:40:28

(b)


Tek Run Trig'd
Noise Filter Off
4.00ms 0.00000 s
0.00 V 40.0509 Hz
5.00 V
2.00 V
-Width 12.48ms
+Width 12.50ms
-Width 15.36 µs
18:37:53

(c)

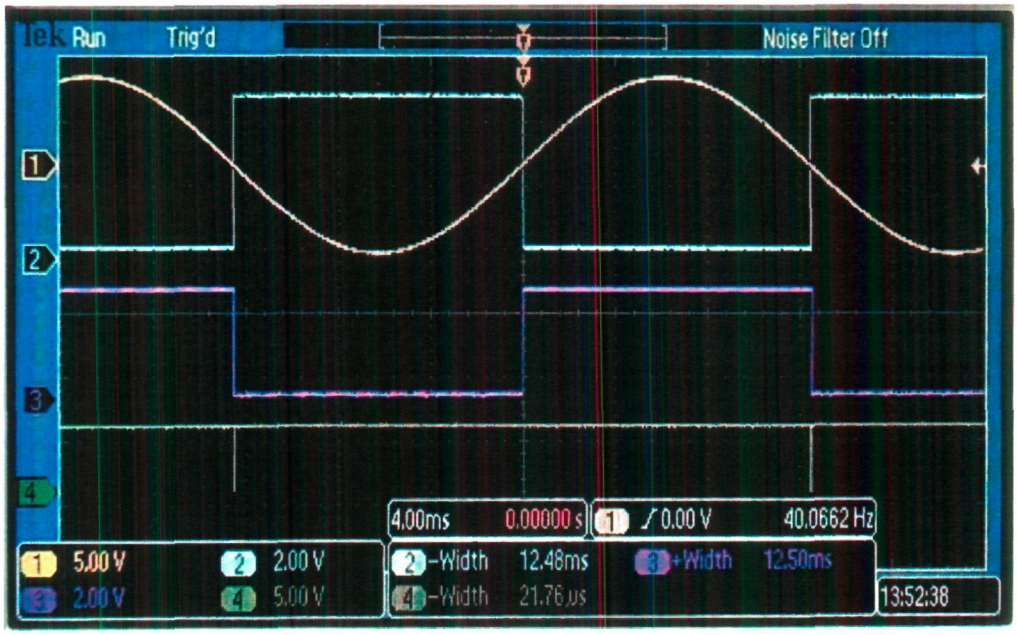
Tek Run Trig'd
Noise Filter Off
4.00ms 0.00000 s
/ 0.00 V 40.0662 Hz
5.00 V
2.00 V
2.00 V
5.00 V
-Width 12.48ms
+Width 12.50ms
-Width 21.76 µs
13:52:38

(d)

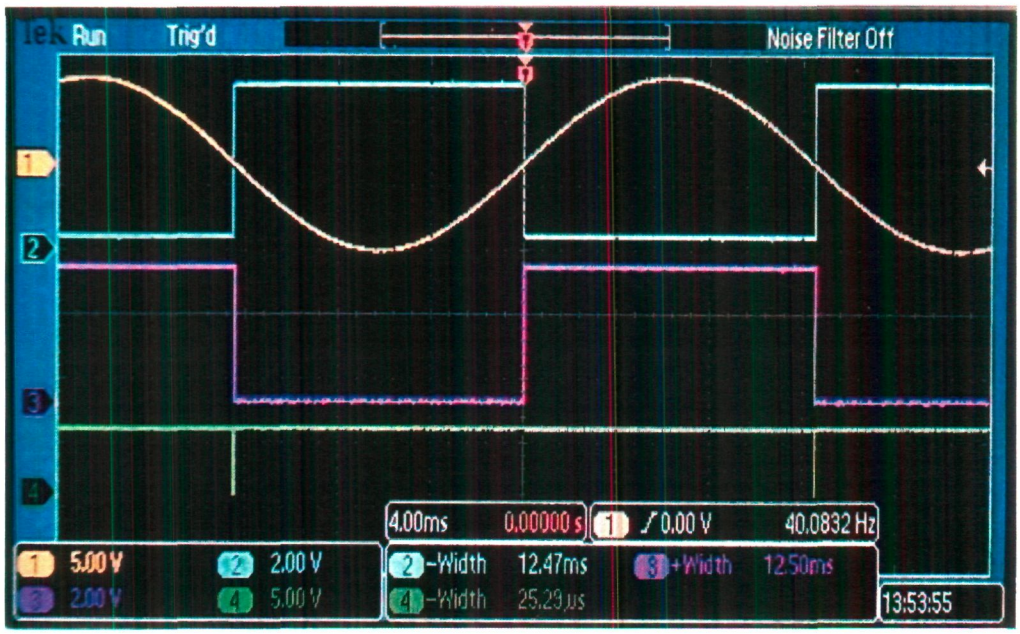
Tek Run Trig'd
Noise Filter Off
4.00ms 0.00000 s
/ 0.00 V 40.0832 Hz
5.00 V
2.00 V
2.00 V
5.00 V
-Width 12.47ms
+Width 12.50ms
-Width 25.29 µs
13:53:55

(e)

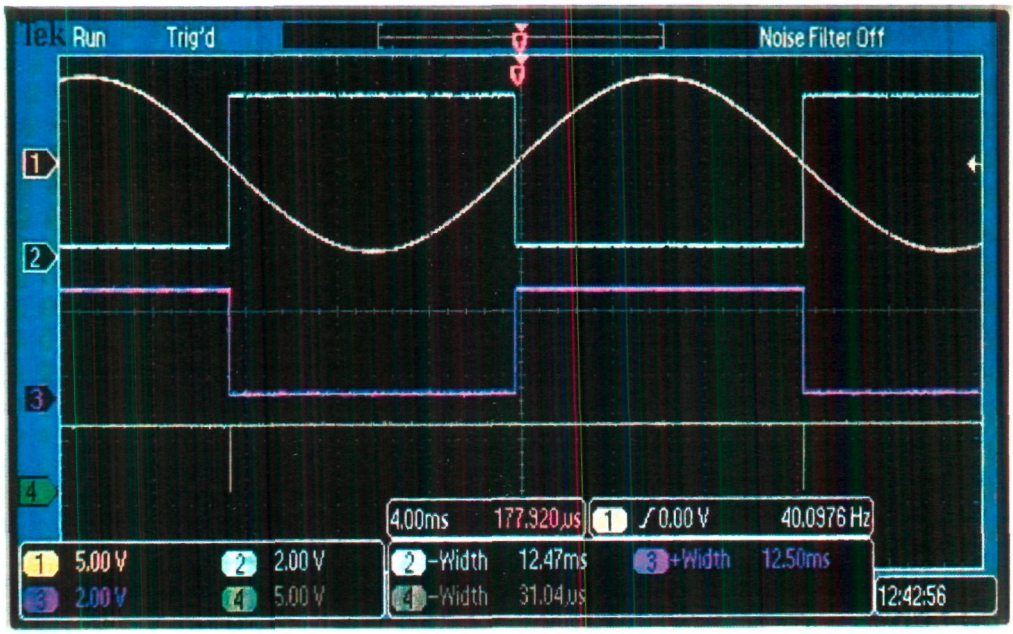
Tek Run Trig'd
Noise Filter Off
4.00ms 177.920µs
∫ 0.00 V 40.0976 Hz
5.00 V
2.00 V
2.00 V
5.00 V
-Width 12.47ms
+Width 12.50ms
-Width 31.04µs
12:42:56

(f)


Tek Run Trig'd
Noise Filter Off
4.00ms 177.920µs
∫ 0.00 V 40.1178 Hz
5.00 V
2.00 V
2.00 V
5.00 V
-Width 12.46ms
+Width 12.50ms
-Width 36.48µs
12:38:42

(g)


Tek Run Trig'd
Noise Filter Off
4.00ms 0.00000 s
1 ƒ 0.00 V
40.1318 Hz
1 5.00 V
2 2.00 V
3 2.00 V
4 5.00 V
2 -Width 12.46ms
3 +Width 12.50ms
4 -Width 41.62 µs
13:39:00

(h)


Tek Run Trig'd
Noise Filter Off
4.00ms 177.920 µs
1 ƒ 0.00 V
40.1493 Hz
1 5.00 V
2 2.00 V
3 2.00 V
4 5.00 V
2 -Width 12.45ms
3 +Width 12.50ms
4 -Width 47.67 µs
12:12:50

(i)

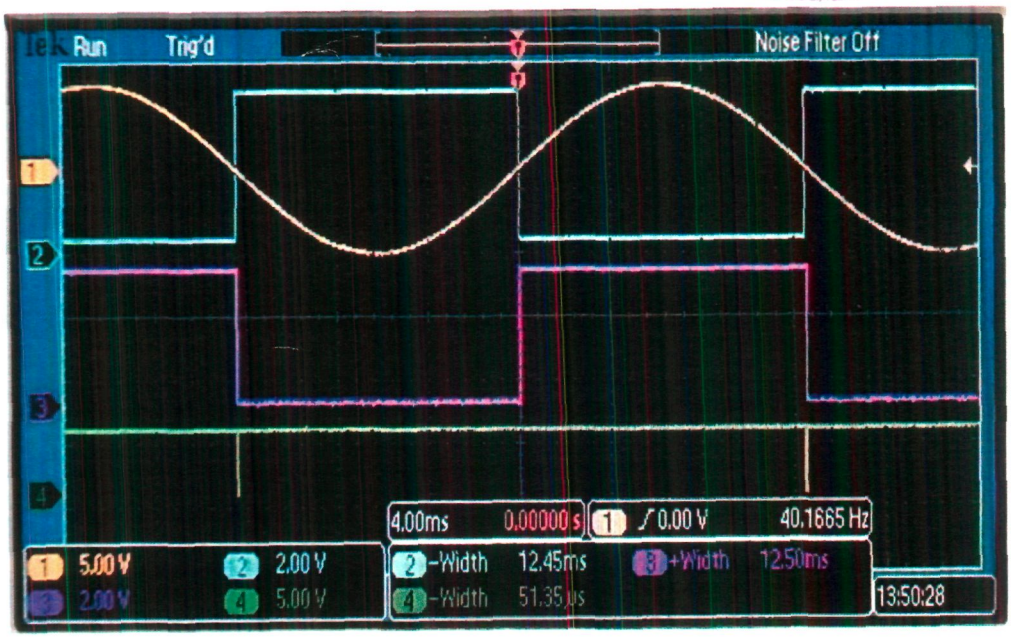

(j)

Figures 4.13 (a)-(j) Output of rotor V_r of synchro (Ch#1), V_R with T_{WR-} (Ch#2), signal Q with T_{WQ+} (Ch#3), and negative width (T_{WG-}) at the output of G-1, corresponding to 1-10 r/min (Ch#4), respectively.

Table 4.2: Theoretical and observed results of the test

T_{WQ+} ms	n_r r/min	f_R (V_R) Hz Theoretical	f_R (V_R) Hz Observed	$T_R = 1/f_R$ ms Theoretical	$T_{WR-} = T_R/2$ ms Theoretical	$T_{WR-} = T_R/2$ ms Observed	T_{WG-} (µs) = $T_{WQ+} - T_{WR-}$ Theoretical	T_{WG-} (µs) = $T_{WQ+} - T_{WR-}$ Observed
12.5	0	40	40	25	12.5	12.5	0	0
12.5	1	40.016	40.018	24.989	12.494	12.49	05.206	5.51
12.5	2	40.033	40.034	24.979	12.489	12.49	10.407	10.10
12.5	3	40.05	40.05	24.968	12.484	12.48	15.605	15.36
12.5	4	40.066	40.066	24.958	12.479	12.48	20.798	21.76
12.5	5	40.083	40.083	24.948	12.474	12.47	25.987	25.29
12.5	6	40.1	40.097	24.937	12.468	12.47	31.172	31.04
12.5	7	40.116	40.117	24.927	12.463	12.46	36.352	36.48
12.5	8	40.133	40.131	24.916	12.458	12.46	41.528	41.62
12.5	9	40.15	40.149	24.906	12.453	12.45	46.699	47.67
12.5	10	40.166	40.166	24.896	12.448	12.45	51.867	51.35

4.3.4 Comparison with Time Response of Tachogenerator

In the experimental setup, an adjustable frequency ac drive is used to control the speed of an induction motor (Figure 4.14). At one side of the shaft of induction motor, a synchro is coupled, whereas on the other side, a dc tachogenerator is mounted and coupled. Thus, both transducers give the output signals for the same speed simultaneously. The adjustable frequency ac drive runs (in start mode) if its feedback terminals #1 and #2 are shorted. When these terminals are open, the voltage across them becomes equal to the internal source voltage (22.6 V), and the drive stops [101]. When the ac drive is set at 1 r/min, induction motor runs at a speed of 1 r/min and the mounted synchro and tachogenerator also crawls at 1 r/min. Corresponding to this speed, a dc voltage of 24.8 mV, as per specification of tachogenerator (2.42 V/ 100 r/min), is generated at its output and measured at CH#1 of DSO, whereas the voltage across terminals #1 and #2 of ac drive remains zero (measured at CH#2), as shown in Figure 4.15 (a). When the feedback terminals of ac drive open, the terminal voltage rises [a step change of 22.6 V in Figure 4.15 (a)], the rotor speed reduces quickly, and, finally it stops. The tachogenerator takes sufficiently large time to register the effects of speed variation and to give the output voltage accordingly. Here, the output voltage of the tachogenerator takes 656 ms to become zero. However, in case of the proposed method, it takes only 12.5 ms, as shown in Figures 4.13 (a)-(j). It may be noted that the variation in the output voltage of tachogenerator is not smooth at very low speed, and the noise level is quite high. The results of the measurement by dc tachogenerator for different speeds are shown in the DSO records [Figures 4.15 (a)-(c)].

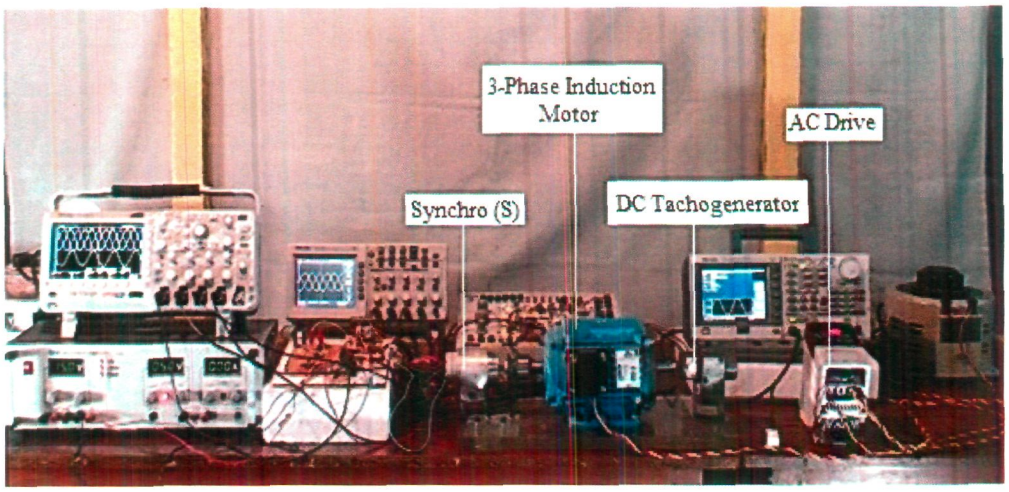

Figure 4.14 Experimental setup for fast measurement of very low speed.

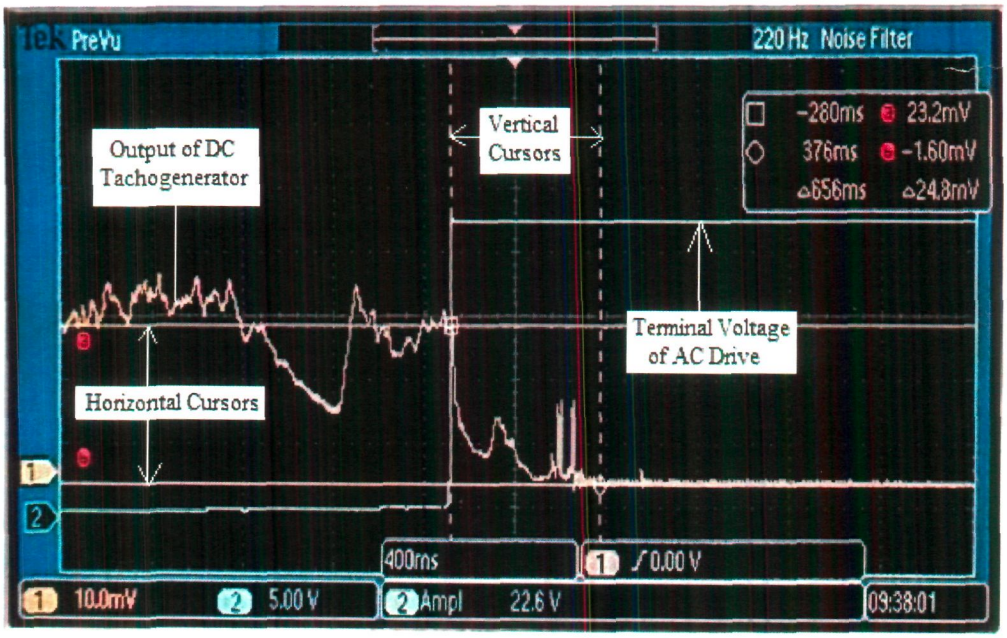

(a)

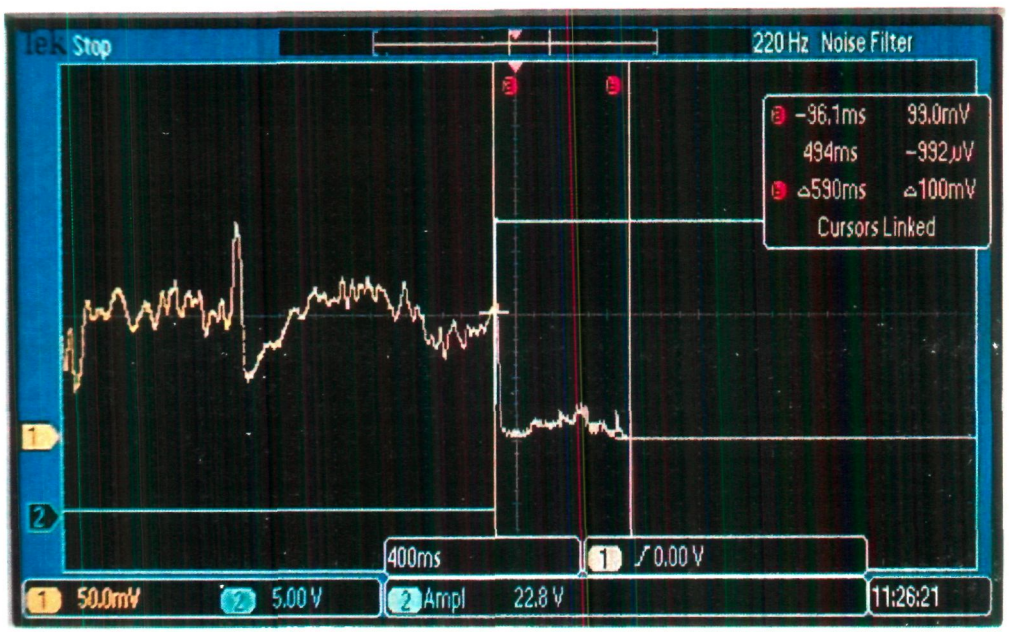

(b)

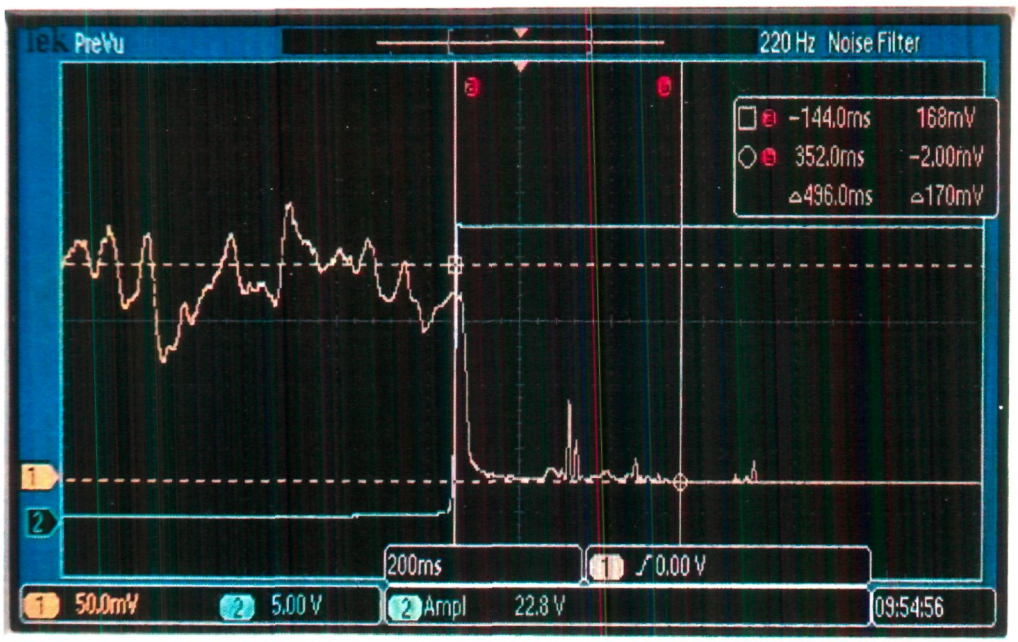

(c)

Figure 4.15(a)-(c) Output voltage of dc tachogenerator for 1, 4 and 7, r/min (CH#1), respectively, and output voltage across terminals #1 and #2 (CH#2).

The output pulses from the gate G-1 can also be used to generate dc output voltage or dc current. This dc output voltage or dc current may be used as feed-back signals for control applications. The pulses from the gate G-1 are applied to an amplifier with averaging circuit (Figure 4.16), which produces an average dc voltage (V_{dc}). This average dc voltage for different speeds (V_{dc}) is calculated by (4.2) and (4.3) as described in Figure 4.17. A current feed-back signal is also generated by connecting a resistance of high value, in series with an ammeter of μA range. The measured output dc voltages (V_{dc}) and currents (I_{dc}) of averaging circuit are given in Table 4.3. The waveforms are also recorded for a speed range, corresponding to 1-10 r/min, as shown in Figures 4.18 (a)-(j).

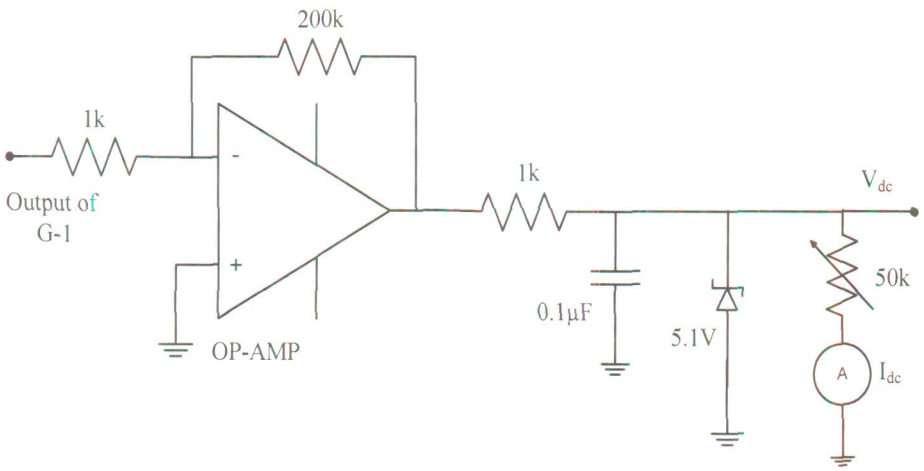

Figure 4.16 Averaging circuit with amplifier.

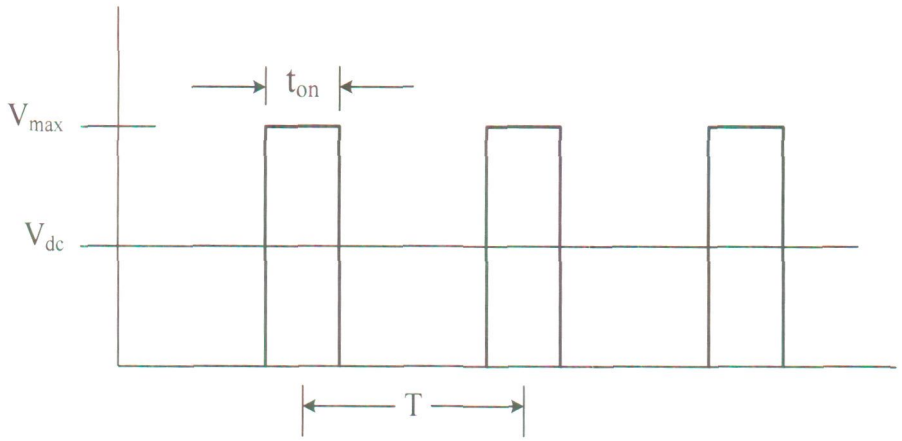

Figure 4.17 Wave forms to calculate the average value (V_{dc}) of pulses at the output of G-1.

$$V_{dc} = \frac{t_{on}}{T} V_{max} \qquad (4.2)$$

$$V_{dc} = t_{on}.f.V_{max} \qquad (4.3)$$

T = Time period of pulse at the output of G-1

t_{on} = On time of pulse at the output of G-1

V_{max} = Maximum amplitude of pulse at the output of G-1

Table 4.3: Measured output dc voltages and currents of averaging circuit

n_r r/min	f_R (V_R) Hz Observed	T_{WG-} (μs) = $T_{WR-} - T_{WQ+}$ Observed	V_{dc} (V) Theoretical	V_{dc} (V) Observed	I_{dc} (μA) Theoretical	I_{dc} (μA) Observed
0	40.00	0	0	0	0	0
1	39.98	5.44	0.21	0.24	5.4	6
2	39.96	10.56	0.42	0.48	10.8	11
3	39.94	16	0.63	0.64	16.3	16.5
4	39.93	21.13	0.83	0.88	21.6	21.5
5	39.91	25.28	1.04	1.04	27	27
6	39.89	31.36	1.28	1.28	32.5	33
7	39.88	36.17	1.44	1.44	37.9	37.5
8	39.86	41.6	1.68	1.68	43.2	43
9	39.84	47.68	1.8	1.76	48.7	48
10	39.83	52.81	2	1.92	54.1	53


Tek Run Trig'd
Noise Filter Off
4.00ms 0.00000 s
800mV 39.9832 Hz
5.00 V
5.00 V
2.00 V
-Width 12.51ms
+Width 12.50ms
-Width 5.446 µs
Ampl 240mV
16:31:21

(a)

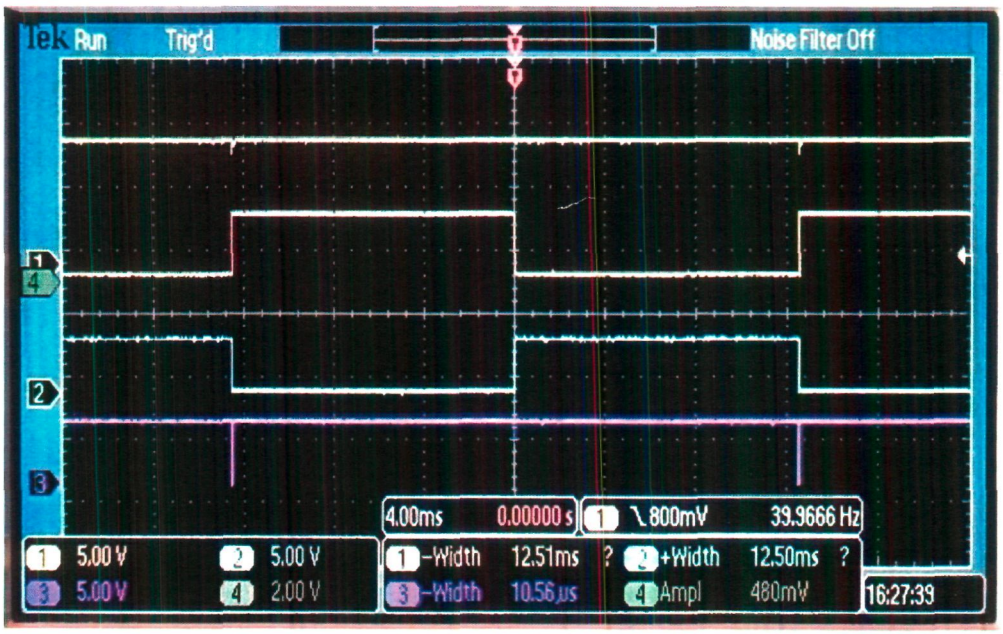
Tek Run Trig'd
Noise Filter Off
4.00ms 0.00000 s
800mV 39.9666 Hz
5.00 V
5.00 V
5.00 V
2.00 V
-Width 12.51ms
+Width 12.50ms
-Width 10.56 µs
Ampl 480mV
16:27:39

(b)

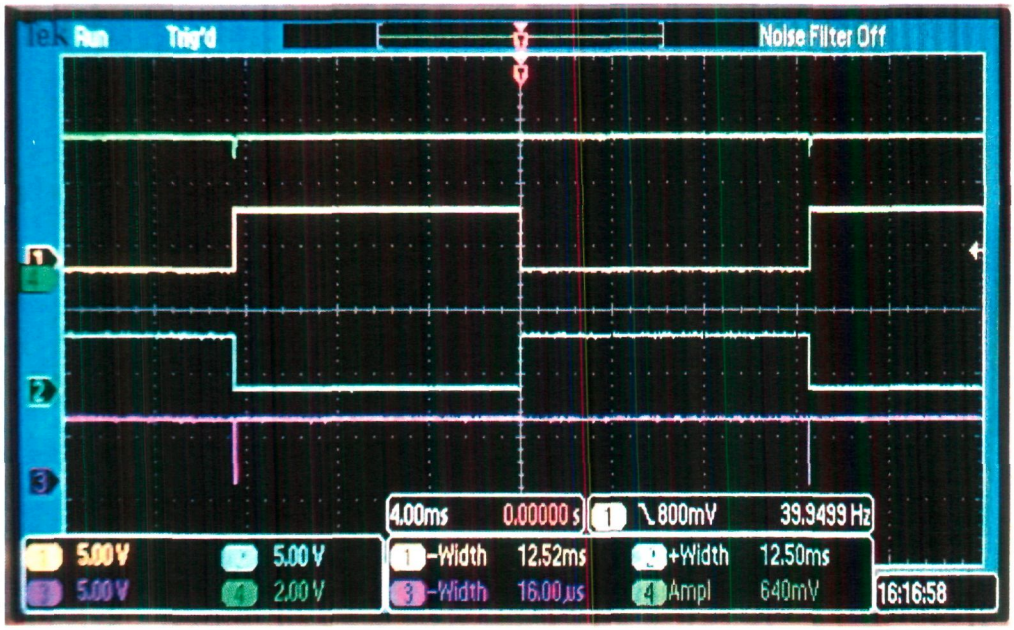
Tek Run Trig'd
Noise Filter Off
4.00ms 0.00000 s
800mV 39.9499 Hz
5.00 V
5.00 V
5.00 V
2.00 V
-Width 12.52ms
+Width 12.50ms
-Width 16.00 µs
Ampl 640mV
16:16:58

(c)

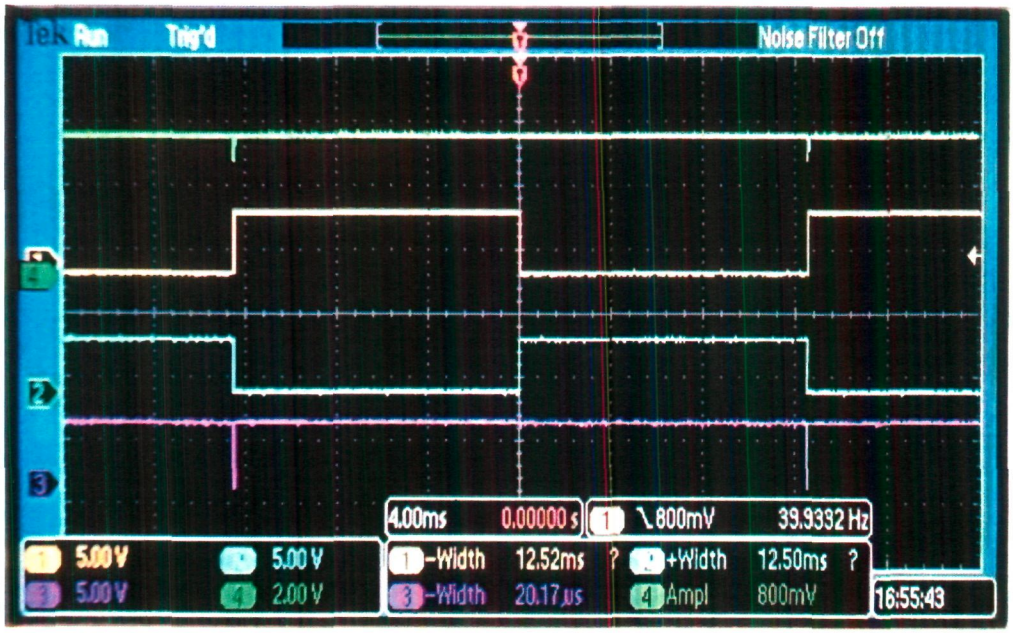
Tek Run Trig'd
Noise Filter Off
4.00ms 0.00000 s
800mV 39.9332 Hz
5.00 V
5.00 V
5.00 V
2.00 V
-Width 12.52ms
+Width 12.50ms
-Width 20.17 µs
Ampl 800mV
16:55:43

(d)

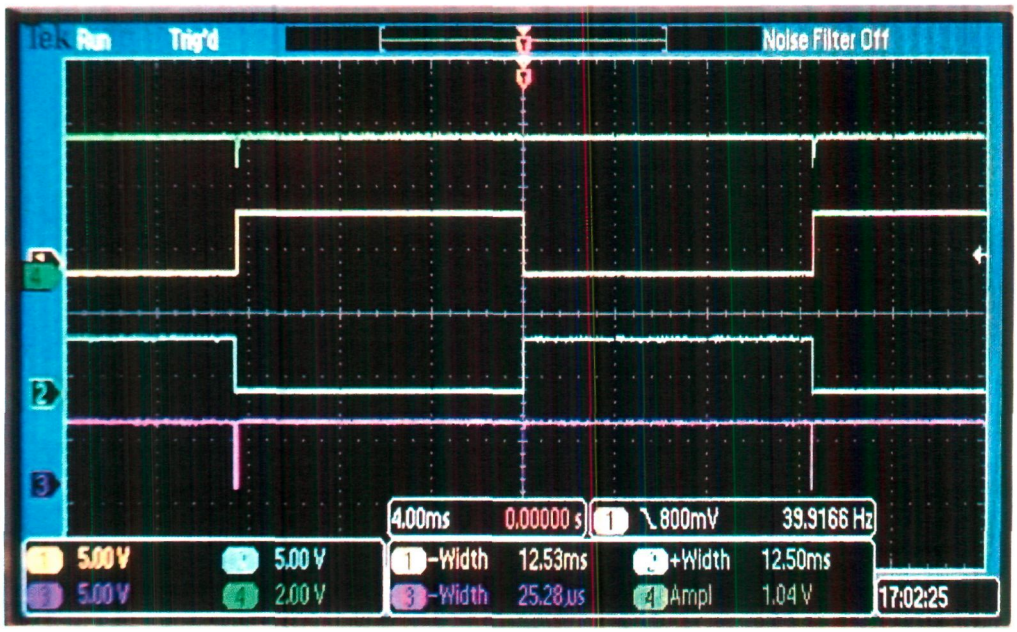
Tek Run
Trig'd
Noise Filter Off
4.00ms 0.00000 s
800mV 39.9166 Hz
5.00 V
5.00 V
5.00 V
2.00 V
-Width 12.53ms
+Width 12.50ms
-Width 25.28 µs
Ampl 1.04 V
17:02:25

(e)

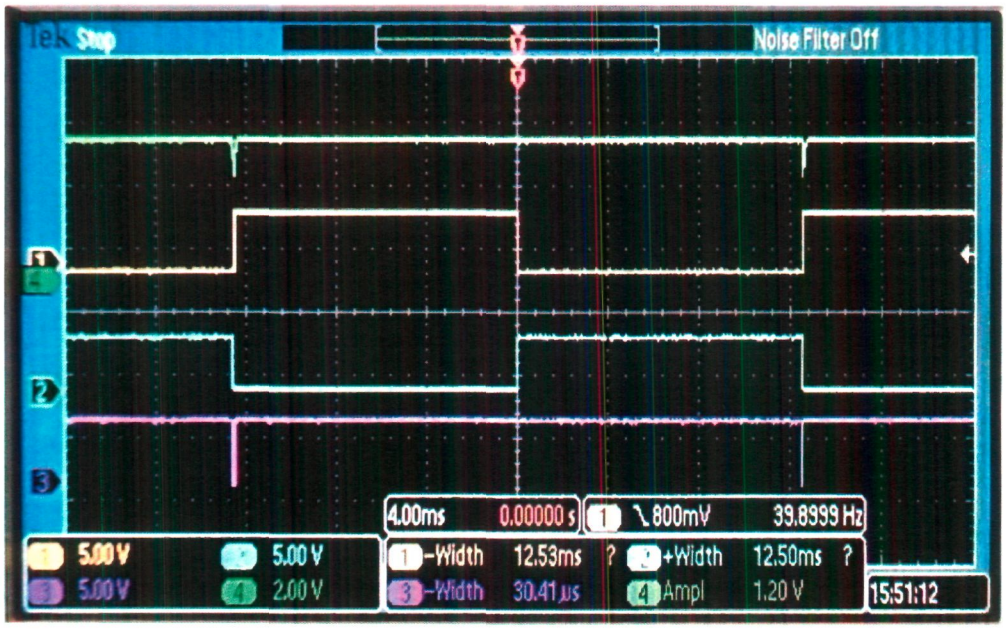
Tek Stop
Noise Filter Off
4.00ms 0.00000 s
800mV 39.8999 Hz
5.00 V
5.00 V
5.00 V
2.00 V
-Width 12.53ms
+Width 12.50ms
-Width 30.41 µs
Ampl 1.20 V
15:51:12

(f)

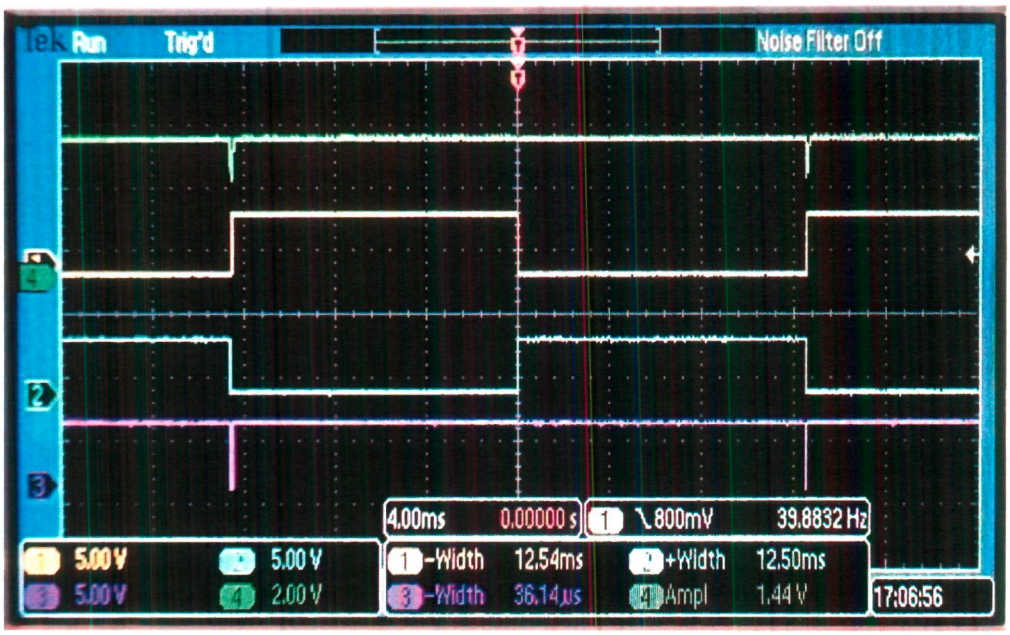
Tek Run Trig'd
Noise Filter Off
4.00ms 0.00000 s
800mV 39.8832 Hz
5.00 V
5.00 V
5.00 V
2.00 V
-Width 12.54ms
+Width 12.50ms
-Width 36.14 µs
Ampl 1.44 V
17:06:56

(g)

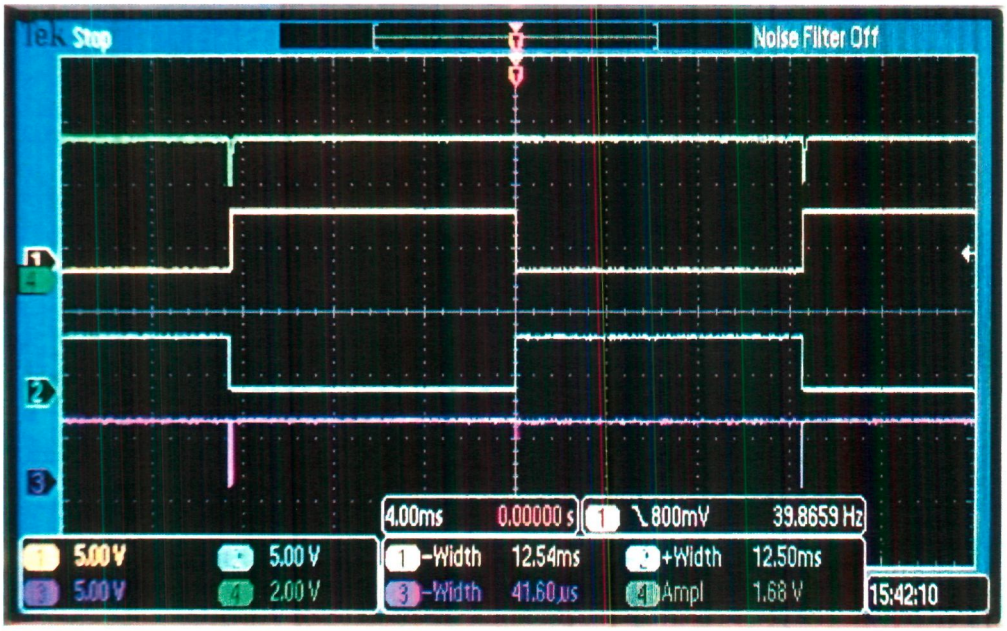
Tek Stop
Noise Filter Off
4.00ms 0.00000 s
800mV 39.8659 Hz
5.00 V
5.00 V
5.00 V
2.00 V
-Width 12.54ms
+Width 12.50ms
-Width 41.60 µs
Ampl 1.68 V
15:42:10

(h)

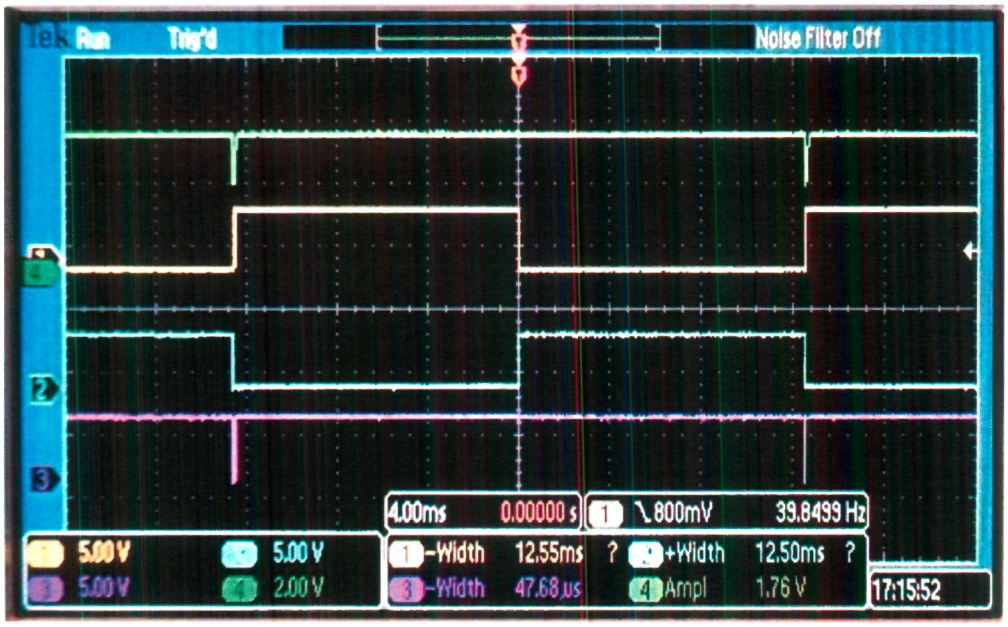

(i)

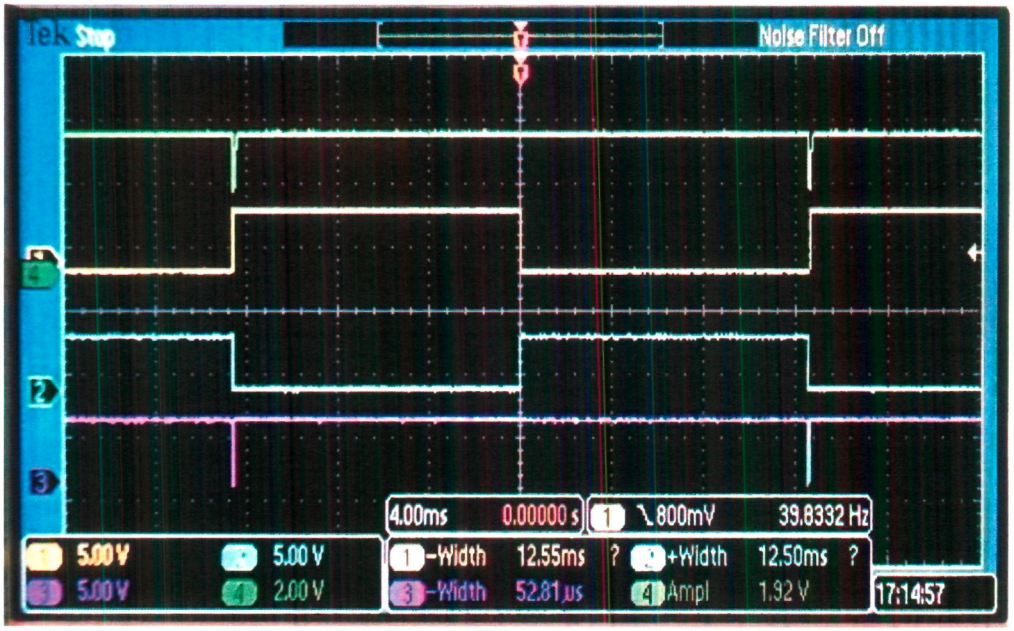

(j)

Figure 4.18 (a)-(j) Negative width of the signal V_R, T_{WR-} (Ch#1), signal Q with T_{WQ+} (Ch#2), output T_{WG-} of G-1 (Ch#3), and output of amplifier and averaging circuit V_{dc}, corresponding to 1-10 r/min (Ch#4), respectively.

4.4 Conclusion

A novel synchro and RMF-based speed measurement technique has been successfully tested for very low speed. Fast measurement of low speed up to 1 r/min has been achieved by the proposed method. The rotor output of synchro (48 V, 2-pole, 3-phase, 50 Hz) has been used for this purpose, whose output varies like a pulse width modulated signal. A linear relationship is practically found in the speed and frequency from 1 to 10 r/min. The DSO records show that the measurement of speed is accomplished within few tens of ms. Even at 1 r/min, the speed is measured at the speed of RMF (40 Hz or 2400 r/min), which is 2400 times faster than the speed of the rotating member. While the RMF completes one revolution in the air gap in 25 ms, but due to the fast measuring mechanism (half-cycle measurement), the deviation in speed is even detected within 12.5 ms. The proposed method is also compared with a conventional tachogenerator method which confirms the fast measurement of speed. The output measurand is also made available in terms of dc voltage and dc current for control applications.

Chapter 5

Rotating Magnetic Field Based Measurement of Velocity and Acceleration of Seismic Vibrations

5.1 Introduction

Earthquake is one of the prime causes of natural disasters, human losses, technological disasters, damage to heavy building structures, water delivery systems and electric power installations. The earth crust is made up of several wide, thin and rigid plates like blocks which are in constant motion with respect to each other. A series of vibrations on the earth surface are produced by the generation of elastic seismic waves due to sudden rupture within the plates during the release of accumulated strain energy [63]. The seismic vibrations (main shock and foreshocks) consist of an adverse combination of extremely high contents of velocity and acceleration superimposed over a very low frequency wave. A number of methods, based on the measurement of velocity and acceleration of seismic vibrations have been reported in the literature [87]-[90]. Conventional instruments like seismometers and accelerometers, usually measure only one parameter that is acceleration and fail to record its peak values, with good accuracy [64]-[65]. Moreover, the response of existing or conventional methods of measurement of seismic vibrations is very slow, which is of the order of several seconds [75], [90]. The findings have also revealed that there is a strong resemblance in the pattern of foreshocks and main shock [70]-[74]. However, the

present measurement of foreshocks with resolution in seconds, does not give a deep insight of the signatures of these small seismic vibrations [68]-[69]. Hence, a systematic and high resolution measurement of velocity and acceleration of these vibrations is required to interpret the pattern of waves and their anomalies accurately which is useful for proper design of buildings and structures.

In the method proposed in this chapter, a fast RMF is used to generate an EMF in the rotor circuit whose frequency depends upon the motion and/or vibration of a stepper motor coupled to the rotor of a synchro. A microprocessor based vibration generation system is developed to generate rocking motion and vibrations similar to the seismic vibrations. The vibration system vibrates the rotor of synchro back and forth, which ultimately varies the frequency and voltage in its rotor circuit. Consequently, a train of pulses with variable pulse width becomes available. A digital logic circuit is developed to measure the width of these pulses to get the instantaneous velocity of vibrations (V_I). An averaging circuit with amplifier is developed to obtain the average velocity of vibrations in terms of dc voltage. A micro ammeter is also calibrated to measure the average velocity of vibrations in terms of dc current. The values of instantaneous acceleration of vibrations (A_I) are obtained from the corresponding values of V_I. Moreover, along with an average value, the peak values of these quantities (velocity and acceleration) are obtained which are useful in proper design of earthquake resistant nuclear power plants, buildings and structures. Here, the angular speed of the rotor of synchro corresponding to the seismic vibrations is in the range of few r/min only, while the speed of RMF is 3000 r/min for a supply frequency of 50 Hz. Therefore the measurement becomes very fast and the resolution becomes very high. The high resolution measurement of small seismic vibrations (foreshocks) is helpful in a better prediction of earthquakes.

5.2 Realization of Setup for the Measurement of Velocity of Seismic Vibrations

In the proposed technique, for the measurement of velocity and acceleration of seismic vibrations, a synchro is used whose rotor is attached with the vibration generation system (Figure 5.1). The three-phase stator winding of the synchro is energized by a 50 Hz voltage signal from a stable arbitrary function generator (F.G). This signal is supplied to a centre-tapped transformer whose output is applied to a single-phase to three-phase conversion circuit, consisting an RC network (R=100 kΩ and C = 0.1μF), to generate a balanced three-phase, 50 Hz voltages V_1, V_2, and V_3 (Figure 5.2). These three voltages are attenuated to a value of about 100 mV (V_4, V_5, and V_6), before feeding into three audio power amplifiers (LM 384N) as shown in Figure 5.3. The outputs of these three amplifiers, V_7, V_8 and V_9, are applied to the stator winding of synchro, to produce a sinusoidal signal V_r with frequency f_r in the rotor winding of synchro (Figure 5.4).

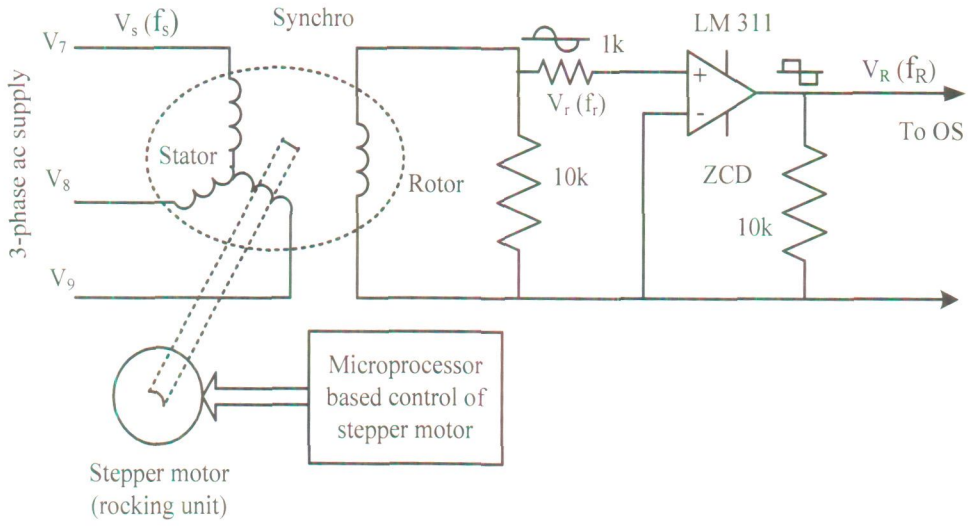

Figure 5.1 Microprocessor based vibration generation and measurement setup.

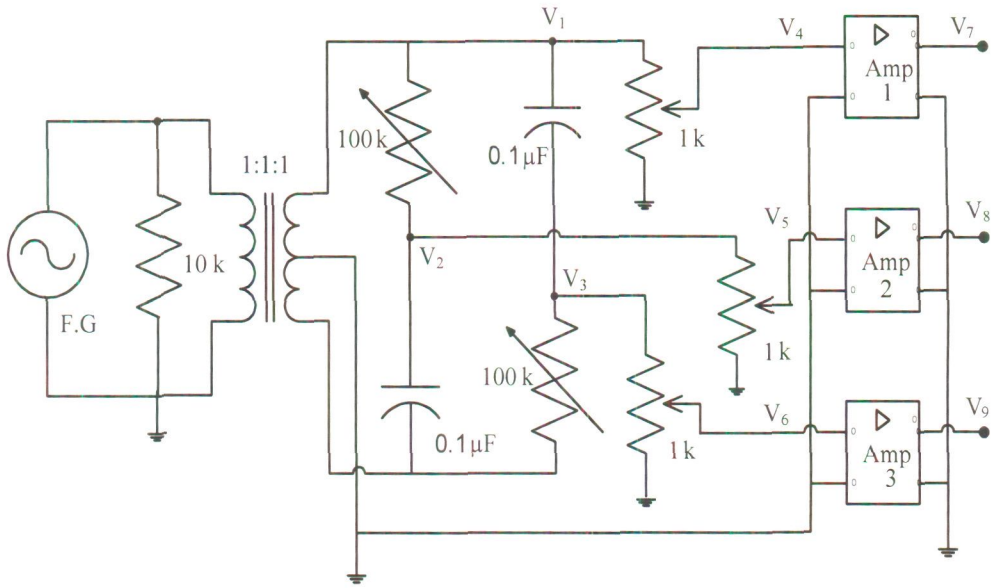

Figure 5.2 Single-phase to three-phase voltage conversion system.

Figure 5.3 Waveforms V_4, V_5, and V_6 at the input of power amplifiers (CH#1, CH#2 and Ch#3).

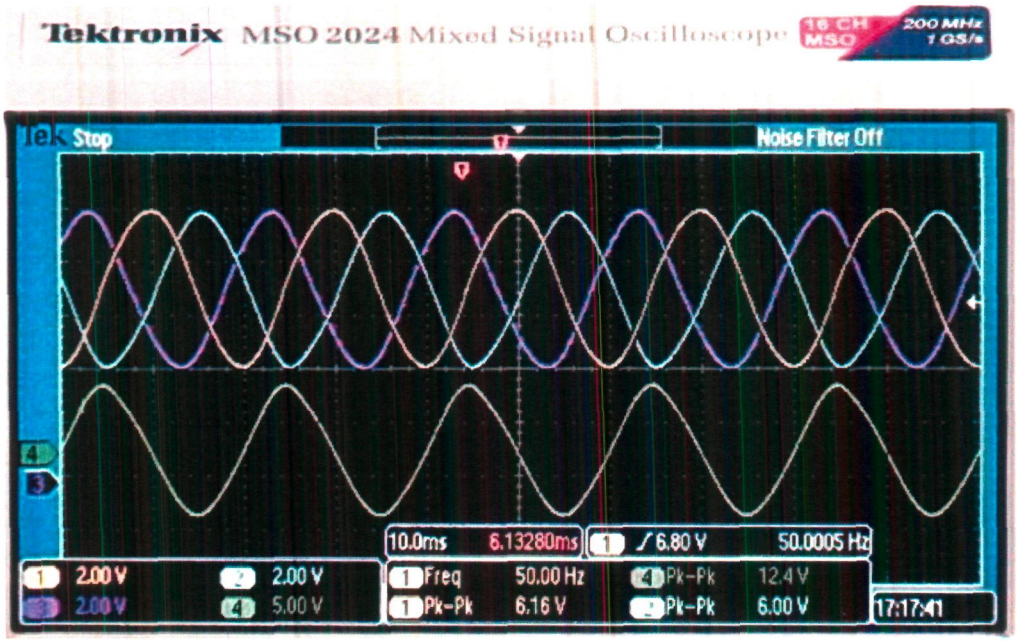

Figure 5.4 Three phase voltages V_7, V_8, and V_9 at the stator winding of synchro (CH #1, CH #2, and Ch #3) and voltage at rotor winding of synchro V_r (CH #4).

5.3 Experimental Results and Discussion

The seismic waves are generated by aircraft impacts, collapse of a large building, underground nuclear explosion and exploding dynamites. But these vibrations are not feasible or allowed for conducting tests. Another method which is generally used is to place a small brick work over a metal platform. That metal platform is given large vibrations using heavy electrical machinery. The instruments are attached with the brick work to study the behavior of vibrations. These instruments are connected to computers in order to record the output. Another method of seismic vibration generation being used in a research institution is by a Shake Table [102]. But these methods are very costly, difficult to realize, non portable, inaccurate and require large installation area and huge seismographic stations.

In order to mechanically simulate seismic vibrations in the laboratory, the records (velocity waveforms) of various earthquakes are investigated [87]-[90].

Some of these earthquake waveforms [2003 Lefkada (Greece), 1994 Northridge (USA), 1992 Landers (USA), 1987 Whittier Narrows (USA)] are taken as reference for the simulation of seismic vibrations [90], as shown in Figure 5.5 (a)-(d). A microprocessor based system is developed to practically realize vibrations which resemble seismic vibrations of these earthquakes. The microprocessor is programmed to control the movement of a stepper motor which generates vibrations with velocity in the range of -20 cm/s to +20 cm/s. The back and forth rotation of stepper motor generates a variable angular movement in both directions with a frequency of one Hz [Figure 5.6 (a)-(b)]. The generated vibrations are having a velocity and frequency similar to the reference seismic waveforms [90]. The stepper motor is coupled to the rotor of a synchro. The fast back and forth movement of different angular span, which resembles the seismic vibrations, is transmitted to the rotor of the synchro. Consequently, this angular movement varies the frequency/time period of rotor voltage of synchro. Thereby, a pulse train of variable pulse width is produced and recorded. Corresponding to the value of each pulse width, V_I is calculated. A waveform with the variation of V_I is shown in Figure 5.6 (a). The same waveform is shown at an enlarged scale in Figure 5.6 (b). This pattern resembles the velocity waveform patterns of earthquakes shown in Figure 5.5 (a)-(d), and confirms the validity of the proposed system for the measurement of actual seismic vibrations. For more clarity, the pattern of variation of V_I, over one cycle, covering a time span of 1 second is shown in Fig 5.7. The proposed method measures 50 values of V_I in one second with a resolution of 20 ms, whereas the resolution of existing methods is in the range of seconds (Figure 5.5). Therefore, it captures those peaks of velocity of vibrations (within 20 ms) which are often missed by conventional measurement systems due to their poor resolution. The details of experiment for generation and measurement of V_I are explained in the following section.

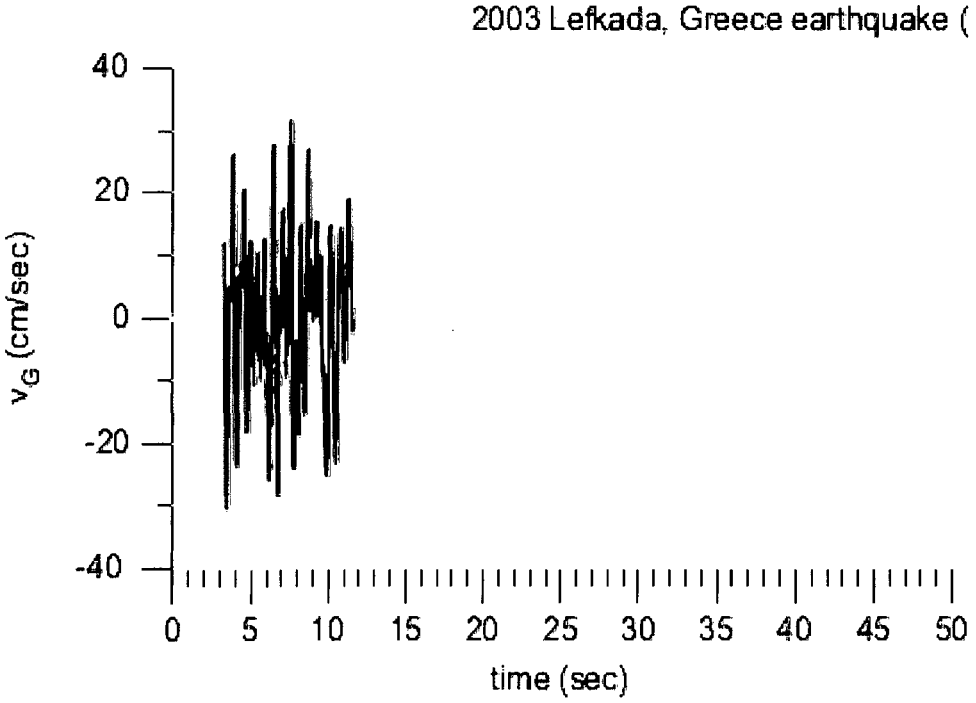
2003 Lefkada, Greece earthquake (
40
20
0
-20
-40
v_G (cm/sec)
0
5
10
15
20
25
30
35
40
45
50
time (sec)

(a)

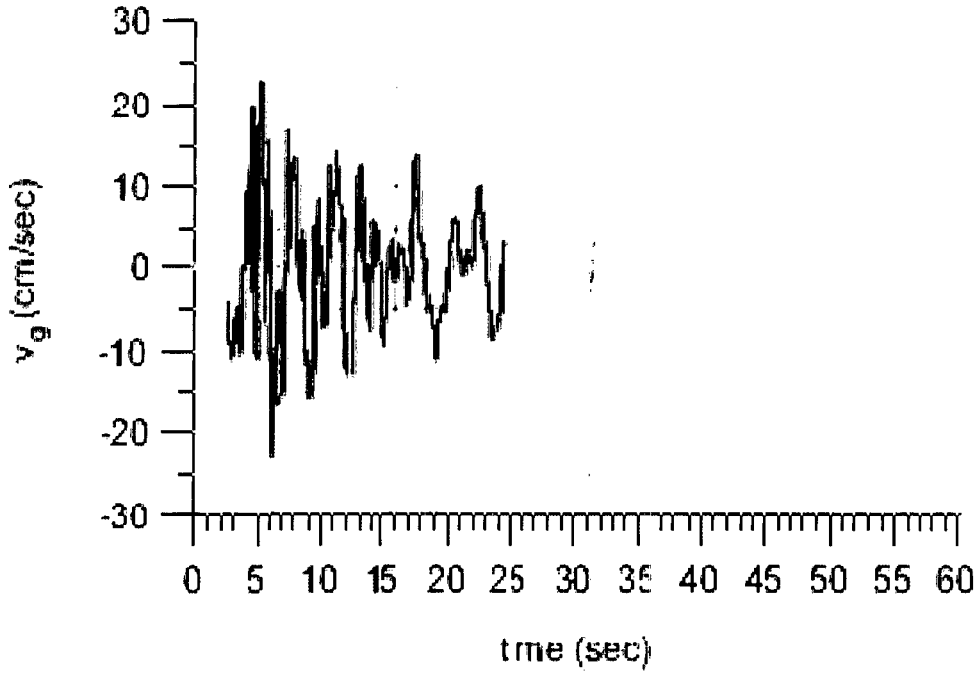
30
20
10
0
-10
-20
-30
v_g (cm/sec)
0
5
10
15
20
25
30
35
40
45
50
55
60
time (sec)

(b)

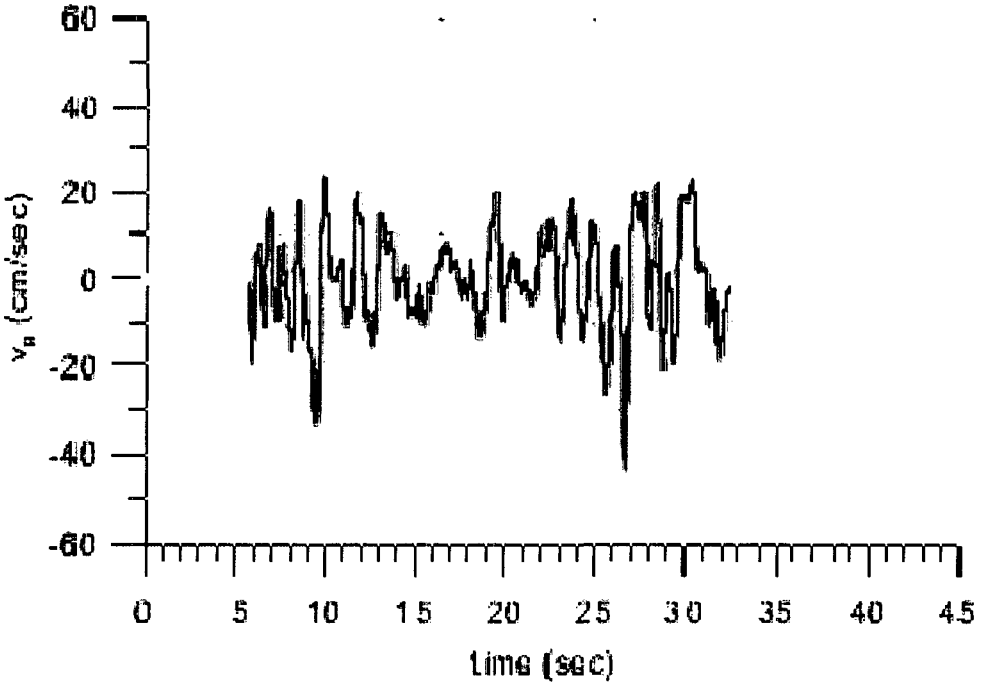

(c)

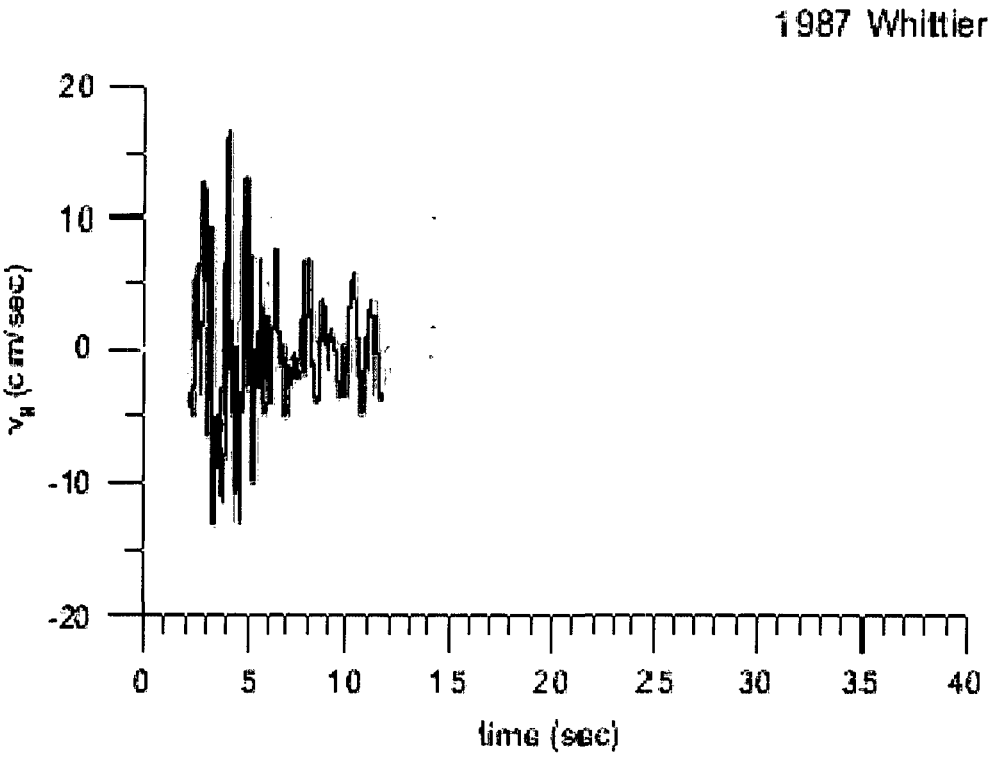

(d)

Figure 5.5 (a)-(d) Velocity waveforms of seismic vibrations of earthquakes [2003 Lefkada (Greece), 1994 Northridge (USA), 1992 Landers (USA), and 1987 Whittier Narrows (USA)].

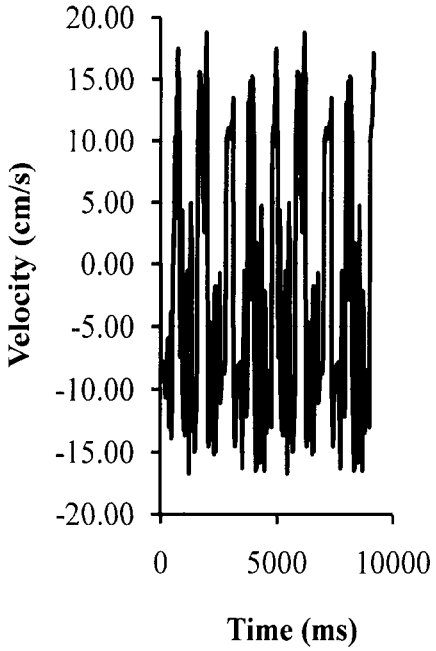

(a)

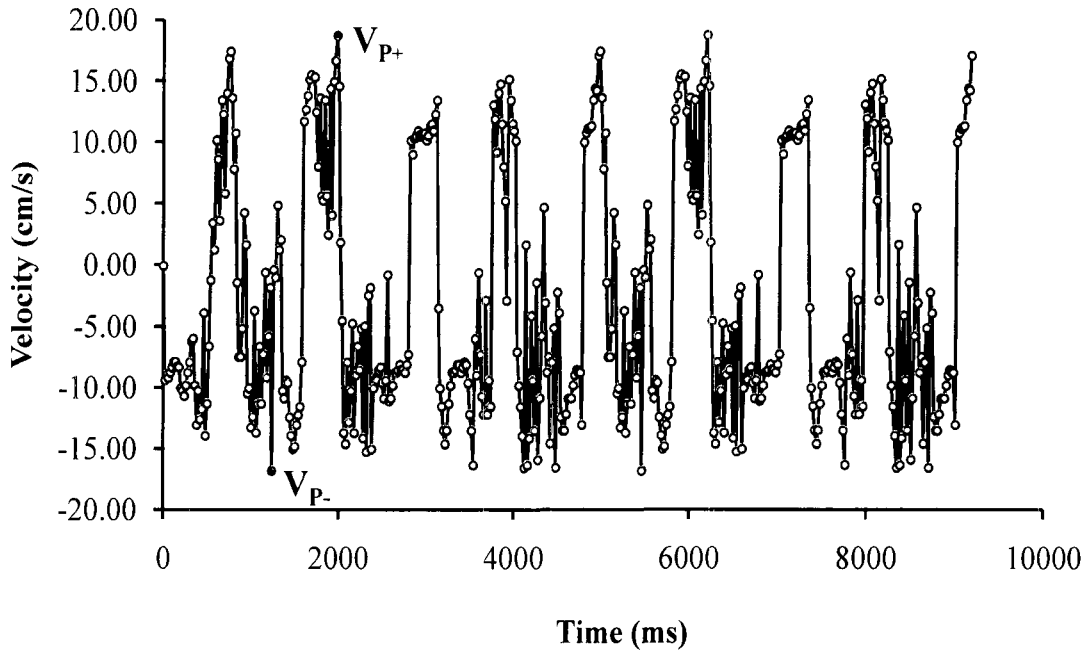

(b)

Figure 5.6 (a)-(b) The pattern with the variation of instantaneous velocity of mechanically generated seismic vibrations using microprocessor, at **(a)** normal scale **(b)** enlarged scale.

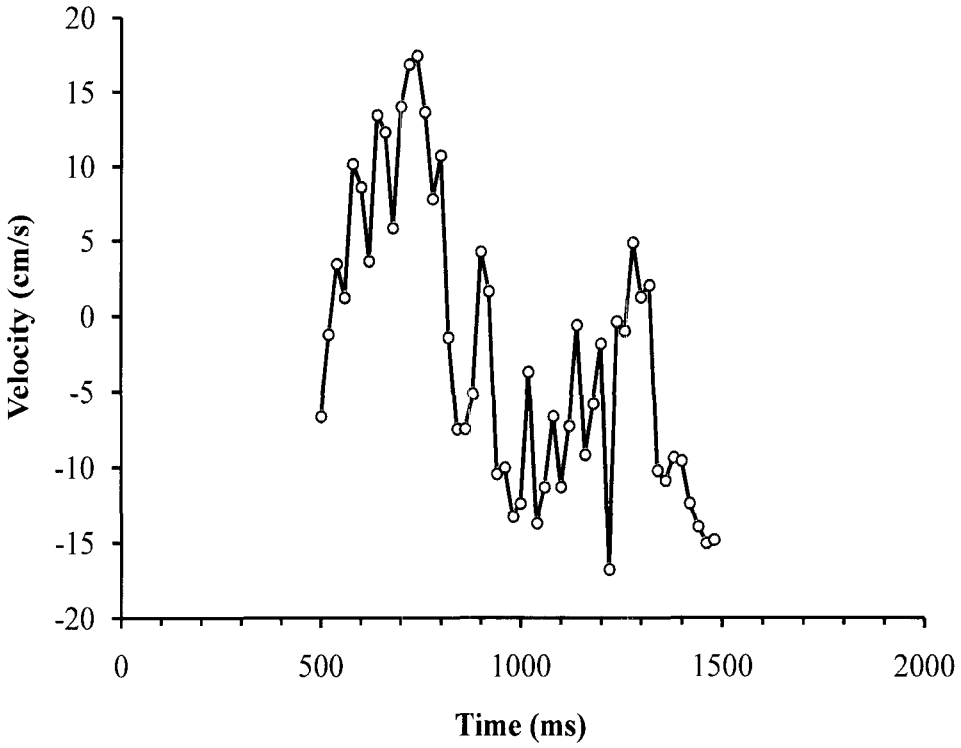

Figure 5.7 The pattern for the variation of instantaneous velocity of mechanically generated seismic vibrations, over one cycle, covering a time span of 1 second.

5.3.1 When the Vibrating System Is Stationary

As long as the vibrating system is stationary, the speed of rotor of the synchro is zero. The synchro acts as a transformer. The frequency of rotor EMF f_r is equal to the frequency of stator voltage f_s. The signal V_r is now applied to a ZCD. It produces a rectangular waveform V_R of frequency f_R where $f_R = f_r$, as shown in Figure 5.8. The positive going transition (PGT) of signal V_R is used to trigger an OS as shown in Figure 5.9. It gives an output signal Q and its complement Q′ with stable positive and negative widths of 10 ms (T_{WQ+} and T_{WQ-} respectively). The signals V_R and Q′ are applied to an EX-OR gate (G-1). The output of G-1 remains HIGH as the positive width (T_{WR+}) of signal V_R is equal to negative width (T_{WQ-}) of signal Q′ and vice versa.

Let

f_R = frequency of signal V_R at the output of ZCD ($f_R = f_r$)

f_s = frequency of stator input voltage or current, in Hz

T_R = time period of the signal V_R at the input of OS

T_{WR+} = positive width of the signal V_R

T_{WQ+} = positive width of signal Q

T_{WQ-} = negative width of signal Q′

T_{WG-} = negative width of the pulse at the output of G-1

Also, $T_{WG-} = T_{WR+} - T_{WQ-}$ (5.1)

When the Vibrating System Is Stationary (n_r = 0), then from (4.1)

$f_R = f_r = f_s = 50$ Hz

$T_R = (1/f_R) = 20$ ms

$T_{WR+} = (T_R / 2) = (1/2f_R) = 10$ ms

$T_{WQ-} = 10$ ms $= 0.01$ seconds

From (5.1)

$T_{WG-} = (1/2f_R) - T_{WQ-}$ (5.2)

Hence, $T_{WG-} = 10 - 10 = 0$

Therefore, the output of gate G-1 = 1 (HIGH)

The waveforms V_r, V_R, Q′ and T_{WG-} are also shown in the DSO records (Figure 5.10).

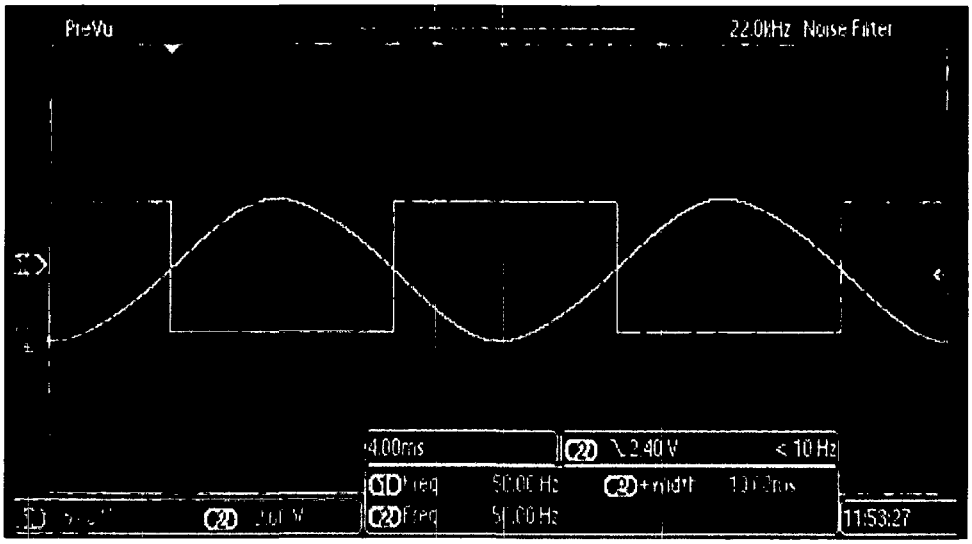

Figure 5.8 Output of rotor V_r, f_r of synchro (Ch#1) and output of ZCD V_R, f_R (Ch#2) at 50 Hz.

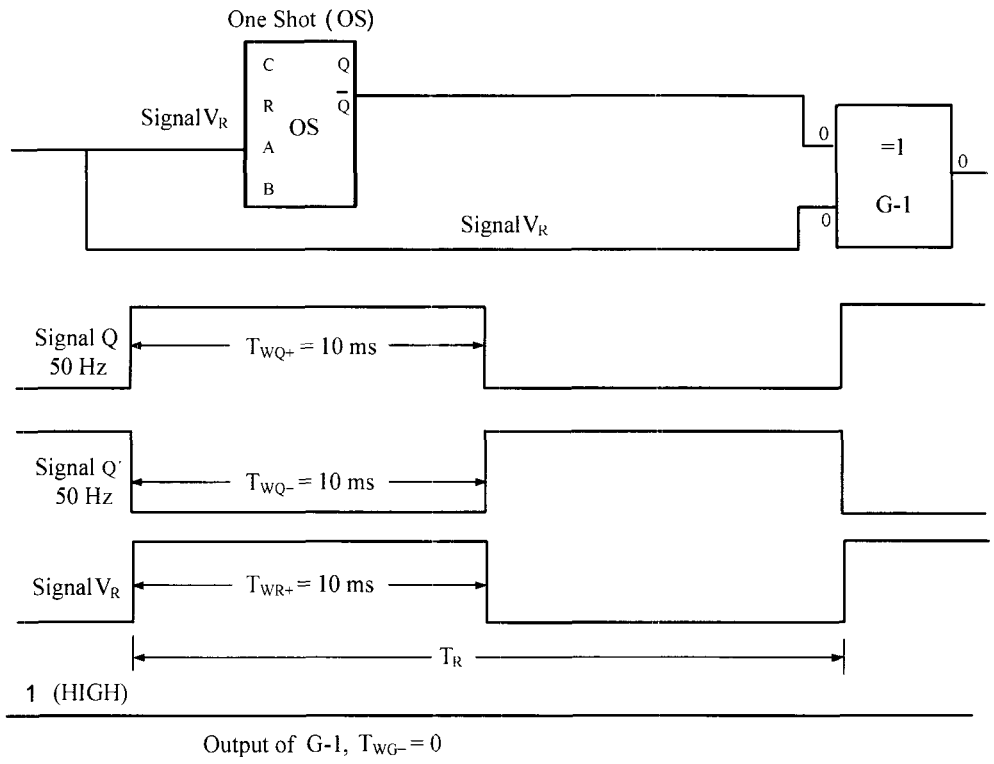

Figure 5.9 Waveforms of signals, V_R, Q, Q′ and output T_{WG-}, when the vibrating system is stationary.

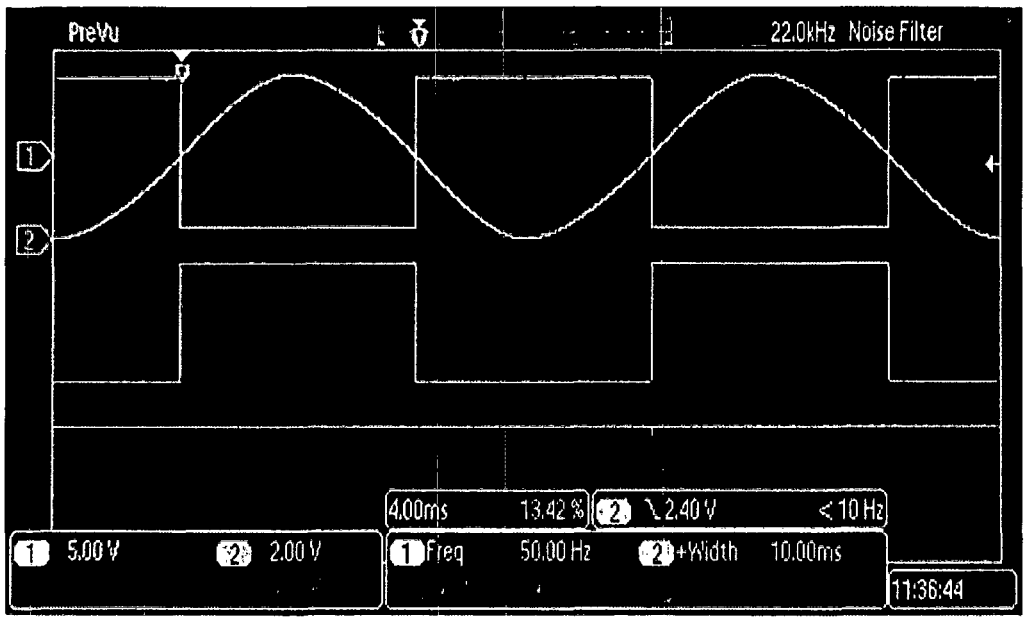

Figure 5.10 Output of synchro V_r (Ch#1), Output of ZCD V_R (Ch#2), output of OS, Q′ (Ch#3), and output of G-1 (Ch#4), at 50 Hz when the vibrating system is stationary.

5.3.2 When the System Starts Vibrating

Now, the stepper motor is vibrated using microprocessor. The rotor of the synchro moves back and forth due to its attachment with the vibrating body (stepper motor). The RMF revolves in the air gap at a very fast speed of 3000 r/min for a 50 Hz, 2 pole machine (synchro). Even a very small angular movement of rotor (one tenth of a radian per second) generates an EMF, of frequency f_r in the rotor circuit which is higher or lower than 50 Hz, depending upon the direction of vibrations. Consequently, a negative pulse appears within 20 ms, for every instantaneous change in the movement of rotor, whose width is proportional to the velocity of the vibrations [Figure 5.11 (a)-(b)]. The associated time period T_R, (or $1/f_R$) and hence the positive width T_{WR+} of signal V_R at the output of ZCD varies instantaneously. The PGT of signal V_R triggers OS to produce a signal Q and its compliment Q′ with stable positive and negative widths of 10 ms (T_{WQ+} and T_{WQ-} respectively). When the signals V_R and Q′ are applied to G-1, a pulse T_{WG-} with a negative width is generated at its output on every trailing edge of signal V_R (Figure 5.11). The width of these pulses depends on the instantaneous speed of rotor of synchro or V_I, at different instants of time. Depending upon the directions of angular movement, the pulses with maximum negative widths are proportional to peak positive and negative velocity of vibrations (V_{P+} and V_{P-}). The calculations for the measurement of V_I with various parameters are as follows.

The pulse width T_{WG-} of instantaneous pulses is obtained using (5.2), therefore

$$T_{WG-} = (1/2f_R) - 0.01$$

$$f_R = f_r = \frac{1}{0.02 + 2T_{WG-}} \qquad (5.3)$$

Equating (5.3) and (4.1), and solving for n_r, the instantaneous speed for any pulse width at the output of gate G-1 is obtained as follows;

$$\frac{1}{0.02 + 2T_{WG-}} = f_s - \frac{n_r P}{120} \qquad (5.4)$$

For, P = 2 and f_s = 50 Hz, from (5.4),

$$n_r = 3000 - \frac{60}{0.02 + 2\,T_{WG-}} \qquad (5.5)$$

V_l is calculated using the basic relationship

$V_l = \omega\, r$

$$V_l = \frac{2\pi \times n_r}{60}\, r \qquad (5.6)$$

ω = angular speed of rotor of synchro in radian per second

r = radius of rotor of synchro = 1.3 cm

$$V_l = 0.136190 \times n_r \qquad (5.7)$$

Now, from (5.7) and (5.5)

$$V_l = 408.57 - \frac{8.17}{0.02 + 2T_{WG-}} \quad cm/sec \qquad (5.8)$$

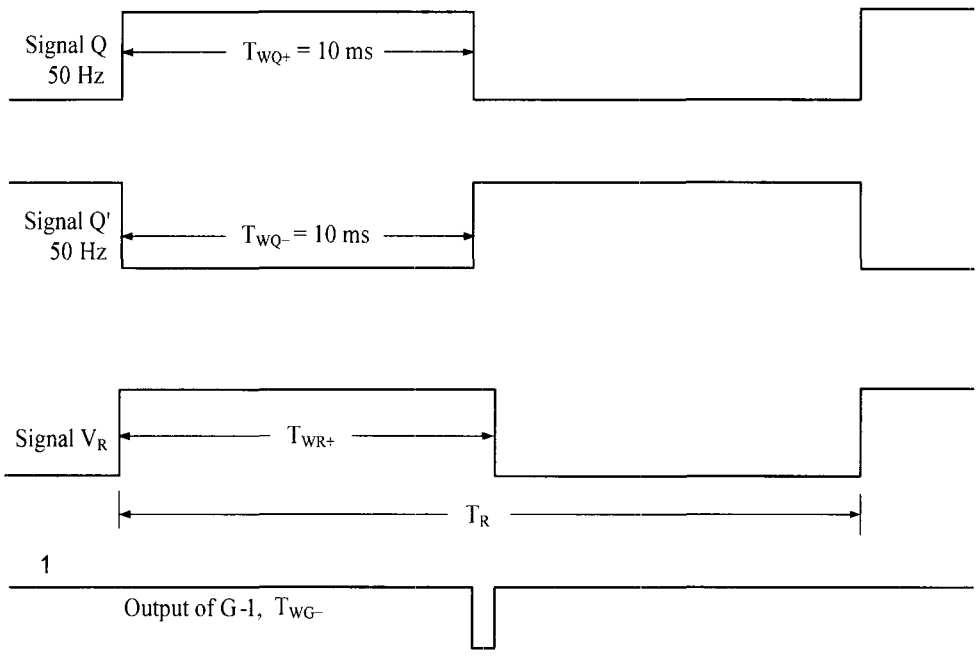

(a)

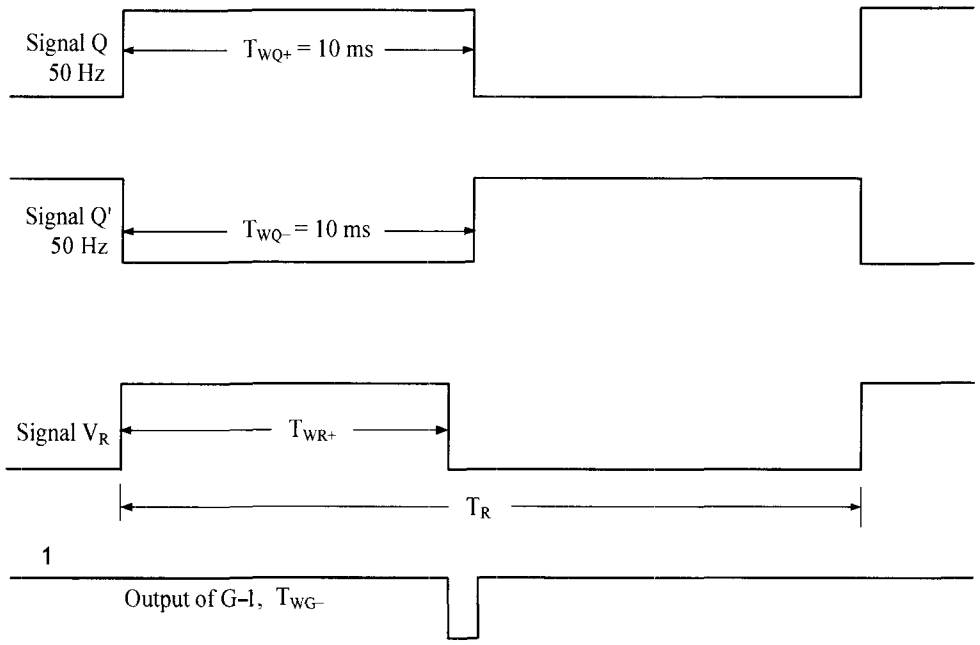

(b)

Figure 5.11 (a)-(b) Waveforms of signals V_R, Q, Q′ and output of G-1, when the rotor of synchro vibrates **(a)** in one direction **(b)** in the other direction.

The voltage waveforms at the output of rotor circuit of synchro V_r, output of ZCD V_R, output of OS Q′, and output of G-1, are recorded by DSO [Figures 5.12 (a)]. The same waveforms are shown at an enlarged scale in Figures 5.12 (b). Table 5.1 shows the measurement results of V_I and A_I. Some of these results with the measurement details of T_{WR+}, T_{WQ-} and T_{WG-} are shown in Figures 5.13 (a)-(j) and **highlighted** in Table 5.1. The data of one second shows 50 values of V_I (1000 ms /20 ms = 50), at intervals of 20 ms [Table 5.1, Figure 5.7]. It shows a significant variation of V_I, even within one second, which is normally not sensed and recorded by the conventional seismic vibration measurement systems. The values of V_{P+} and V_{P-}, corresponding to the maximum widths of T_{WG-} are found using (5.8) as **+18.78 cm/s** and **−16.73 cm/s** respectively, and **marked** in Figure 5.6 (b).

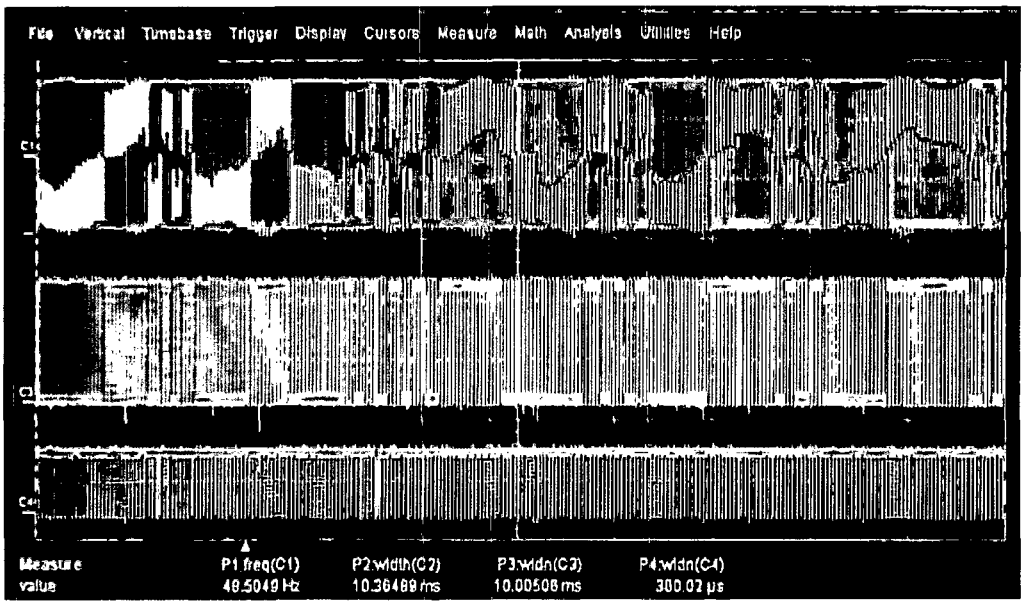

(a)

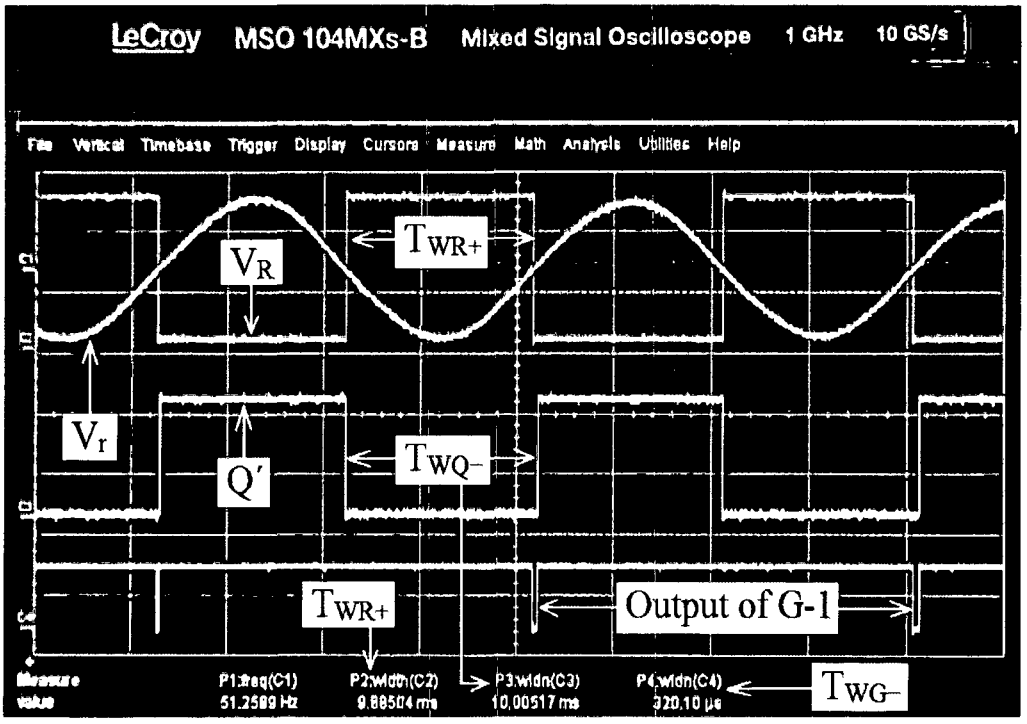

(b)

Figures 5.12 (a)-(b) Output of rotor circuit of synchro V_r (Ch#1), output of ZCD V_R with T_{WR+} (Ch#2), output of OS Q′ with T_{WQ-} (Ch#3), and output of G-1 with T_{WG-} (Ch#4), at **(a)** normal scale **(b)** enlarged scale.

Table 5.1: Results of the mechanically simulated seismic vibration measurement

S.No.	Time (ms)	T_{WR+} (ms)	T_{WQ-} (ms)	T_{WG-} (μs) = $T_{WR+} - T_{WQ-}$ (observed)	V_I (cm/s)	A_I (cm/s^2)
1	**500**	**09.84506**	**10.00515**	**-160.07**	**-06.56**	**234.59**
2	520	09.97161	10.00006	-030.09	-01.16	269.92
3	540	10.08992	10.00515	084.77	03.50	233.33
4	560	10.03483	10.00516	029.91	01.29	-110.78
5	580	10.25999	10.00498	254.83	10.22	446.76
6	600	10.21999	10.00511	214.94	08.67	-077.90
7	620	10.34010	10.00012	339.71	13.50	490.09
8	**640**	**10.31488**	**10.00512**	**309.99**	**12.35**	**-057.19**
9	660	10.14992	10.00520	144.43	05.89	-323.36
10	680	10.35995	10.00516	354.89	14.07	409.22
11	700	10.43485	10.00513	429.93	16.91	141.91
12	720	10.44992	10.00515	444.86	17.47	027.99
13	**740**	**10.34989**	**10.00508**	**345.25**	**13.69**	**-189.03**
14	760	10.19992	10.00497	194.93	07.88	-290.36
15	780	10.27504	10.00517	269.87	10.80	146.19
16	800	09.96985	10.00503	035.09	-01.37	-608.65
17	820	09.81996	10.00009	179.86	-07.41	-302.17
18	840	09.81996	10.00006	179.84	-07.41	000.04
19	**860**	**09.87481**	**09.99999**	**125.08**	**-05.10**	**115.44**
20	880	10.11004	10.00511	105.01	04.32	470.86
21	900	10.04331	10.00539	039.91	01.69	-131.06
22	920	09.75504	10.00521	249.79	-10.40	-604.46
23	940	09.76504	10.00520	239.77	-09.97	021.51
24	960	09.69002	10.00520	314.59	-13.20	-161.66
25	**980**	**09.70996**	**10.00510**	**295.24**	**-12.34**	**043.05**
26	1000	09.91413	10.00502	089.92	-03.64	435.05
27	1020	09.67992	10.00512	324.84	-13.65	-500.43
28	1040	09.73491	10.00502	269.87	-11.26	119.26

29	1060	09.84506	10.00516	159.93	-06.57	234.53
30	**1080**	**09.73500**	**10.00521**	**269.98**	**-11.25**	**-234.12**
31	1100	09.82999	10.00135	174.84	-07.20	202.62
32	1120	09.98496	10.00015	014.93	-00.54	332.93
33	1140	09.78250	10.00566	0219.7	-09.11	-428.28
34	1160	09.86491	10.00510	139.93	-05.73	168.95
35	1180	09.95492	10.00011	044.86	-01.77	197.82
36	**1200**	**09.60989**	**10.00524**	**395.25**	**-16.73**	**-747.82**
37	1220	09.99493	10.00520	009.86	-00.33	819.70
38	1240	09.97496	10.00007	024.78	-00.94	-030.58
39	1260	10.12500	10.00493	119.76	04.90	292.45
40	1280	10.03492	10.00512	030.03	01.29	-180.56
41	**1300**	**10.05515**	**10.00521**	**050.20**	**02.10**	**040.28**
42	1320	09.75999	10.00503	244.79	-10.18	-613.96
43	1340	09.74505	10.00508	259.78	-10.83	-032.22
44	1360	09.77981	10.00503	224.78	-09.32	075.08
45	1380	09.77397	10.00511	229.96	-09.54	-011.08
46	**1400**	**09.70996**	**10.00510**	**295.24**	**-12.35**	**-140.32**
47	1420	09.67504	10.00506	329.92	-13.86	-075.46
48	1440	09.64976	10.00515	354.85	-14.96	-054.92
49	1460	09.65492	10.00515	349.78	-14.74	011.13
50	**1480**	**09.69487**	**10.00519**	**310.01**	**-12.99**	**087.50**


File Vertical Timebase Trigger Display Cursors Measure Math Analysis Utilities Help
Measure value
P2:width(C2) 9.84506 ms
P3:width(C3) 10.00515 ms
P4:width(C4) 160.07 µs

(a)

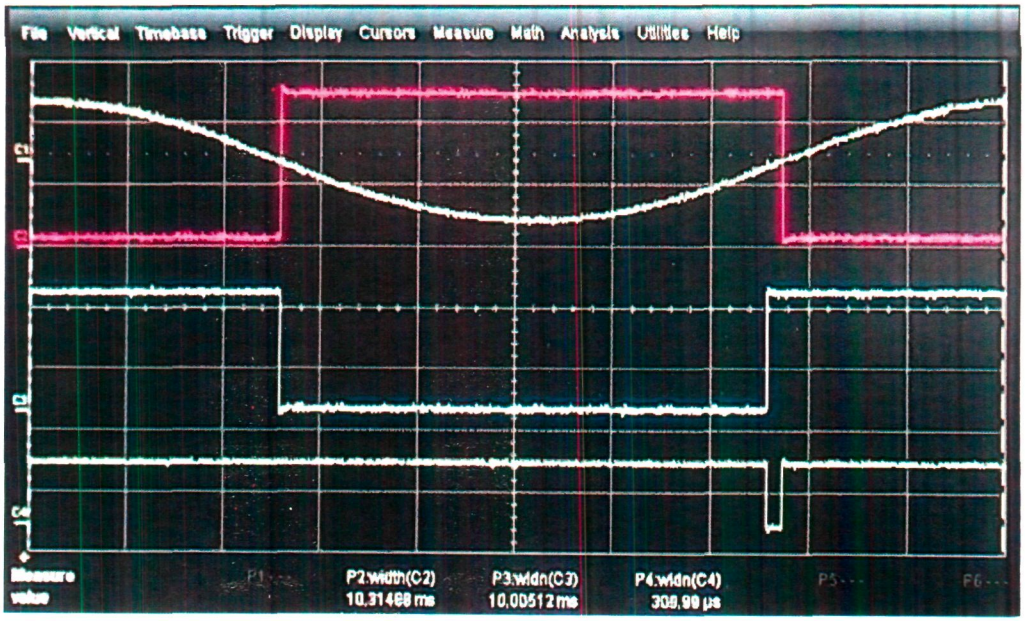
File Vertical Timebase Trigger Display Cursors Measure Math Analysis Utilities Help
Measure value
P2:width(C2) 10.31468 ms
P3:width(C3) 10.00512 ms
P4:width(C4) 309.99 µs

(b)

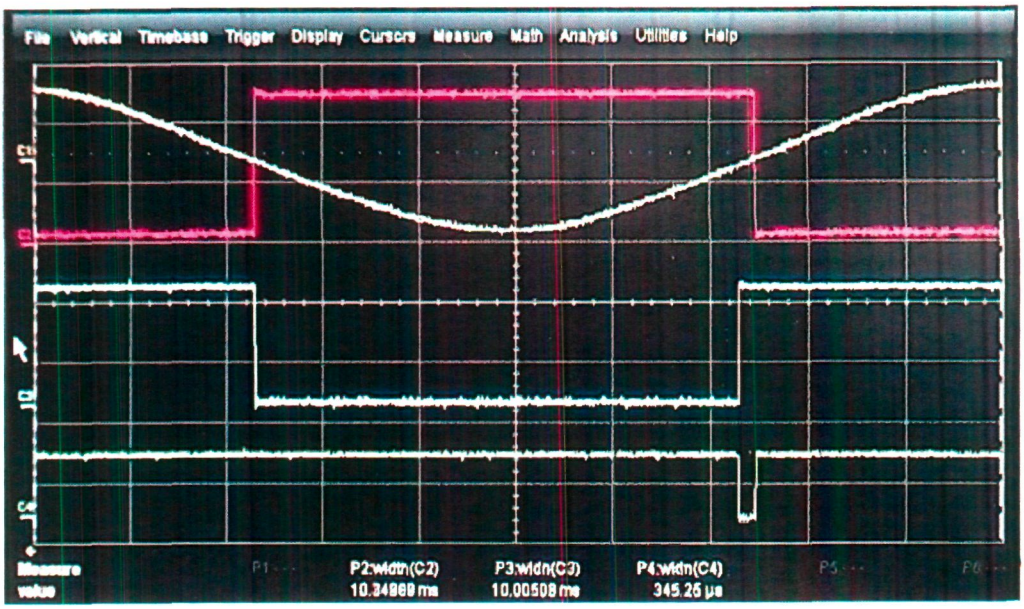
File Vertical Timebase Trigger Display Cursors Measure Math Analysis Utilities Help
P2:width(C2)
10.34869 ms
P3:widh(C3)
10.00508 ms
P4:widh(C4)
345.25 µs

(c)

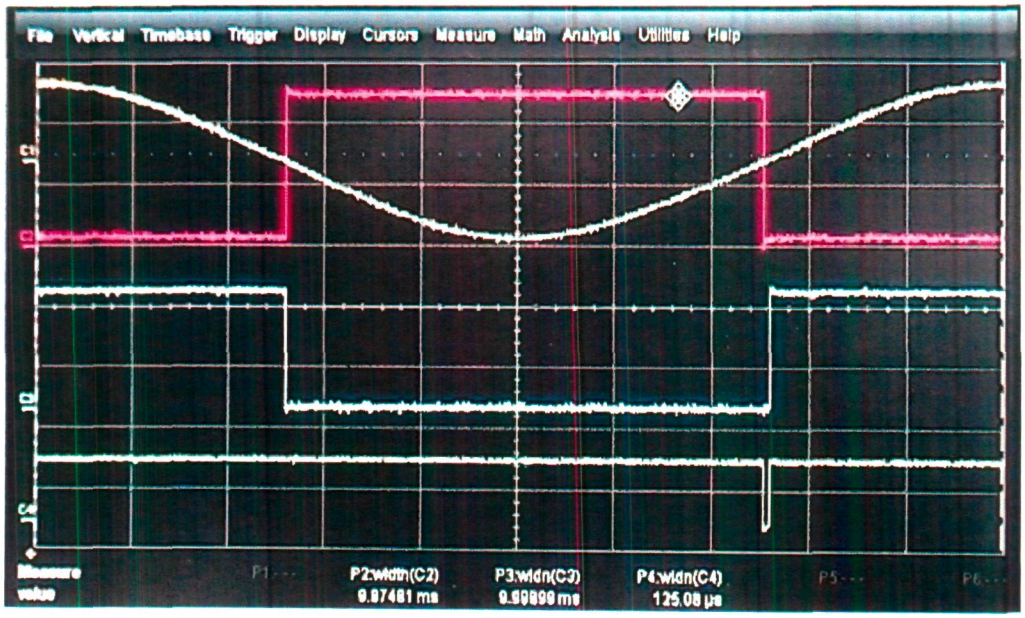
File Vertical Timebase Trigger Display Cursors Measure Math Analysis Utilities Help
P2:width(C2)
9.97481 ms
P3:widh(C3)
9.99899 ms
P4:widh(C4)
125.08 µs

(d)

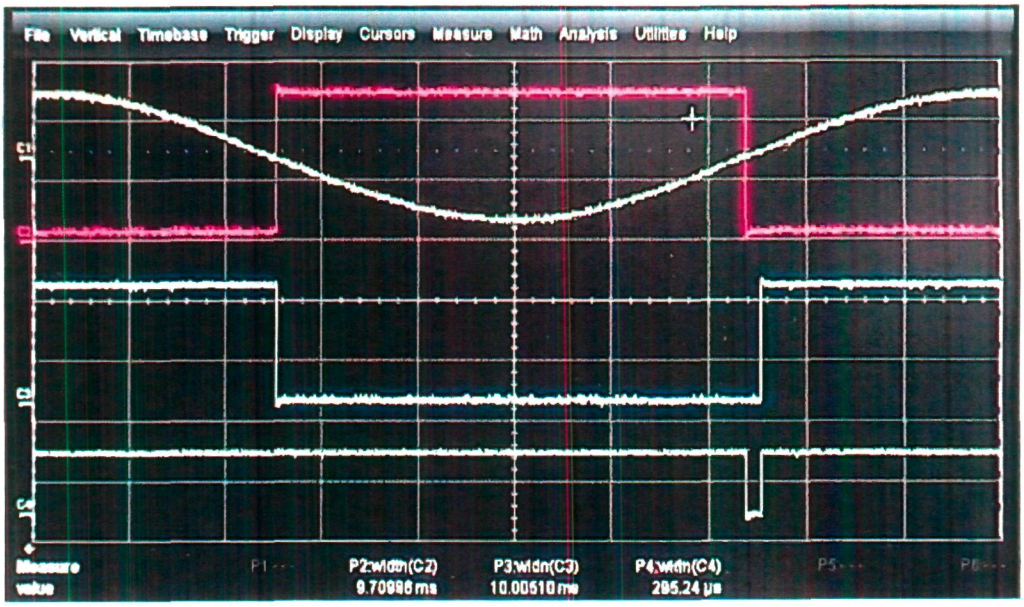
File Vertical Timebase Trigger Display Cursors Measure Math Analysis Utilities Help
Measure
value
P2:widn(C2)
9.70998 ms
P3:widn(C3)
10.00510 ms
P4:widn(C4)
285.24 µs

(e)

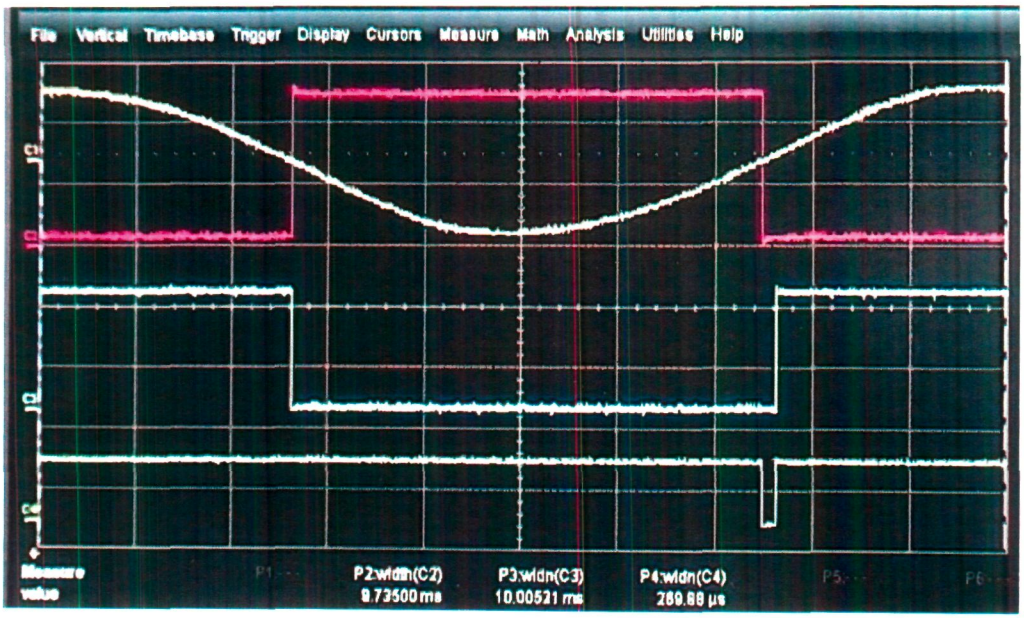
File Vertical Timebase Trigger Display Cursors Measure Math Analysis Utilities Help
Measure
value
P2:widn(C2)
9.73500 ms
P3:widn(C3)
10.00521 ms
P4:widn(C4)
289.68 µs

(f)

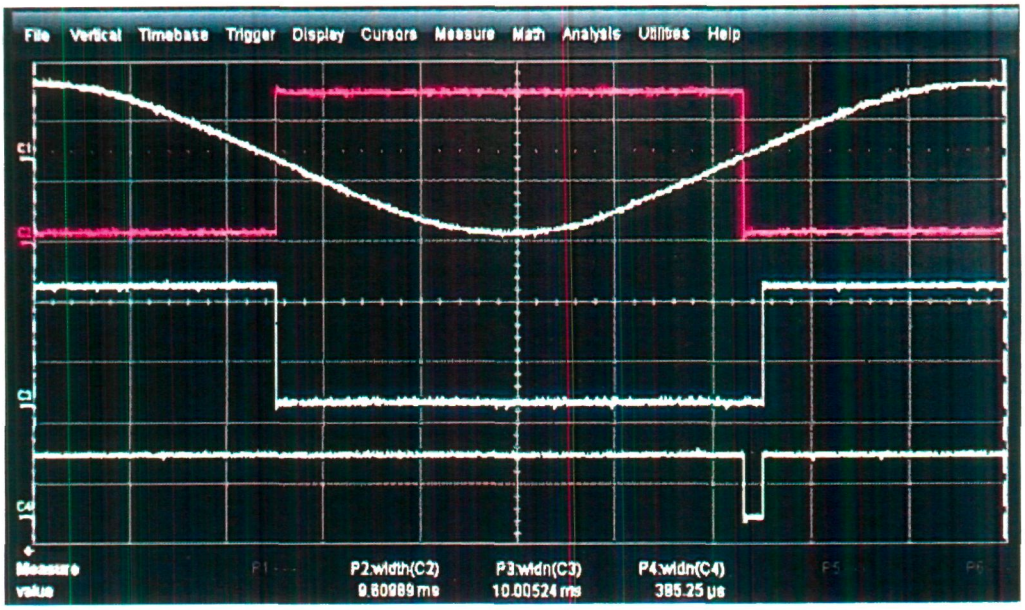
File Vertical Timebase Trigger Display Cursors Measure Math Analysis Utilities Help
Measure
value
P2:width(C2)
9.80989 ms
P3:widn(C3)
10.00524 ms
P4:widn(C4)
385.25 µs

(g)

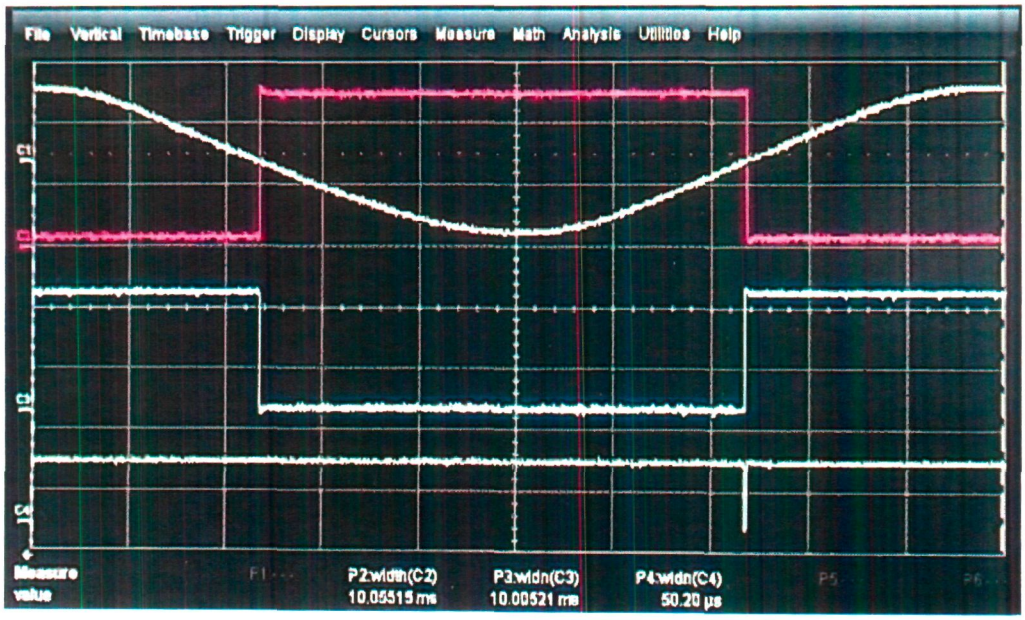
File Vertical Timebase Trigger Display Cursors Measure Math Analysis Utilities Help
Measure
value
P2:width(C2)
10.05515 ms
P3:widn(C3)
10.00521 ms
P4:widn(C4)
50.20 µs

(h)

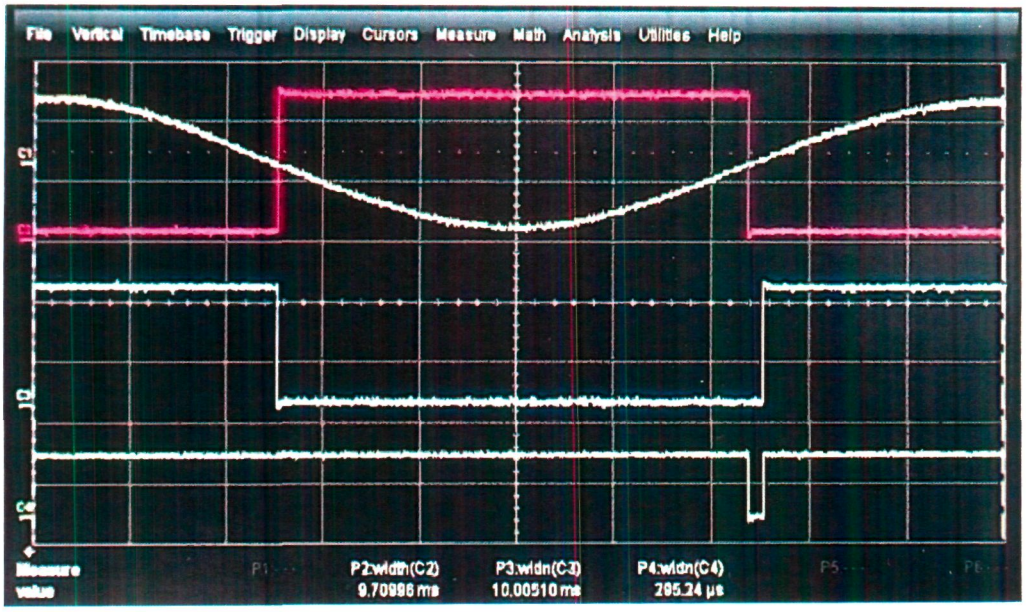

(i)

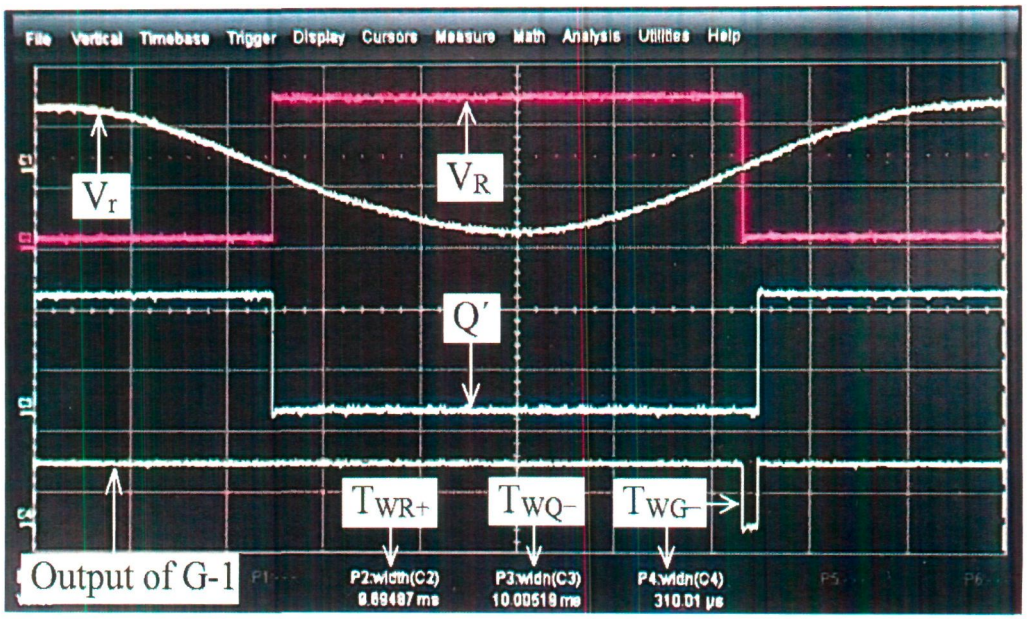

(j)

Figures 5.13 (a)-(j) Output of rotor circuit of synchro V_r (Ch#1), output of ZCD V_R with T_{WR+} (Ch#2), output of OS Q′ with T_{WQ-} (Ch#3), and output of G-1 with T_{WG-} (Ch#4), as **highlighted** in Table 5.1.

The proposed method measures A_I also, within 20 ms [Table 5.1, Figure 5.15 (a)], which is shown at an enlarged scale in Figure 5.15 (b). For more clarity, the pattern of variation of A_I, over one cycle, covering a time span of 1 second is shown in Figure 5.16. It is evident from Figure 5.16 that the proposed method measures 50 values of A_I in one second with a resolution of 20 ms, whereas, the resolution of existing methods is in the range of seconds as shown in Figure 5.17 [90]. Hence, due to high resolution of measurement, it easily captures the small variation (within 20 ms) and those peaks of acceleration of vibrations which are often missed by conventional measurement systems due to their poor resolution. The values of peak positive and negative acceleration (A_{P+} and A_{P-}), are found as **+1229.37 cm/s^2** and **−898.60 cm/s^2** respectively, as **marked** in Figure 5.15 (b).

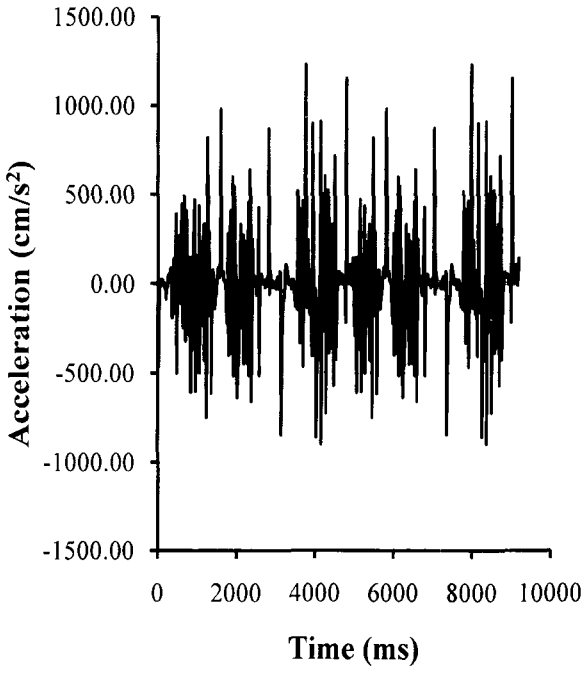

(a)

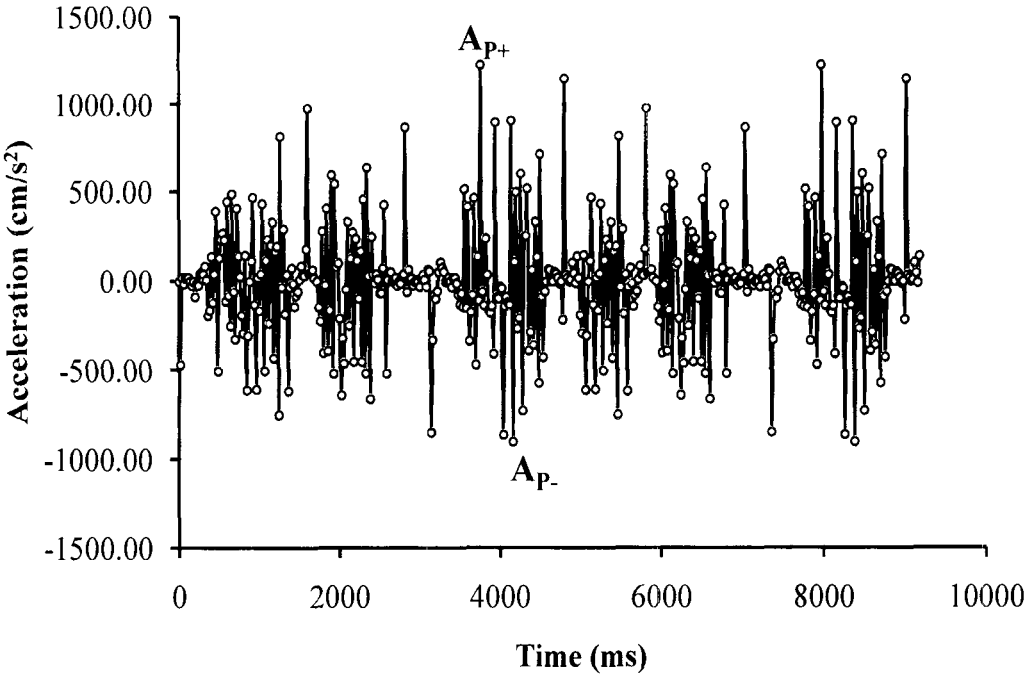

(b)

Figures 5.15 (a)-(b) The pattern for the variation of A_I, at **(a)** normal scale **(b)** enlarged scale.

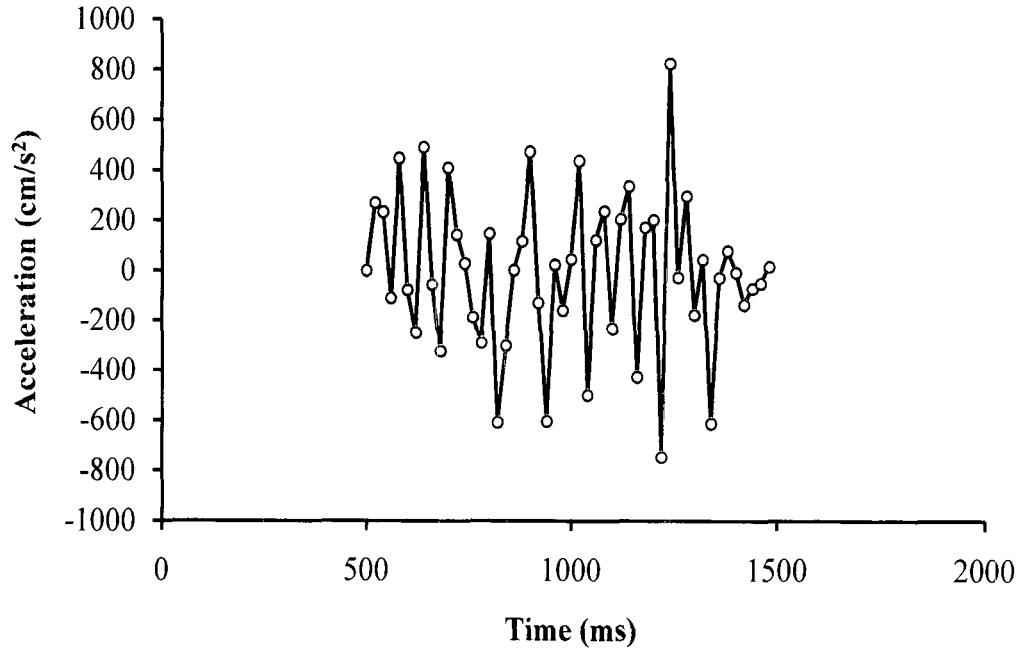

Figures 5.16 The pattern for the variation of A_I, over one cycle, covering a time span of 1 second.

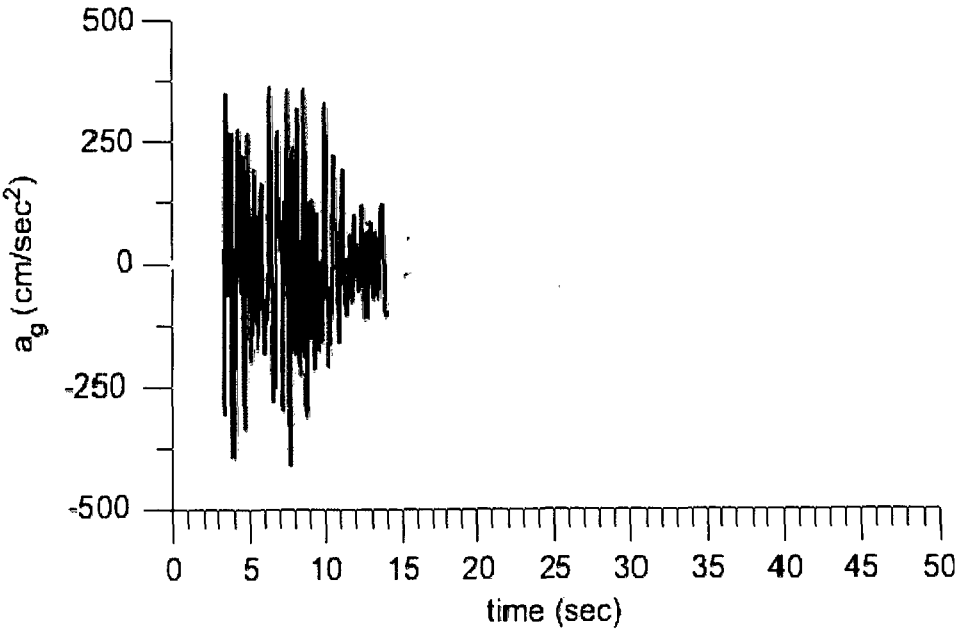

(a)

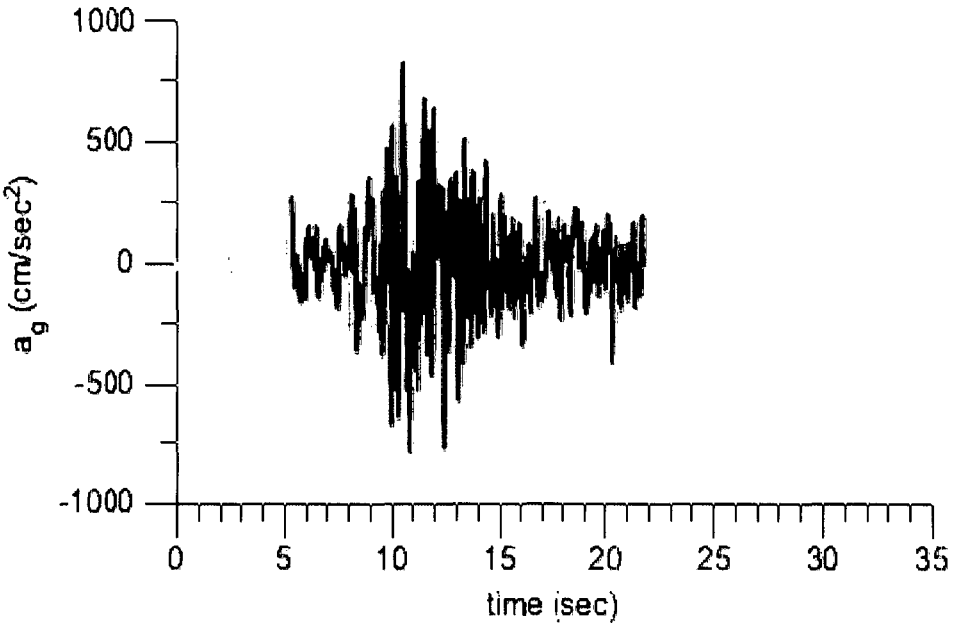

(b)

Figure 5.17 (a)-(b) Waveforms for the acceleration of seismic vibrations of **(a)** 2003 Lefcada (Greece) earthquake and **(b)** 1978 Tabas, Iran earthquake.

The sensitivity of the proposed method is 3.25×10^{-5} s^2 per cm, obtained as a ratio of infinitesimal change in pulse width and angular motion of the rotor of synchro. The accuracy of the method may be affected by the variation in frequency generated by the function generator. Here, we have used a very high resolution, arbitrary/function generator (Tektronix, AFG-2022 B) with an accuracy (Stability) of ± 1ppm ± 1μHz, 0 °C to 50 °C. Therefore, our apparatus is sufficiently accurate for the proposed instrumentation. The noise level introduced in the apparatus by the power amplifiers (LM384N) is removed by connecting capacitors of high values (4700 μF) at different stages.

5.4 Foreshocks

Generally, before any earthquake (main shock), there are foreshocks with hidden signatures of velocity and acceleration. The researchers have explored that there is a strong correlation (in seismicity rate and stacked amplitude etc) and physical linkage in the foreshocks and main shock which is helpful for the prediction of earthquakes [70]-[74]. Like main shock, the foreshocks consist of very low frequency wave but high frequency spikes are superimposed, which have extremely high instantaneous velocity and acceleration. Hence, due to this adverse combination, the existing low resolution accelerometers and seismometers are unable to get an insight of signatures present in these foreshocks [75]. The foreshocks are best forecaster of earthquakes, as there is very much resemblance in the pattern of velocity and acceleration of foreshocks and main shock [76]. However the magnitude of velocity and acceleration of foreshocks is less than that of main shock. These vibrations (foreshocks) are generated and measured in the same way as explained in sections 5.3.1 and 5.3.2 [93]. The existing and conventional instruments measure the velocity of foreshocks with a resolution of seconds, whereas due to fast measurement, the proposed scheme gives a high measurement resolution in the range of 20 ms. Consequently, it provides a better insight to recognize the signature of these vibrations (foreshocks), which will help in a better prediction of earthquakes and prevention of heavy losses.

5.5 Conclusion

A novel RMF and synchro based seismic vibration measurement technique is proposed in this chapter. It provides fast measurement of seismic vibrations with high accuracy and resolution. The rotor output of synchro is used to sense the instantaneous variation of velocity of seismic vibrations. A microprocessor based system is used to generate the vibrations in the range of -20 cm/s to +20 cm/s, with a vibration frequency of about 1 Hz. The vibrations change the frequency of induced EMF in the rotor circuit of synchro which is detected in terms of pulses of different pulse width. The output varies like a pulse width modulated signal. The instantaneous velocity of vibrations are measured using the widths of pulses at the output of G-1. The values of peak positive and negative velocity of vibrations, are found as +18.78 cm/s and −16.73 cm/s respectively. Average velocity of the vibrations in terms of dc voltage (5.03 V) and current (101.2 μA) are also measured using averaging circuits. The values of peak positive and negative acceleration are obtained as +1229.37 cm/s^2 and −898.60 cm/s^2 respectively. The conventional systems measure the velocity and acceleration of vibrations in the range of seconds, while the proposed method measures these values with a resolution of 20 ms. Hence, it easily captures the small variations and peaks of velocity and acceleration of vibrations (within 20 ms) which are often missed by conventional measurement systems due to their poor resolution. Thus, fast measurement of velocity and acceleration of seismic vibrations/foreshocks from the proposed system will help in a proper design of earthquake resistant nuclear power plants, buildings and structures and better prediction of earthquakes. The proposed system has to be simply attached with the conventional standard spring attachment system to measure the actual velocity and acceleration of seismic vibrations. A number of such units at earthquake prone areas may be placed and connected to supervisory monitoring centre for a continuous monitoring of seismic vibrations. The data from these units may be remotely sensed and simultaneously communicated for the centralized monitoring through the internet.

Chapter 6

Conclusions

6.1 Concluding Remarks

In this thesis, a novel contact type RMF based measurement technique is proposed which provides fast measurement of speed and deviation in speed while retaining high accuracy. The change in speed, changes the frequency of induced EMF in the rotor circuit of a synchro immediately as the RMF is rotating at a speed faster than the rotating member. The change in frequency is quickly monitored by the change in pulse width or time period of its output voltage. As the RMF rotates at a high speed (24000 r/min) for an input voltage frequency of 400 Hz, the measurement of speed and the deviation in speed are practically monitored in the very next cycle of the induced EMF (i.e. within 2.5 ms). In comparison to a dc tachogenerator, the time response of the proposed method is very fast and the measurement is very accurate as it is directly related to the frequency or time period of EMF of the rotor circuit. A microcontroller is also used for the generation of digital output corresponding to the measured speed and its variation. It gives 16-bit digital output corresponding to the width of the output pulse. This digital output can be used as a feedback signal for controlling the speed and deviation in speed accurately. For fast speed motors, the resolution may be increased to a very high value by utilizing 32-bit digital output signal of microcontroller or by increasing the frequency of the input voltage which generates the RMF.

The concept of RMF based speed measurement technique has also been successfully applied for the measurement of very low speed. Fast measurement of

low speed up to 1 r/min has been achieved by the proposed method. The rotor output of synchro (48 V, 2-pole, 3-phase) has been used for this purpose. A linear relationship is practically found in the speed and frequency from 1 to 10 r/min. The DSO records show the measurement of speed is done within few tens of ms. Even at 1 r/min, at the completion of one revolution of the rotating member, the RMF rotates 2400 times around the rotating member. Thus, the speed is measured at the speed of RMF which is 2400 times faster than the speed of the rotating member. The RMF completes one revolution in 25 ms, but due to the fast measuring mechanism (half cycle measurement), the deviation in speed is even detected within 12.5 ms. The proposed method of speed measurement is also compared with the response of a conventional tachogenerator method. The DSO records confirm the fast measurement of speed by the proposed method. The output measurand is also made available in terms of dc voltage and dc current using a separate analog circuit for feedback control applications.

The proposed technique is also used for the calibration of different tachometers which includes contact type, non-contact type, and both analog and digital tachometers. Normally limiting (guarantee or maximum) error or full-scale error (in terms of percent of full scale) is provided from the manufacturer. It does not tell anything about the actual error (point error) at different values of measurand. Moreover, due to the aging effect of permanent magnet of dc type tachometers and tachogenerators, a regular calibration is required for these devices. With the help of calibration chart, the actual speed can be found for the whole range of the measurement. For example the errors of an analog contact-type tachometer, provided in the data specification sheet, are ± 3 r/min for 0 to 300 r/min and ± 10 r/min, for 300 r/min to ± 1200 r/min. However, the point error found by the proposed method is within ± 2 r/min to ± 10 r/min, over these ranges, respectively. According to the calibration report provided with the tachometer, the error of digital non-contact type tachometer is ± 1 r/min over a range of 5 to 1200 r/min. Whereas, the point error found at different speed varies between ± 2 to ± 6 r/min in this speed range. Similarly, according to the data sheet, the error of digital contact type tachometer is ± 7 r/min in the range of 0 to

± 1200 r/min. However, the error found by the proposed method is ± 3 to ± 13 r/min in this range. It clearly shows the importance of calibration and finding of point error over the whole range of measurement for high accuracy of measurand.

The RMF based technique is also proposed in this thesis for the measurement of seismic vibrations and foreshocks. It provides fast measurement of seismic vibrations with high accuracy and high resolution. The rotor output of synchro is used to sense the instantaneous variation of velocity of seismic vibrations. A microprocessor based system is developed to simulate (generate) the vibrations of 1 Hz, with velocity in the range of -20 cm/s to +20 cm/s, similar to the seismic vibrations of 2003 Lefkada (Greece), 1994 Northridge (USA), 1992 Landers (USA), and 1987 Whittier Narrows (USA) earthquakes. The instantaneous velocity of vibrations are measured using the widths of pulses at the output of G-1. The peak positive and negative velocity of vibrations are found as +18.78 cm/s and −16.73 cm/s respectively. An analog dc output (5.03 V) is obtained corresponding to the velocity of vibrations. A micro ammeter is also calibrated to measure the average velocity of seismic vibrations in terms dc current. Further, the instantaneous values of acceleration of vibrations are obtained from the corresponding instantaneous values of velocity. The values of peak positive and negative acceleration are found as +1229.37 cm/s^2 and −898.60 cm/s^2 respectively. The time resolution of conventional systems, measuring the velocity and acceleration of vibrations are of the order of seconds, while the proposed method measures these values with a resolution of only 20 ms. Hence, it easily captures those peaks of velocity and acceleration which are missed by conventional measurement systems due to their poor resolution. Thus, high accuracy and resolution of the proposed method, shall help in better understanding of seismic records and better forecasting. The high resolution measurement of foreshocks also provides a deep insight to recognize the signature of these vibrations, which will help in a better prediction of earthquakes and prevention of heavy losses. Therefore, the seismic records may also help for selecting proper location of a nuclear power plant, dams and structures. A number of proposed measuring units may be placed at different locations of earthquake

prone areas and a supervisory monitoring centre may be used for a continuous monitoring of seismic vibrations of these places. The data from these units may be communicated through the internet.

6.2 Scope of Future Work

- The proposed RMF based measurement technique is basically a contact type measurement technique which provides fast measurement of speed and deviation in speed at high resolution and accuracy. A non-contact type RMF based measuring system may be developed in future to avoid the limitations of contact type instrumentation.
- For the calibration of different tachometers, the only source of error is the error due to the instruments used. Therefore if 'Bench Mark' instruments are used for measurement, then the accuracy of the measurement will increase further.
- The RMF based seismic vibration and foreshocks measurement technique provides high accuracy and high resolution of measurement of seismic vibrations which can also be made contactless type. If 'Bench Mark' instruments are used for measurement, then the accuracy and resolution shall improve further. It may be helpful for better and accurate prediction of earthquakes to safeguard the heavy losses.
- The RMF based measurement technique may also be applied for the vibration measurement of automobiles and diesel engines. The existing methods measure the vibration of diesel engines in frequency domain. These methods are costly and complex. The proposed method can measure these vibrations in time domain which is simple and cost effective.

References

[1] G. B. Foo and M. F. Rahman, "Direct torque control of an IPM-synchronous motor drive at very low speed using a sliding-mode stator flux observer," *IEEE Trans. Power Electron.*, vol. 25, no. 4, pp. 933-942, Apr. 2010.

[2] P. Kulkarni, M. T. Abraham, and S. P. Das, "Design and simulation of a matrix converter-fed scalar controlled synchronous motor drive," *Annual IEEE Conference*, INDICON, pp. 69-74, Dec. 2008.

[3] X. Feng, L. Zhenting, C. Yufeng, M. Xinbang, and Y. Hui, "Processing optimization and quality control of rotor spinning," Henan Textile College, Xiangcheng, Textile Co., Ltd., Henan, China, 2007.

[4] J. Zhang, F. Zhao, W.Wang, X. Ze and D. Su, "Dynamic analysis of tip set extra hard load of vertical shaft impact crusher," International conference on measuring technology and mechatronics automation, Zhangjiajie, Hunan, China, April 11-12, 2009.

[5] T. K. Boukas, and T. G. Habetler, "High-performance induction motor speed control using exact feedback linearization with state and state derivative feedback," *IEEE Trans. Power Electron.*, vol. 19, no. 4, pp. 1022-1028, July 2004.

[6] J. D. Park, C. Kalev, and H. F. Hofmann, "Control of high-speed solid rotor synchronous reluctance motor/generator for flywheel-based uninterruptible power supplies," *IEEE Trans. Ind. Electron.*, vol. 55, no. 8, pp. 3038–3046, Aug. 2008.

[7] R. D. Lorenz, T. Lipo, and D. W. Novotny, "Motion control with induction motors," *IEEE Proceedings,* vol. 82, no. 8, pp. 1215-1240, Aug. 1994.

[8] M. Aiello, A. Cataliotti, and S. Nuccio, "An induction motor speed measurement method based on current harmonic analysis with the chirp-Z transform," *IEEE Trans. Instr. Measr.*, vol. 54, no. 5, pp. 1811-1819, Oct. 2005.

[9] T. Fabian and G. Brasseur, "A robust capacitive angular speed sensor," *IEEE Instrumentation and Measurement Technology Conference, IMTC/1997, Process.*, Ottawa, Canada, vol. 2, pp. 1267-1272, May 19-21, 1997.

[10] C. Schauder, "Adaptive speed identification for vector control of induction motors without rotational transducers," *IEEE Trans. Ind. Appl.*, vol. 28, no. 5, pp. 1054-1161, Sept./Oct.1992.

[11] U. Baader, M. Depenbrock, and G. Gierse, "Direct self control (DSC) of inverter-fed Induction machine: A basis for speed control without speed measurement," *IEEE Trans. Ind. Appl.*, vol. 28, no. 3, pp. 581-588, May/June 1992.

[12] C. Michael and A. Safacas, "Behavior of a drive system consisting of two DC motors with elastic shafts driving the Yankee drying cylinder of a tissue paper machine," *The 4th International Conference on Power Electronics and Motion Control, IPEMC 2004.*, vol. 3, pp. 1460-1465, Aug. 2004.

[13] S. I. Ahson and M.H. Ali, "A microprocessor–based scheme for torque angle and speed measurement," *IEEE Trans. Ind. Electron.*, vol. IE-34, no. 2, pp. 135-138, 1987.

[14] E. Galviin, A.Torralba, and L.G.Franquelo, "A simple digital/optical tachometers with high precision in a wide speed range," in *Proc. IEEE Ind. Electron. Conf. IECON'94*, vol. 2, pp. 920-923, Sept. 1994.

[15] Y. Li, F. Gu, G. Harris, A. Ball, N. Bennet and K. Travis, "The measurement of instantaneous angular speed," *Mechanical Systems and Signal Processing, Elsevier*, vol. 19, issue 4, pp. 786-805, July 2005.

[16] E. Galvan, A. Torralba, and L. G. Franquelo, "ASIC implementation of a digital tachometer with high precision in a wide speed range," *IEEE Trans. Ind. Electron.*, vol. 43, no. 6, pp. 655–660, Aug. 2002.

[17] A. Sanchez, L. R. G. Carrillo, E. Rondon, R. Lozano, and O. Garcia "Hovering flight improvement of a quad-rotor mini UAV using brushless dc motors," *Journal of Intelligent and Robot System 2011, Springer Science*, vol. 61, pp. 85-101, Oct. 2010.

[18] F. Gu, I. Yesilyurtb, Y. Li, G. Harris, and A. Ball, "An investigation of the effects of measurement noise in the use of instantaneous angular speed for machine diagnosis," *Mechanical Systems and Signal Processing, Elsevier,* vol. 20, issue 6, pp. 1444-1460, Aug. 2006.

[19] S. Sarma, V.K. Agrawal, S. Udupa, and K. Parameswaran, "Instantaneous angular position and speed measurement using a DSP based resolver-to-digital converter," *Mechanical Systems and Signal Processing, Elsevier,* vol. 41, issue 7, pp. 788-796, Aug. 2008.

[20] H. In-Joong and S. Lee, "An online identification method for both stator and rotor resistances of induction motors without rotational transducers," *IEEE Trans. Ind. Electron.*, vol. 47, no.4, pp. 842-853, Aug. 2000.

[21] L. Rovati, M. Bonaiut, and P. Pavan, "Design of a high-performance optical system for angular position measurement: optical and electronic strategies for uncertainty reduction," *IEEE Trans. Inst. Measr.*, vol. 54, no. 5, pp. 2075-2081, Oct. 2005.

[22] A. S. Morris, *Measurement and Instrumentation Principles*, 3rd ed., USA: Butterworth-Heinemann, 2001.

[23] A. H. Kadhim, T. K. M. Babu, and D. O'Kelly, "Measurement of steady - state and transient load-angle, angular velocity, and acceleration using an optical encoder," *IEEE Trans. Instr. and Measr.*, vol. 41, no. 4, pp. 486-489, Aug. 1992.

[24] US Digital Products, HD25A Absolute Industrial Rugged Metal Optical Encoder, 1400 NE 136th Avenue, Vancouver, Washington 98684, USA, www.usdigital.com, info@usdigital.com.

[25] Computer Optical Products, Inc. (COPI), Emoteq Corporation, 10002 E 43rd Street, Tulsa, OK 74146-3638, USA, inquiry@alliedmotion.com.

[26] O. Al-Ayasrah, T. Alukaidey, and G. Pissanidis, "DSP based n-motor speed control of brushless dc motors using external FPGA design," in *Proc. IEEE Ind. Techn. Conf. (ICIT99)*, 2006, vol. 1, pp. 627-631, Dec. 2006.

[27] K.M. Lee and D. Zhou, "A real-time optical sensor for simultaneous measurement of three-DOF motions," *IEEE/ASME Trans. Mechatronics,*

vol. 9, no. 3, pp. 499-507, Sept. 2004.

[28] T. O. Kowalska and M. Dybkowski, "Stator-current-based MRAS estimator for a wide range speed-sensorless induction-motor drive," *IEEE Trans. Ind. Electron.*, vol. 57, no. 4, pp.1296-1308, April 2010.

[29] G. Foo and M. F. Rahman, "Sensorless sliding-mode MTPA control of an IPM synchronous motor drive using a sliding-mode observer and HF signal injection," *IEEE Trans. Ind. Electron.*, vol. 57, no. 4, pp. 1270-1278, April 2010.

[30] M. Hajian, J. Soltani, G. A. Markadeh, and S. Hosseinnia, "Adaptive nonlinear direct torque control of sensorless im drives with efficiency optimization," *IEEE Trans. Ind. Electron.*, vol. 57, no. 4, pp. 975-985, April 2010.

[31] J. Lee, J. Hong, K. Nam, R. Ortega, L. Praly, and A. Astolfi, "Sensorless Control of Surface-Mount Permanent-Magnet Synchronous Motors Based on a Nonlinear Observer," *IEEE Trans. Power Electron.*, vol. 25, no. 2, pp. 290-297, Feb. 2010.

[32] M. S. Zaky, M. M. Khater, S. S. Shokralla, and H. A. Yasin, "Wide-speed-range estimation with online parameter identification schemes of sensor less induction motor drives," *IEEE Trans. Ind. Electron.*, vol. 56, no. 5, pp. 1699-1708, May 2009.

[33] M. Barut, S. Bogosyan, and M.Gokasan, "Experimental evaluation of braided EKF for sensorless control of induction motors," *IEEE Trans. Ind. Electron.*, vol. 55, no. 2, pp. 620-632, Feb. 2008.

[34] R. Cárdenas, R. Peña, J. Clare, G. Asher, and J. Proboste, "MRAS Observers for sensorless control of doubly-fed induction generators," *IEEE Trans. Power Electron.*, vol. 23, no. 3, pp. 1075-1084, May 2008.

[35] D. Shi, P. J. Unsworth and R. X. Gao, "Sensorless speed measurement of induction motor using Hilbert transform and interpolated fast Fourier transform," *IEEE Trans. Inst. Measr.*, Vol. 55, No.1, pp. 290-299, Feb. 2006.

[36] A. Haddoun, M. E. H. Benbouzid, D. Diallo, R. Abdessemed, J. Ghouili and K. Srairi, "Comparative analysis of estimation techniques of SFOC induction motor for electric vehicles," in *Proc. IEEE Elect. Machines*

Conf. (ICEM), vol. 1, pp. 1-6, Sept. 2008.

[37] E. Levi and M. Wang, "A speed estimator for high performance sensorless control of induction motors in the field weakening region," *IEEE Trans. Power Electron.*, vol. 17, no. 3, pp. 365-378, May 2002.

[38] D. Shi, P. J. Unsworth and R. X. Gao, "Sensorless speed measurement of induction motor using hilbert transform and interpolated fast Fourier transform," *IEEE Trans. Instr. Measr.*, vol. 55, no. 1, pp. 290-299, Feb. 2006.

[39] A. Piipo, M. Hinkkanen, and J. Luomi, "Signal injection in sensor less PMSM drives equipped with inverter output filter," *IEEE Trans. Ind. Appl.*, vol. 44, no. 5, pp. 1614-1620, Sep./Oct. 2008.

[40] J. M. Aller, T. G. Habetler, R. G. Harley, and R. M. Tallam, "Sensor less speed measurement of ac machines using analytic wavelet transform," *IEEE Trans. Ind. Appl.*, vol. 38, no. 5, Sept. 2002.

[41] N. K. Boggarpu and R. C. Kavanagh, "New learning algorithm for high-quality velocity measurement and control when using low-cost optical encoders," *IEEE Trans. Inst. Measr.*, Vol. 59, no.3, pp. 565-574, March 2010.

[42] R. C. Kavanagh, "An enhanced constant sample-time digital tachometer through oversampling," *Transaction of institute of measurement and control,* vol. 4, no. 2, pp. 83-98, June 2004.

[43] R. C. Kavanagh, "Performance analysis and compensation of M/T- type digital tachometers," *IEEE Trans. Inst. Measr.*, Vol. 50, no.4, pp. 965-970, Aug. 2001.

[44] R. C. Kavanagh, "Improved digital tachometer with reduced sensitivity to sensor non ideality," *IEEE Trans. Ind. Electron.*, vol. 47, no. 4, pp. 890-897, Aug 2000.

[45] J. N. Lygouras, T. P. Pachidis, K. N. Tarchanidis, and V. S. Kodogiannis, "Adaptive high performance velocity evaluation based on a High-Resolution time-to digital converter," *IEEE Trans. Inst. Measr.*, Vol. 57, no.9, pp. 2035-2043, Sept. 2008.

[46] W. Yang, P. J. Tavner, C. J. Crabtree, and M. Wilkinson, "Cost-effective

condition monitoring for wind turbines," *IEEE Trans. Ind. Electron.*, vol. 57, no. 1, pp. 263-271, Jan. 2010.

[47] Rino Mechanical Components Inc., 216 North Main Street, Freeport, NY 11520, 1-888-260-7466, sales@rinomechanical.com.

[48] S. J. Arif and S. H. Laskar, "A rotating magnetic field based ultra fast measurement of speed," Patent Application 777/DEL/2011A, *Indian Official Journal of the Patent Office,* Issue no. 18/2011, p-8219, May 6, 2011.

[49] S. J. Arif, M. S. J. Asghar and Adil Sarwar, "Measurement of speed and calibration of tachometers using rotating magnetic field," *IEEE Tnans. on Inst. & Measr.*, vol., 60, pp. 1-11, Digital Object Identifier 10.1109/TIM.2013.2283136., Aug. 2013.

[50] S. J. Arif and M. S. J. Asghar, "A Rotating Magnetic Field Based Ultra Fast Transducer for the Measurement of Very Low Speed," Patent Application 2183/DEL/2010A, *Indian Official Journal of the Patent Office,* Issue No. 14/2011, p-6126, Apr. 8, 2011.

[51] S. J. Arif, M. S. J. Asghar, and Imdadullah, "Very fast measurement of low speed of rotating machines using rotating magnetic field," *IEEE Trans. Instrum. Meas.*, vol. 61, no. 3, pp. 759-766, March 2012.

[52] David A. Bell, *Electronic Instrumentation and Measurements, 2nd ed.*, New York, USA: Oxford University Press, 2012.

[53] A. K. Swahney, *A Course in Electrical and Electronic Measurements and Instrumentation*, 4th ed., Delhi, India: Dhanpat Rai & Co. Pvt. Ltd., 1997.

[54] Tachometer Calibration Using Pulse Generator and Electronic Counter, Integrated Publishing, http://operatormanuals.tpub.com.

[55] Easy method to calibrate tachogenrator using computer and tone generating program, http://www.nch.com.au/tonegen/.

[56] Calibration Services for Rotational Speed Measurement, Standard and Calibration Laboratory, Hoklas, tkchan@itc.gov.hk.

[57] Calibration of Tachometers, Electronics Automation Pvt. LTD, Banglore, India, www.eaplindia.com.

[58] Optical Tachometer Calibration Option for the 2000 Series Calibrators V 2.00 Transmille solution in Calibration, http://www.transmille.co.uk/pdf/tacho_info.pdf.

[59] Calibration of Tachometers and Measure of Speed, Sanas South African National Accreditation System http://www.sanas.co.za/manuals/pdfs/tr_4501.pdf.

[60] Hand Tachometer, Jeclock Type H, Fuji Kogoyo Co., Ltd, Japan.

[61] Contact/Surface Speed Digital Tachometer, Model DT-2235 B, Lutron, India.

[62] Non-Contact Digital Tachometer, Model DT-2001 B, EAPL Pvt. Ltd., Banglore, India, www.eaplindia.com.

[63] T. Bleier and F. Freund, "Earthquake alarm," *IEEE Spectr.*, vol. 42, no. 12, pp. 22–27, Dec. 2005.

[64] C. Albertini, Ispra, K. Labibes, and Orino, "Seismic wave measuring devices," U.S. Patent 6,823,963 B2, Nov. 30, 2004.

[65] P. C. Jenkins, *Engineering seismology from earthquakes: observation, theory and interpretation*, North Holland, H. Kanamori and E. Boschi, 1983.

[66] K. Okubo, M. Takayama, and N. Takeuchi, "Electrostatic field variation in the atmosphere induced by earth potential difference variation during seismic wave propagation," *IEEE Trans. on Electromagnetic Compatibility,* vol. 49, no. 1, pp.163-169, Feb. 2007.

[67] D. M. Tralli, W. Foxall, A. Rodgers, E. Stappaerts, and C. Schultz, "Suborbital and space borne monitoring of seismic surface waves," *proc. of IEEE Aerospace Conf., Pasadena*, CA, USA, pp. 1- 6, 2005.

[68] Emily E. Brodsky, "The spatial density of foreshocks," *Geophysical Research Letters*, vol. 38, L10305, doi: 10.1029/2011GL047253, pp.1-6, May 2011.

[69] M. Gong, J. Sun, T. Kashima, and L. Xie, "Parameter Identification of a 9-Story Building for Earthquake Damage Detection." *3rd International Congress on Image and Signal Processing (CISP2010),* pp. 3650-3654,

2010.

[70] K. R. Felzer, R. E. Abercrombie, and G. Ekstrom, "A common origin for aftershocks, foreshocks, and multiplets," *Bulletin of the Seismological Society of America*, vol. 94, no. 1, pp. 88–98, Feb. 2004.

[71] A. Helmstetter, D. Sornette, and J. R. Grasso, "Main shocks are aftershocks of conditional foreshocks: How do foreshock statistical properties emerge from aftershock laws," *Journal of Geophysical Research*, vol. 107, 108(B1), 2046, doi:10.1029/2002JB001991, 2003.

[72] J. J McGuire, M. S. Boettcher, and T. H. Jordan (2005), "Foreshock sequences and short-term earthquake predictability on East Pacific Rise transform faults," *Nature,* 434, 457–461, doi:10.1038/nature03377, Sept. 2005.

[73] Z. Peng, J. E. Vidale, M. Ishii, and A. Helmstetter, "Seismicity rate immediately before and after main shock rupture from high frequency waveforms in Japan," *Journal of Geophysical Research*, vol. 112, B03306, doi:10.1029/2006JB004386, March 2007.

[74] J. Zhuang, A. Christophersen, M. K. Savage, D. Vere-Jones, Y. Ogata, and D. D. Jackson (2008), "Differences between spontaneous and triggered earthquakes: Their influences on foreshock probabilities," *Journal of Geophysical Research*, vol. 113, B11302, doi:10.1029/2008JB005579, Nov. 2008.

[75] R. Rupakhety, and R. Sigbjornsson, "A note on the L'Aquila earthquake of 6 April 2009: Permanent ground displacements obtained from strong-motion accelerograms," *Journal of Soil Dynamics and Earthquake Engineering,* vol. 30, pp. 215–220, 2010.

[76] P. Varotsos, K. Alexopoulos, and K. Nomicos, "Seismic electric currents," *Proc. of the Academy of Athens Conf.*, pp. 277–286, *1981.*

[77] P. Varotsos, K. Alexopoulos, K. Nomicos, G. Papaioannou, M. Varotsou and E. Revelioti-Dologlou, "Determination of the epicenter of impending earthquakes from precursor changes of the telluric current," *Proc. of the Academy of Athens Conf.*, pp. 434–446, 1981.

[78] P. Varotsos, K. Alexopoulos, and K. Nomicos, "Electro telluric precursors to earthquakes," *Proc. of the Academy of Athens Conf.*, pp. 341–363,

1982.

[79] P. Varotsos, K. Alexopoulos, K. Nomicos and M. Lazaridou, "Earthquake prediction and electric signals," *Nature*, vol. 322, pp. 120, July 1986.

[80] P. Varotsos, N. Sarlis, M. Lazaridou, and P. Kapiris, " Transmission of stress induced electric signals in dielectric media," *Journal of Applied Physics,* vol. 83, pp. 60–70, Jan. 1998.

[81] S. J. Lighthill, A critical review of VAN - Earthquake prediction from seismic electrical signals, London, UK: World Scientific Publishing Co Pvt. Ltd., ISBN 978-9810226701, 1996.

[82] Y. Y. Kagan, "Special section-assessment of schemes for earthquake prediction; Are earthquakes predictable?" *Geophys. J. Int.*, vol. 131, pp. 505-525, 1997.

[83] M.S. Lazaridou-Varotsos, Earthquake Prediction by Seismic Electric Signals. The success of the VAN method over thirty years. Springer-Verlag, Berlin Heidelberg, 2011.

[84] C. Y. King, W. C. Evans, T. Presser, and R. Husk, "Anomalous chemical changes in well water and possible relation to earthquakes," *Geophys. Res. Lett.* vol. 8, pp. 425–428, 1981.

[85] C. Y. King, N. Koizumi, and Y. Kitagawa, "Hydro geochemical anomalies and the 1995 Kobe earthquake," *Science 7,* vol. 269, pp. 38–39, July 1995.

[86] N. M. Pérez, P. A. Hernández, G. Igarashi, I. Trujillo, S. Nakai, H. Sumino, and H. Wakita, "Searching and detecting earthquake geochemical precursors in CO_2-rich ground waters from Galicia, Spain," *Geochemical Journal*, vol. 42, pp. 75-83, 2008.

[87] P. Mandal, "Crustal shear-wave splitting in the epicentral zone of the 2001 Mw 7.7 Bhuj earthquake, Gujarat, India," *Journal of Geodynamics*, vol. 47, pp. 246–258, 2009.

[88] W. R. Stephenson, "Late resonant response at Wainuiomata, New Zealand, during distant earthquakes," *Journal of Soil Dynamics and Earthquake Engineering*, vol. 25, pp. 187–196, 2005.

[89] E. Durukal, "Critical evaluation of strong motion in Kocaeli and Du¨zce (Turkey) Earthquakes," *Journal of Soil Dynamics and Earthquake Engineering,* vol. 22, pp. 589–609, 2002.

[90] M. Taflampas, C. C. Spyrakos, and I. A. Koutromanos, "A new definition of strong motion duration and related parameters affecting the response of medium–long period structures," *Journal of Soil Dynamics and Earthquake Engineering,* vol. 29, pp. 752–763, 2009.

[91] S. J. Arif and Shahedul Haque Laskar, "A rotating magnetic field based high resolution measurement of velocity and acceleration of seismic vibrations," *Indian Official Journal of the Patent Office,* Issue no. 17/2011, Application No.778/DEL/2011A, p. 7116, April 29, 2011.

[92] S. J. Arif, M. S. J. Asghar, and Imdadullah, "Accurate measurement of velocity and acceleration of seismic vibrations near nuclear power plants," *Elsevier's Journal of Physics Procedia,* vol., 37, pp. 43-50, Oct. 2012.

[93] S. J. Arif, M. S. J. Asghar, and K. F. Khan, "A high resolution Measurement of foreshocks for the prediction of earthquakes," *Journal of Earth Science and Climate Change,* vol., 3, Issue 2, pp. 1-6, Oct. 2012.

[94] A. E. Fitzgerald, C. Kingsley, and S. D. Umans, *Electric Machinery*, 6th ed., New Delhi: McGraw-Hill, 2006.

[95] Voltage Comparator, LM311, National Semiconductors, Texas Instruments, Literature Number: SNOSBJ1C, p. 1, www.national.com.

[96] PIC16F877A: Flash 40-pin, 4MHz, 8kB Microcontroller, Microchip, USA. www.futurelec.com/Microchip/PIC16F877A.shtml.

[97] Arbitrary function generator (AFG-2022 B), Tektronix: www.tektronix.com.

[98] Mixed signal oscilloscope (Wave Surfer 104 MXs-B), LeCroy: www.lecroy.com.

[99] I. J. Nagraj and D. P. Kothari, *Electric Machines*, 3rd ed., New Delhi: Tata McGraw Hill, 1994.

[100] H. N. Norton, *Handbook of transducer for electronic measuring systems*, Prentice-Hall, Inc. Englewood Cliffs, N.J., 1969.

[101] PowerFlex4: adjustable frequency ac drive, www.abpowerflex.com, www.rockwellautomation.com/literature.

[102] Department of Earthquake Engineering, Indian Institute of Technology, Roorki, U.P., India.

Appendix A

A.1 Ratings of Different Machines Used in the Experiment for Ultra Fast Measurement of Speed and Deviation in Speed Using Rotating Magnetic Field

Rating of Synchro	
Rated voltage	48V
Frequency	50 Hz
Number of phase at stator side	3
Number of phase at rotor side	1
Number of poles	2
Rating of Permanent Magnet dc Tachogenerator	
Maximum r/min	10000
Output dc voltage at 100 r/min	2.43V
Rating of dc Motor	
Input voltage	415 V
Rated power	0.5 kW
Number of r/min	1440
Rated current	2 A
Number of poles	2
Input voltage range	200-240 V

A.2 Program for the Fast Measurement of Time Period T_Z Using Microcontroller

```
LIST p=16f877a
        #include <p16f877a.inc>
        ORG 0x000
        GOTO START
        ORG 0X04
        GOTO STARTTIMER
```

```
START       BSF STATUS,RP0 ;
        BCF STATUS,RP1 ;Select Bank1
                MOVLW b'01111111'
                MOVWF OPTION_REG
                MOVLW b'00000001'
                MOVWF TRISB
                MOVLW b'00000000'
                MOVWF TRISD
                MOVLW b'00000000'
                MOVWF TRISC
                BCF STATUS,RP0
                CLRF PORTA              ;Clear PORTA output latches
                CLRF PORTD
                BCF INTCON,INTF
                BSF INTCON,GIE
                BSF INTCON,INTE
                GOTO $

STARTTIMER
                BCF STATUS,RP0 ;
        BCF STATUS,RP1 ;Select Bank0
                MOVF TMR1L,W
                MOVWF PORTC
                MOVF TMR1H,W
                MOVWF PORTD
                BCF STATUS,RP0 ;
        BCF STATUS,RP1 ;Select Bank0
                BTFSS INTCON,INTF
                GOTO NOTRB0
                BCF STATUS,RP0
                BCF INTCON,INTF
                BCF STATUS,RP0 ;
        BCF STATUS,RP1 ;Select Bank0
                CLRF TMR1L
                CLRF TMR1H
                MOVLW 0X039
                MOVWF T1CON
                BSF T1CON, TMR1ON ; Timer1 starts to increment DELAY

                RETFIE

NOTRB0      BCF INTCON,INTF
                RETFIE

                END
```

A.3 Specifications of Different Tachometers

Rating of Analog/Mechanical Tachometer #1	
Test range and accuracy	± 2 r/min from 1 to 1000 r/min, ± 0.1 % over 1000 r/min
Rating of Digital/Optical Non-contact Type Tachometer #2	
Test range and accuracy	± 1 r/min from 1 to 5000 r/min, ± 0.05 % over 5000 r/min
No. of pulses per revolution	1
Rating of Digital Contact Type Tachometer #3	
Test range and accuracy	± 1 r/min from 1 to 1000 r/min, ± 0.05 % over 1000 r/min

A.4 Ratings of Different Machines Used for Very Fast Measurement of Low Speed of Rotating Machines Using Rotating Magnetic Field

Rating of Induction Motor	
Input voltage	415 V
Rated power	0.75 kW/1 HP
Frequency	50 Hz
Number of phase	3
Number of r/min	1390
Rated current	1.8 A
Number of poles	4
Rating of ac Drive	
Rated power	0.75 kW/1 HP
Input voltage range	200-240 V
Input frequency range	48-63 Hz
Number of phase at input	1
Input rated current	10 A
AC voltage range at output	0-230V
Output frequency range	0-240 Hz
Number of phase at output	3
Continuous output current	4.5 A
60 Second overload output current	6.75 A